National Aeronautics and
Space Administration

TIDE-FHWS-04
July 1993

George C. Marshall Space Flight Center
Marshall Space Flight Center, Alabama 35812

INTERNATIONAL SOLAR TERRESTRIAL PHYSICS PROGRAM

GLOBAL GEOSPACE SCIENCE PROGRAM

POLAR SPACECRAFT

THERMAL ION DYNAMICS EXPERIMENT
AND
PLASMA SOURCE INSTRUMENT

TIDE/PSI FLIGHT HARDWARE SPECIFICATIONS

Rev. 0 June 1988
Rev. 1 October 1988
Rev. 2 June 1989
Prepared by: David T. Young

Rev. 3 March 1993
Rev. 4 July 1993 (AS BUILT)
Prepared by: Thomas E. Moore

TABLE OF CONTENTS

Sections

Tables

Figures

Acronyms

ADC, A/D	Analog-to-Digital Converter
c/sec	Counts per Second
c/sam	Counts per Sample
DAC, D/A	Digital to Analog Converter
DE	Direct Events
DP	Data Processing microprocessor
DPU	Data Processing Unit
E/Q	Energy per Unit Charge
FOV	Field-of-View
FWHM	Full Width Half Maximum
GSE	Ground Support Equipment
HV	High Voltage
HVPS	High Voltage Power Supply
I/F	Interface
IMP	Instrument Mode Processing microprocessor
LEIF	Low Energy Ion Facility
LVPS	Low Voltage Power Supply
LZW	Lempel-Ziv-Welch (compression algorithm)
MAGAZ	Magnetic Field Azimuthal Angle
MAGEL	Magnetic Field Elevation
MCP	Microchannel Plate
M/Q	Mass Per Unit Charge (proton charge Q = +1)
PSI	Plasma Source Instrument
R_B	Bias Resistor
R_L	Load Resistor
RPA	Retarding Potential Analyzer
S/C	Spacecraft
S/N	Signal-to-Noise Ratio
START	TOF start-associated signal
STOP	TOF stop-associated signal
TAC	Time-to-Amplitude Converter
TIDE	Thermal Ion Dynamics Experiment
TLM	Telemetry
TCM	Telecommand
TOF	Time-of-Flight
UHV	Ultra High Vacuum

1. INTRODUCTION

1.1. Scope

The purpose of this document is to specify the performance requirements and resulting design specifications for the Thermal Ion Dynamics Experiment (TIDE) and Plasma Source Instrument (PSI) for the International Solar Terrestrial Physics program, Global Geospace Science mission, POLAR spacecraft. The intent of this revision is to document the requirements to which TIDE has been built, since they have shifted in detail from what was originally proposed, owing to numerous practical considerations. To keep this document compact and useful, reference is made to other project documents where appropriate. A summary of the existing and planned TIDE/PSI documents is given in the next section. Comments or questions should be directed to T. E. Moore.

1.2. Relevant Documents

EXISTING:

TIDE Original Proposal, 1980
PSI Original Proposal, 1980
TIDE Flight Proposal, 1988
PSI Flight Proposal, 1988
TIDE/PSI Data Handling Plan, 1991
TIDE/PSI Performance Assurance Implementation Plan (MSFC, SwRI, and LANL), 1989
TIDE/POLAR Interface Control Document, GE IS-32821262
PSI/POLAR Interface Control Document, GE IS-3282450
TIDE SwRI/LANL Interface Control Document, SwRI-15-3348-TOF-00
TIDE/PSI Flight Software Requirements Document, SwRI-15-3348-FSRD-01
TIDE/PSI Flight Software Test Requirements, MSFC-TIDE-FSTR-00
TIDE/PSI Preliminary Flight Software Test Procedure, SwRI-15-3348-FSTP-00
TIDE Functional Test Procedure, SwRI-15-3348-FTP-01
TIDE Comprehensive Test Procedure, MSFC-TIDE-CTP-01
TIDE Calibration Procedure, MSFC-TIDE-CP-01
"The Thermal Ion Dynamics Experiment and Plasma Source Instrument", submitted to*Space Science Reviews* , May, 1993.

PLANNED:

TIDE/PSI Flight Software Design Package, SwRI-15-3348-FSWD-00
TIDE/PSI Flight Software Test Procedure, SwRI-15-3348-FSTP-01
TIDE/PSI Flight Software Users Guide, SwRI-15-3348-FSUG-00
TIDE/PSI Flight Operations Guide, MSFC-TIDE-FOG-00
TIDE/PSI Key Parameters Generation Software Design, MSFC-TIDE-KPSD-00
TIDE/PSI Key Parameters Users Guide, MSFC-TIDE-KPUG-00
TIDE/PSI Data Base Users Guide, MSFC-TIDE-DBUG-00

1.3. Key Contacts and Personnel

[** Institution lead science investigator; * Institution development manager]

Space Science Laboratory
Marshall Space Flight Center
Huntsville, AL 35812
FAX: 205-544-5244

T. E. Moore**, Code ES53	205-544-7633	mooret@ssl.msfc.nasa.gov
M. O. Chandler, Code ES53	205-544-7645	chandler@ssl.msfc.nasa.gov
C. R. Chappell, Code DS01	205-544-3033	cchappell@nasamail.nasa.gov
W. L. Chisholm, Code ES53	205-544-7652	chisholm@ssl.msfc.nasa.gov
S. A. Fields*, Code ES51	205-544-7592	fields@ssl.msfc.nasa.gov
D. L. Gallagher, Code ES53	205-544-7587	gallagher@ssl.msfc.nasa.gov
C. J. Pollock, Code ES53	205-544-7638	pollock@ssl.msfc.nasa.gov

Los Alamos National Laboratory
P.O. Box 1663
Los Alamos, NM 87545
FAX: 505-665-3332

D.J. McComas**	505-667-0138	mccomas@essdp1.dnet.nasa.gov
K. McCabe	505-667-0728	mccabe@essdp1.dnet.nasa.gov
J. E. Nordholt*	505-667-3897	beth@alfven.lanl.mil.gov
M. F. Thomsen	505-667-1210	thomsen@essdp1.dnet.nasa.gov

Southwest Research Institute
P.O. Drawer 28510
San Antonio, TX 78284
FAX: 512-647-4325

D. T. Young**	210-522-2743	nick@swri.dnet.nasa.gov
R. K. Black	210-522-3562	rblack@space.swri.edu
R. P. Bowman	210-522-3369	nick@swri.dnet.nasa.gov
J. L. Burch	210-522-2526	jim@swri.dnet.nasa.gov
P. J. Casey	210-522-5031	nick@swri.dnet.nasa.gov
N. Eaker*	210-522-3140	nick@swri.dnet.nasa.gov
D. L. Kloza	210-522-3989	dana@swri.dnet.nasa.gov
J. H. Waite	210-522-3493	hunter@swri.dnet.nasa.gov

Centre de Recherches en Physique de l'Environment
CNET/CNRS
4. Avenue de Neptune
94107 St. Maur-des-Fosses
FRANCE
FAX: 33-1-4889-4433

J. J. Berthelier**	33-1-4886-1263	berthelier@crpeis.dnet.nasa.gov
N. Dubuloz	33-1-4886-1263	dubuloz@crpeis.dnet.nasa.gov
D.C. Delcourt	33-1-4511-4269	delcourt@crpeis.dnet.nasa.gov

Hughes Research Laboratories
3011 Malibu Canyon Road
Malibu, CA 90265
FAX: 213-317-5483

B. Beatty	213-317-5550	
R. Robson*	213-317-5391	
T. Williamson**	213-317-5206	

Center for Space Plasma and Aeronomic Research
The University of Alabama in Huntsville
Huntsville, AL 35899
FAX: 205-895-6382

R. H. Comfort**	205-895-6663	comfort@cspar.dnet.nasa.gov
J. L. Horwitz	205-544-6662	horwitz@cspar.dnet.nasa.gov

Center for Space Sciences
The University of Texas at Dallas
Richardson, TX 75083
FAX: 214-690-2761

W. B. Hanson**	214-690-2853	hanson@utd750.utdallas.edu
R. L. Heelis	214-690-2822	heelis@utd750.utdallas.edu
J. H. Hoffman	214-690-2846	hoffman@utd750.utdallas.edu

Space Physics Research Laboratory
The University of Michigan
Ann Arbor, MI 48109-2143
FAX: 313-747-3083

A. F. Nagy**	313-764-6592	nagy@sprl.dnet.nasa.gov
P. M. Banks	313-764-8475	

Center for Space Sciences
Utah State University
Logan, UT 84322

J. Raitt**	801-750-2849	raitt@cc.usu.edu

National Institute for Polar Research
9-10, Kaga, 1-Chome,
ITABASHI-KU
Tokyo 173 JAPAN
FAX: 03-962-5704

M. Ejiri	03-962-4711	ejiri@nipr.ac.jp

Naval Postgraduate School
Mail Code
Monterey, CA 93943
FAX: 408-646-2834

R. C. Olsen	408-646-2019	olsen@npspac.dnet.nasa.gov

1.4. Science Objectives and Heritage

The Thermal Ion Dynamics Experiment (TIDE) and Plasma Source Instrument (PSI) have been developed in response to the requirements of the ISTP program for three-dimensional (3D) plasma composition measurements capable of tracking the outflow of ionospheric plasma throughout the magnetosphere. Large and relatively steady outflows of ionospheric plasma were identified by the Dynamics Explorer 1 Retarding Ion Mass Spectrometer (DE 1/RIMS) as originating in the dayside auroral zone cleft region (heavy upwelling ion outflows, the cleft ion fountain), and from the entire high latitude region (light ion polar wind). This plasma is in part lost to the downstream solar wind and in part recirculated within the magnetosphere, participating in the formation of the diamagnetic hot plasma sheet and ring current plasma populations. The 2 x 9 R_E orbit of the POLAR spacecraft will position it high over the polar caps in the lobes of the magnetotail where it will extensively sample these outflows.

Significant obstacles which have previously made this task impossible include the low density and energy of the outflowing ionospheric plasma plume and the positive spacecraft floating potentials which exclude the low-energy plasma from detection on ordinary spacecraft. Based on a unique combination of focusing electrostatic ion optics and time-of-flight detection and mass analysis, TIDE provides the unprecedented sensitivity (seven channels having an effective aperture of nearly 1 cm^2 each) and resolution required for this purpose. PSI will produce a low-energy plasma locally at the POLAR spacecraft which will provide the ion current required to balance the photoelectron current, along with a low temperature electron population, thus regulating the spacecraft potential at a few tenths of a volt positive relative to the space plasma. Thus it will be possible with TIDE/PSI to:

(a) investigate the extent to which ionospheric ions are recirculated within the distant magnetotail neutral sheet or lost to the solar wind, by measuring their density and flow velocity,

(b) investigate the mass dependent degree of energization achieved as ionospheric plasma flows antisunward on merged flux tubes through the lobes and into the distant tail, by measuring the thermodynamic properties of these plasmas, and

(c) investigate the ionosphere as a source of plasma to the plasma sheet and ring current, by identifying the ionospheric species and distinguishing them from solar plasmas.

2. FUNCTIONAL DESCRIPTION

TIDE combines large aperture electrostatic mirrors and retarding potential analyzers (M/RPAs) with time-of-flight (TOF) ion optics to provide an effective area per aperture over two orders of magnitude greater than the Retarding Ion Mass Spectrometer on Dynamics Explorer 1 (DE 1/RIMS). This large increase permits improved angular resolution and enhanced sensitivity. With an angular aperture on the order of 10% that of RIMS at ~ 0.1 sr, the resulting geometric factor $A\Omega \sim 0.1$ cm^2 sr per 22.5° sector is still roughly one order of magnitude greater than that of RIMS.

Seven such polar angle sectors operate simultaneously, arranged in a fan, each containing an independent collimator, mirror, RPA and TOF optics. Figure 2.0-1 shows the relative location and orientation of TIDE and the PSI on the Polar spacecraft. The sensor field-of-view (FOV) is coplanar with the spacecraft spin axis and one edge of the FOV is aligned with the spin axis. In order to achieve this orientation of the FOV it is necessary to mount the entire instrument on a wedge-shaped platform so that the sensor is tipped up off of the mounting platform by 11.25°, as may be seen clearly in the sensor photograph of Figure 2.0-2.

Figure 2.0-1 Spacecraft mounting with coordinate systems.

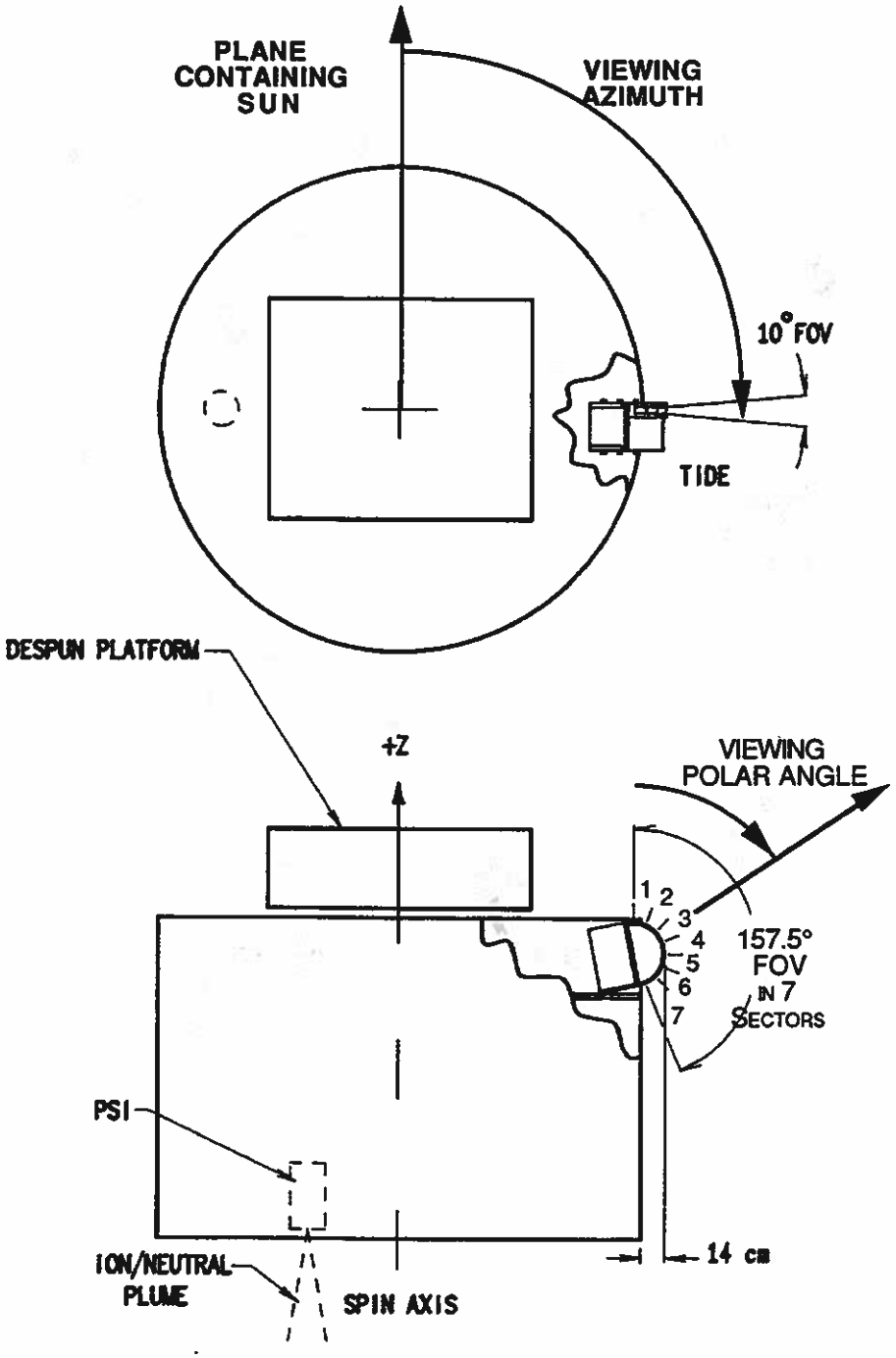

Figure 2.0-2 Photograph of sensor in flight configuration.

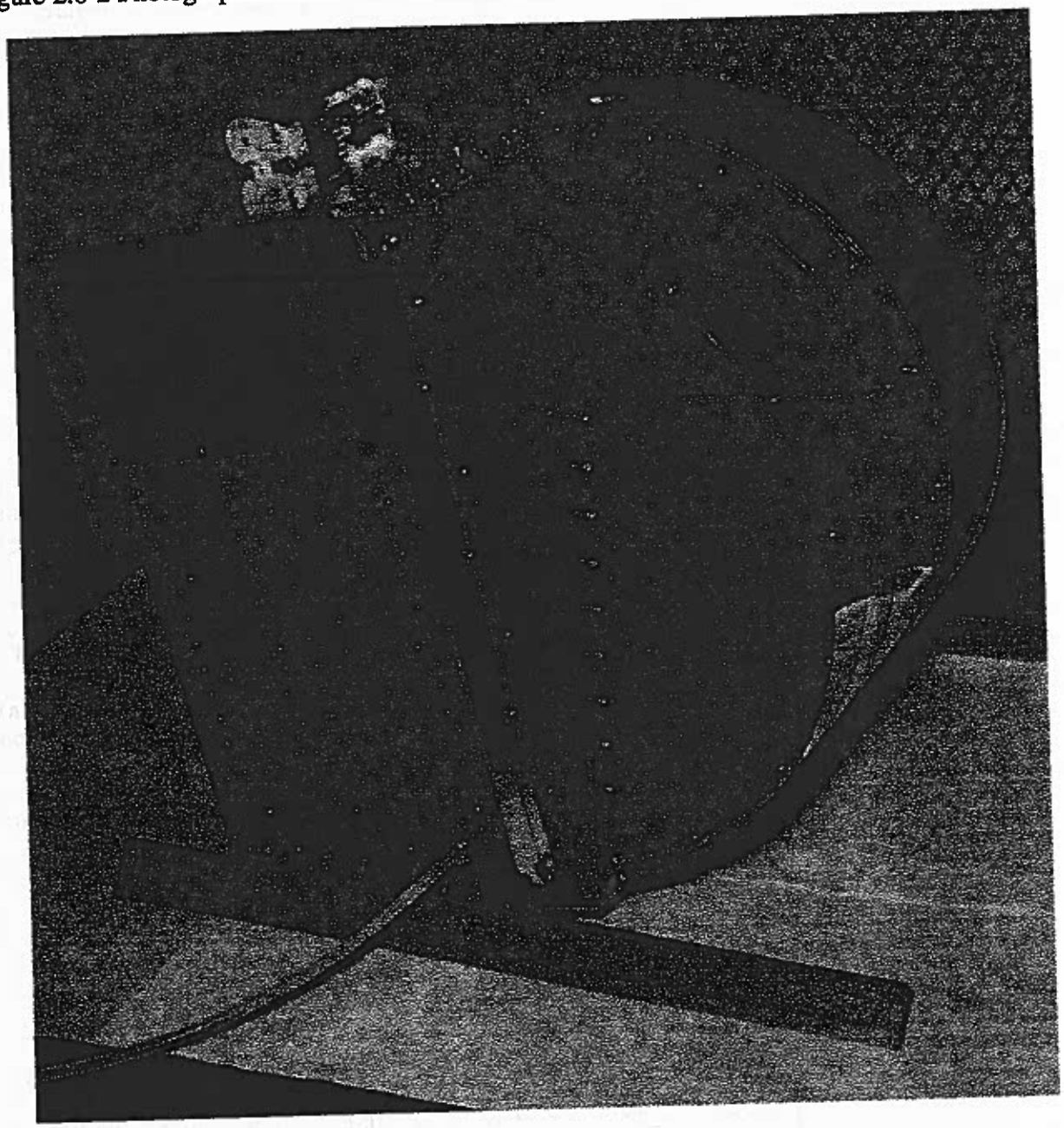

The electrostatic mirrors are preceded by collimators that restrict the angular acceptance of each aperture to that acceptable to the full optics system. Following the mirror is an RPA similar in principle to those of DE 1/RIMS. Coupled with each mirror and RPA system is a TOF mass analyzer and electronics similar to that developed for the LOMICS instrument on the CRRES mission. A pre-acceleration potential sufficient for penetration of carbon foils with small energy losses is used in conjunction with the low-energy front end optics. The large pre-acceleration voltage provides benefits in accommodating the large angular spread of ions delivered to the TOF unit by the focusing mirror optics. In addition, the TOF technique allows simultaneous measurement in multiple directions of all ionospheric species likely to be encountered along the POLAR spacecraft orbit (viz. H^+, He^{++}, He^+, O^{++}, O^+, and molecular species such as NO^+). The overall operation of the sensor optics system is illustrated in Figure 2.0-3, which shows an ensemble of simulated ion trajectories passing through the entire instrument. In this case, the aperture has been filled by initiating particles over a range of angles and energies.

Owing to its multiple look directions and simultaneous detection of all ion species, TIDE generates very high data rates (~ 35k data words per satellite spin period) so a powerful onboard DPU is required. This DPU is based on twin SA3300 radiation-hardened microprocessors, one to control the instrument, optionally performing data collapse and lossless compression, the other to perform onboard computations while queuing the data for telemetry. Other features of the TIDE design include built-in pulse generators for testing of amplifiers and TOF electronics, enclosure of the highly sensitive detectors and foils in a sealed housing with a removable aperture cover, and a shorting plug which prevents the accidental application of detector and TOF high voltages.

2.1. Basic Sampling Intervals

The Polar spacecraft spins at a nominal rate of 10 rpm. Because TIDE should give nearly three-dimensional (3D) sampling of velocity space, this spin rate determines TIDE's fundamental time resolution. During one spin period (6 s) the voltages on the mirror and RPA are swept 32 times in a pre-determined sequence of 32 voltage levels, giving 32 = 1024 samples from each of the 7 polar-angle sectors. The nominal azimuthal angular resolution is then 11.25° (32 energy sweeps per spin) which implies an energy sweep of 32 steps and an interval of 187.5 ms. Thus a nominal sample period is 6.00 s /1024 = 5.86 ms long. Ten percent of this period (586 μs) is allowed for voltage settling and data read-out so that the actual live time is 0.90 x 5.86 = 5.273 ms. In order to ensure synchronization between the TIDE goal of 1024 samples per spin and slight variations in POLAR spin rate (~ ±3% expected) the TIDE sample interval of 5.86 ms will be adjusted automatically on-board by up to ±7.5%.

Individual TOF events are accumulated in two parallel memories. Events corresponding to identified major ion species are accumulated in 16-bit registers with maximum (non-compressed) count storage of 65535. The maximum allowable count rate for these events is thus 1.24×10^7 c/sec which exceeds both the TOF processing and MCP count rate capabilities. The TOF event processing requires a nominal 3 μs giving a maximum TOF event rate of 3.3×10^5 c/sec for the entire TIDE sensor, corresponding to 1933 counts/sample. On the other hand, the MCP linear count rate response is limited (for a single plate) at ~ 3% of the plate bias current of ~ 10 μA. At a gain of ~ 10^7 the allowable input current per MCP is thus $3 \times 10^{-2} \times 1.0 \times 10^{-5} \times 1 \times 10^{-7}$ A = 3.0×10^{-14} A = 1.9×10^5 c/sec. This corresponds to a singles rate of 1187 c/sample per MCP or 8306 c/sample total events over all seven channels. All TOF events are also accumulated in a "direct event" memory, providing full TOF spectral resolution for each of the seven channels, but summed over all energy sweep steps and spin azimuths. This data is accumulated and reported over 32 spins or 192 sec, or 32764 basic samples. The accumulation registers for this data are allocated 32 bits each, which is well in excess of the most extreme requirements.

Figure 2.0-3 Sensor radial cross section with simulated particle rays.

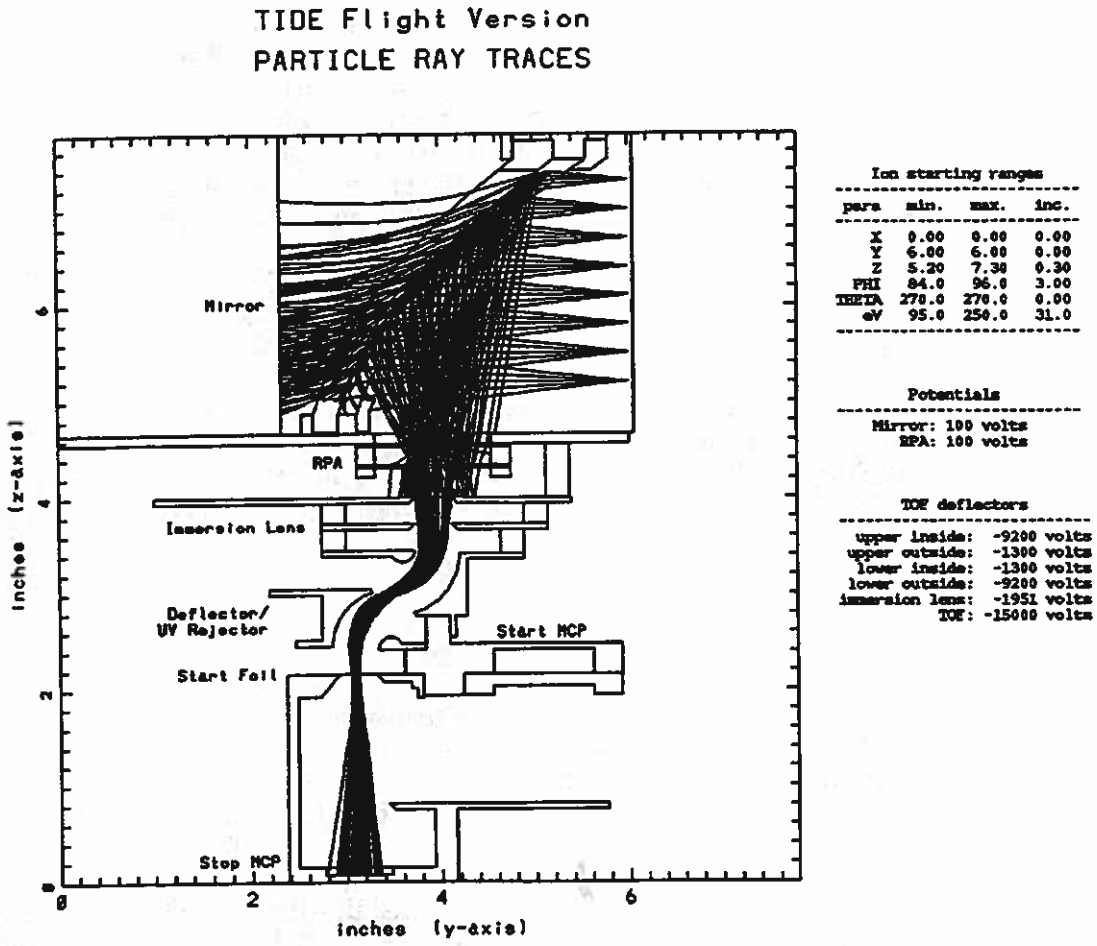

2.2. Energy Sampling

The nominal RPA bias range for TIDE is ~ 0.1 to 300 eV and the RPA voltage is controlled by a 12-bit DAC (73.2 mV resolution). The mirror potential is controlled as a fraction of the RPA potential by an 8-bit DAC over the range from zero to 100% (0.4% resolution). The RPA and mirror supplies are controlled by the active sweep table which is chosen from a menu of available tables, but may be modified by uplink. If the mirror table consists of a single value, the mirror is swept in proportion to the RPA and a fixed $\Delta E/E$ results. The current sweep table is always documented in the telemetry stream for unambiguous interpretation of the data on the ground. This is particularly important for the mirror supply values, which are controlled dynamically so as to prevent over counting of the detectors, as described below in the section on dynamic range

2.3. Mass Identification

The TOF spectrum results in two types of data: that binned into M/Q bins on the basis of TOF channel and "direct" events containing full TOF information, but unsorted by energy, spin angle, or polar-angle sector. The correspondence of TOF channels to specific mass peaks is determined by calibration. A preliminary mass calibration obtained in Dec. 1992, results in the binning given in Table 2.3-1. The location of peaks follows a nominal TOF equation, with an offset owing to electronic effects: TOF $\approx$ -20 + 39 $M^{1/2}$ ns. Because of telemetry limitations, full energy and angular distributions are telemetered only for the 5 most important mass peaks, as selected by means of an uplinkable mass lookup table. Minor species may be monitored by means of the Direct Event data, and the primary table may be updated based upon this experience.

Table 2.3-1 Preliminary mass peak locations

Species	M/Q range	TOF (ns)	Center (chan)	Width (chan)
H^+	1	19	14	8-20
He^{++} (H_2^+)	2	35	33	25-40
He^+	3-6	58	57	45-70
O^{++}	7-11	90	88	75-100
O^+	12-20	136	123	110-145
H_2O^+	17-20	145.5	140	135-145
Na^+, Mg^+	20-26	167	157	146-169
N_2^+, NO^+, O_2^+	26-41	193	232	210-255
Bkgnd	0.25	7-8	20	0-6
Bkgnd	21.1	145.1	185	180-190

2.4. Angle Sampling

2.4.1. Polar Angle Sampling

There are 7 polar-angle sectors on centers of 22.5°. The polar sector of origin for each TOF event is obtained from the TOF electronics as a 3-bit sector ID code. The TOF events from each accumulation are logged to the memory location appropriate to the polar sector in which it occurred.

2.4.2. Azimuth Angle Sampling

The energy sweeps of TIDE are phase-loop-locked to the spacecraft sun pulse and spin clock, which synchronizes 32 sweeps to each spin of the spacecraft. The TOF events from each accumulation are logged to the memory location appropriate to the azimuth sector during which it occurred. Each event is then logged in memory by incrementing the appropriate array location, resulting in an event distribution by energy, mass, polar angle sector, and azimuth angle sector.

2.5. Dynamic Range

The TIDE effective area is unusually large and nearly 100 times that of its predecessors. In some regions of the spacecraft orbit this may result in correspondingly high count rates at the TIDE detectors if measures were not taken to limit the exposure of the instrument detectors. Moreover, initial operation of the plasma contactor, prior to trimming its vernier bias supply, may result in large fluxes of Xe^+ ions reaching the TIDE aperture. DE 1/RIMS experienced count rates approaching 10^7 c/sec with a much smaller geometric factor, and suffered detector gain loss which was to some extent recoverable, but created difficulties in data analysis. A variable aperture feature is incorporated in TIDE to deal with this problem, along with the software required to implement automated operation of the aperture control when desired.

2.5.1. Sensitivity Adjustment

The combined action of the RPA and mirror potentials can be used to modulate the energy pass band and overall sensitivity of TIDE so as to limit the effective aperture of the instrument and thereby the count rates corresponding to a particular flux level. The action of the RPA and mirror intrinsically modulates the energy pass band, the angular aperture, and the effective area of the mirror which is passing ions to the TOF section, so that there is a multiplicative reduction of the geometric factor of the instrument. Consequently, the instrument sensitivity can be modulated over a very wide dynamic range by this technique. The mirror/RPA combination has an energy dependent geometric factor whose magntude is dependent upon one parameter, the ratio of the mirror and RPA potentials. This dependence has been extensively modeled using trajectory tracing codes, and is fully documented during calibration.

As illustrated in Figure 2.5-1, based on simulation, the ratio of the mirror potential to the retarding potential controls the the instrument energy (dE/Ebar) and angular (dA, dP) pass bands, and the effective area (AEPS). This adjustment may be controlled by commands from the ground or generated onboard by the DPU in response to high flux levels. The programmable power supplies which control these potentials have a resolution which ultimately limits the overall dynamic range of the sensitivity adjustment to approximately three orders of magnitude.

Implementation of this automatic sensitivity control is discussed below under Flight/GSE Software.

Figure 2.5-1 M/RPA energy-angle response from simulation of the TIDE optics.

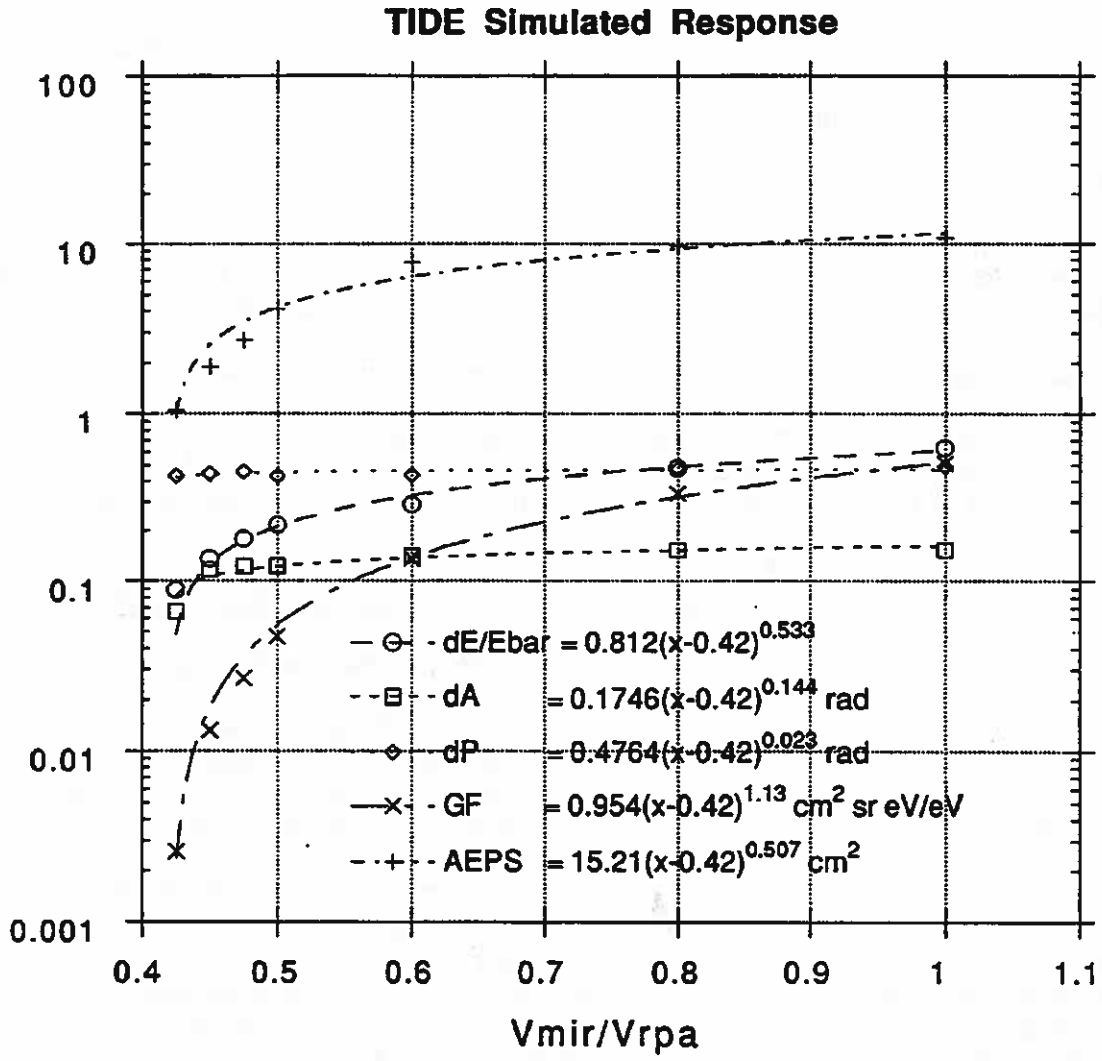

2.6. Performance Specifications

A fundamental design goal for TIDE has thus been to achieve a geometric factor much greater than that of previous instruments. However, an extremely large dynamic range of low-energy plasma fluxes is seen by a spacecraft in the course of an orbit from the ionosphere to the polar regions at several R_E altitude. DE 1/RIMS, for example, routinely experienced fluxes which ranged from well above detector saturation levels to low levels requiring long accumulations, to levels so low they could not be measured above an extremely low detector noise rate ($\leq$ 1 Hz). Therefore, an extended dynamic range is required in order to adequately sample both the lowest and highest density/flux regions. Unknown regimes await discovery by an instrument with higher sensitivity.

TIDE has also been designed to provide low-energy measurements which are differential in energy and angle as well as mass, with range and resolution adequate for the full characterization of features known to exist in the low-energy plasma populations. These features include polar wind flows of very high Mach number which were unresolved in angle or energy by DE 1/RIMS. Also included are flow features which appeared to DE 1 as crosswinds and could be lost between the RIMS fields of view due to insufficient angular coverage. Another important type of feature is the angle-dependent energy distribution of transversely accelerated ion distributions or ion conics, which required differentiation of the RIMS Retarding Potential Analyzer (RPA) curves with a resulting loss of signal relative to noise. TIDE produces intrinsically differential data.

Table 2.6-1 TIDE performance specifications

Parameter	Value
Energy Range	0.1 - 500 eV
Energy Resolution	5% - 100%, command selectable
Mass Range	1 - 40 amu
Mass Resolution*	$M/\Delta M = 4$ at 10% of peak height
Angular Coverage	instantaneous: 10° x 157.5° in 7 sectors per spin: 360° x 157.5° in 32 x 7 sectors
Angular Resolution	10° x 22.5°
Total Field of View	96% of 4π sr
Nominal Pixels per Image	35 k = 32Energy x 32Az x 7Polar x 5 Mass
Aperture*	1.0 cm^2 per 22.5° sector
Geometric Factor	0.10 cm^2 sr per 22.5° sector
Time Resolution 1 Sample	5.86 ms
Time Resolution 2D	1/32 spin period (0.1875 sec)
Time Resolution 3D	1 spin period (6 sec)
Dynamic Range	10^8 using variable $\Delta E/E$
RESOURCES:	
Mass	17.1 kg
Power	9.1 W
Telemetry	4.0 kbps

* Final values to be determined by calibration.

Time resolution is of primary importance on a rapidly moving spacecraft when it passes through localized structures. The larger the number of variables scanned during instrument operations, the more difficult it becomes to achieve adequate temporal resolution of phenomena. This problem is all the more serious for mass spectrometers. Recent prototypes of TIDE have used an electrostatic deflection system for angular scanning with a single mass analyzer section. It has become apparent during sounding rocket flights of TIDE predecessors (e.g., the SuperThermal Ion Composition Spectrometer or STICS) that this provides an imperfect solution to the problem

of angular sampling, placing extreme requirements on the stepping power supplies which sweep the angle, energy, and mass selection. TIDE solves this problem by implementing multiple independent angular detection channels, each equipped with independent TOF mass analyzers which monitor all mass species simultaneously. The only variable which must be swept using stepping power supplies is the ion energy. This can be accomplished in a time small compared with the POLAR spin period, so that single spin time resolution of the multi-species 3D distribution function is achieved.

The performance specifications of the TIDE instrument are summarized in Table 2.6-1.

3. SENSOR DESIGN

3.1. Energy and Angle Selection Optics

Figure 3.1-1 shows a cross section of a single 22.5° sector of the TIDE instrument. A total of 7 such sectors, with apertures on 22.5° centers, span a total FOV of 157.5°, as shown in Figure 3.1-2. The Collimator and Mirror configuration is shown in the first panel, while the RPA configuration is shown in the second panel. The individual sectors have polar angle response widths nominally equal to their spacing. In this section the specifications and design considerations relevant to the energy and angle selection optics are discussed.

Ions enter each TIDE aperture through a two-dimensional (2D) collimator system, which serves to limit the angular FOV as specified above. After traversing a field-free region they are incident upon a focusing electrostatic mirror system, reflected specularly through 90°, brought to a focus as they pass through a retarding potential analyzer (RPA), and then transmitted into a UV rejector/deflector system which in turn delivers them to the TOF analyzer. Those with energies below the mirror cutoff energy E_2 (nominally twice the mirror potential V_m) are reflected downward toward the RPA section. Ions with higher energies, as well as electrons and most UV photons, pass through the mirror and are absorbed in the baffle system beyond the mirror. As the reflected ions traverse the RPA, those with energies below the RPA cutoff energy E_1 are reflected while those with energies above E_1 are transmitted. The M/RPA combination transmits only ions with energies $E_1 < E < E_2$. Both the location and width of this energy pass band can be controlled in a programmed manner by the experiment electronics. The effective aperture of the mirror and width of its angular response are also reduced as the energy pass band is reduced.

The mirror itself plays an important role in the achievement of the large TIDE geometric factor, through its focusing geometry, which is similar to the action of focusing lenses and mirrors in optical telescopes. An electrostatic mirror for charged particles consists of a biased surface suspended behind a grounded grid, and the penetration depth is in general non-negligible relative to mirror dimensions. Focusing is accomplished through the implementation of a mirror geometry which differs slightly from parabolic in a functionally-significant way. The shape is derived from the requirement that incoming ions following parallel trajectories are directed through a common focal line. This focusing action translates a large collection area and small solid angle at the entrance aperture, to a smaller collection area/larger solid angle at the entrance to the TOF section. The large solid angle acceptance at the TOF entrance is attributable to the large attractive potential encountered by ions upon entry to that section.

Figure 3.1-1 Sensor radial cross section

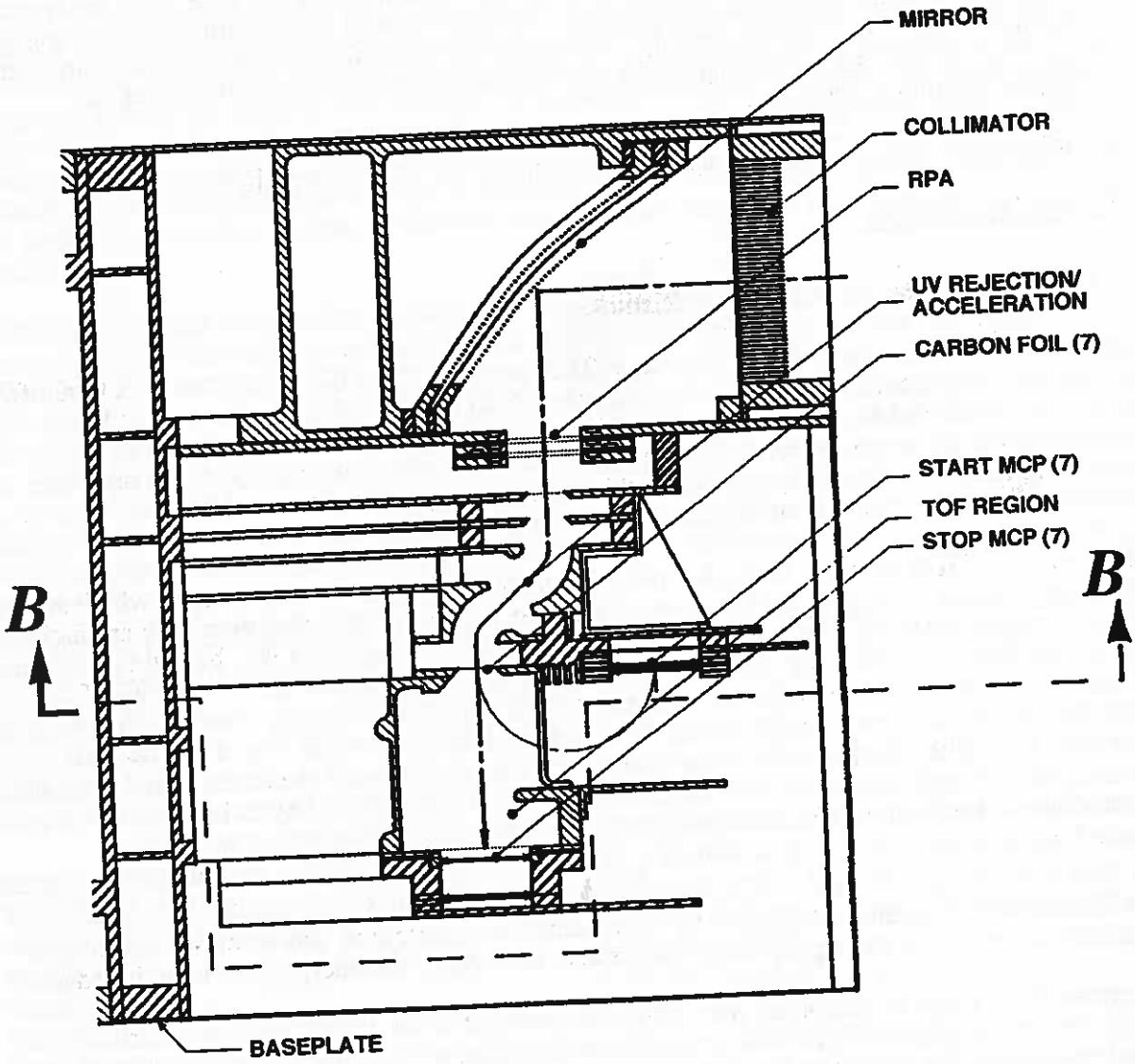

3.1.1. Mirror/RPA System

The TIDE electrostatic mirror/RPA system provides differential energy analysis, rejecting ions which are too energetic as well as those of insufficient energy. The actual energy response is asymmetric with a sharp cut-off on the low-energy side (due to the RPA), and a more gradual cutoff on the high-energy end (due to the mirror). Adjustment of the energy response width is used to control overall instrument sensitivity, as described below.

The corrected parabolic mirror consists essentially of two conducting grids separated by a constant spacing, and curved in the direction corresponding to spin azimuth as mounted on the spacecraft. The mirror is flat and non-focusing in the direction corresponding to polar angle relative to the spacecraft spin axis. The first grid encountered by entering ions is maintained at instrument chassis ground potential, while the second grid is at a programmable potential proportional to the energy of the ions which are to be selected. A third grid is mounted behind the two active girds, at the same potential as the reflecting grid, to smooth the potential in the vicinity of the latter grid. The grids are mounted so as to conform to a shape which brings to a focus all ions entering the mirror parallel to the optic axis. Ions passing the front grounded grid execute nearly parabolic ballistic trajectories between the grids, and exit the mirror at a point translated from that at which they entered, but in a direction which represents specular reflection with respect to a normal to the grid surface which coincides with the symmetry axis of the trajectory. Figure 3.1-3 illustrates the trajectory of the ions in the grid region. Based upon this trajectory, imposing the condition that all particles entering parallel to the optic axis pass through a common focal line leads to a nonlinear differential equation for the shape of the grid surface. This equation has been solved numerically for the grid shape.

Ion scattering is produced by encounters with the inevitable irregularities associated with the finite grid spacing, and it has been shown that scattering becomes a severe problem for $D/d < 10$, where D is the spacing between the front and center mirror grids, and d is the grid wire spacing. A design trade-off has been made between the fineness of the grid wire and its transparency. The corrected mirror can have D as large as desired and still maintain focusing, so this helps to reduce scattering for a fixed value of d. The final choices for these parameters are $D = 5.0$ mm and $d = 0.36$ mm.

Ideal optical mirrors are parabolic. This is the shape required to bring a parallel incoming photon beam through a focal line or point, in the cases of one or 2D focusing, respectively. The fact that the photons penetrate the mirror to a depth which is negligible in comparison to the system dimensions is essential to the simplicity of the parabolic focusing shape. In the case of an electrostatic mirror, the required focusing shape departs from parabolic and the shape and placement of the mirror, with respect to the desired focal line or point, is not intuitively obvious.

Figure 3.1-2a Sensor axial section: Collimators and Mirror/RPA

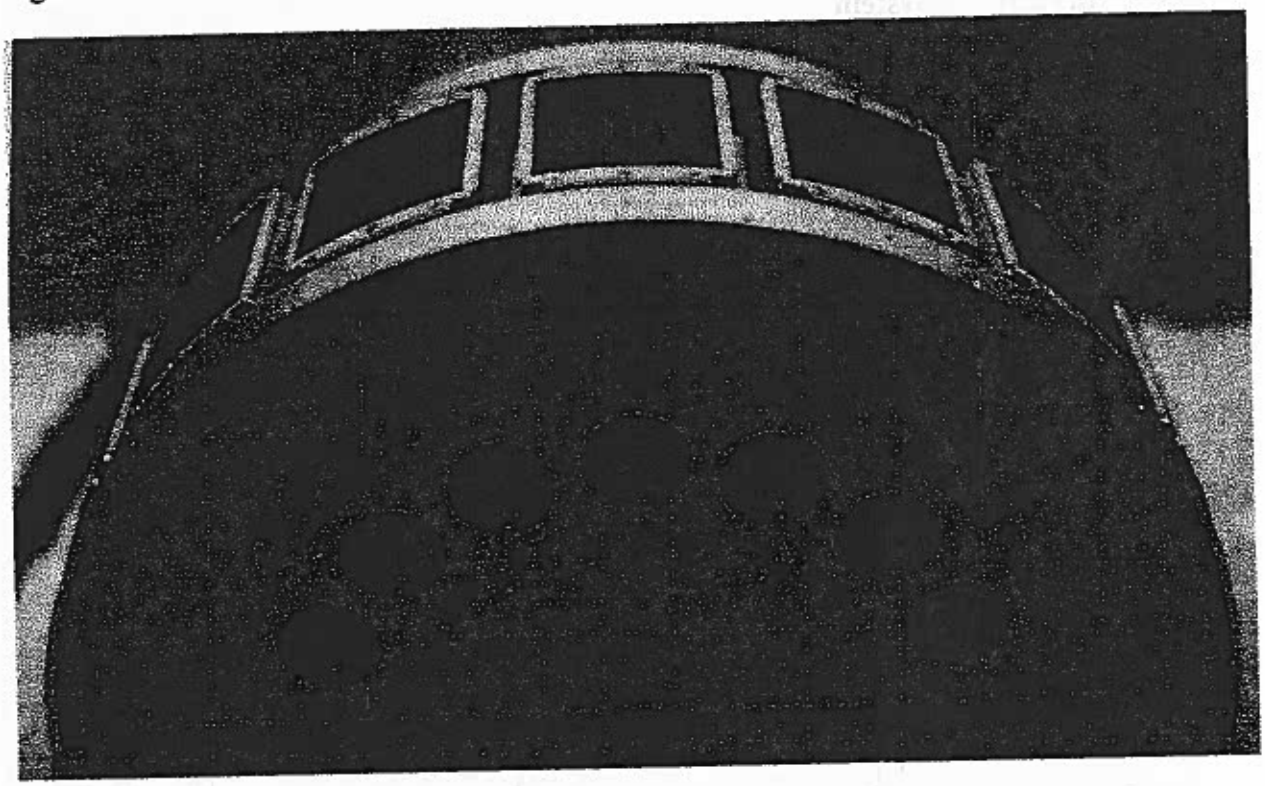

Figure 3.1-2b Sensor axial section: Mirrors

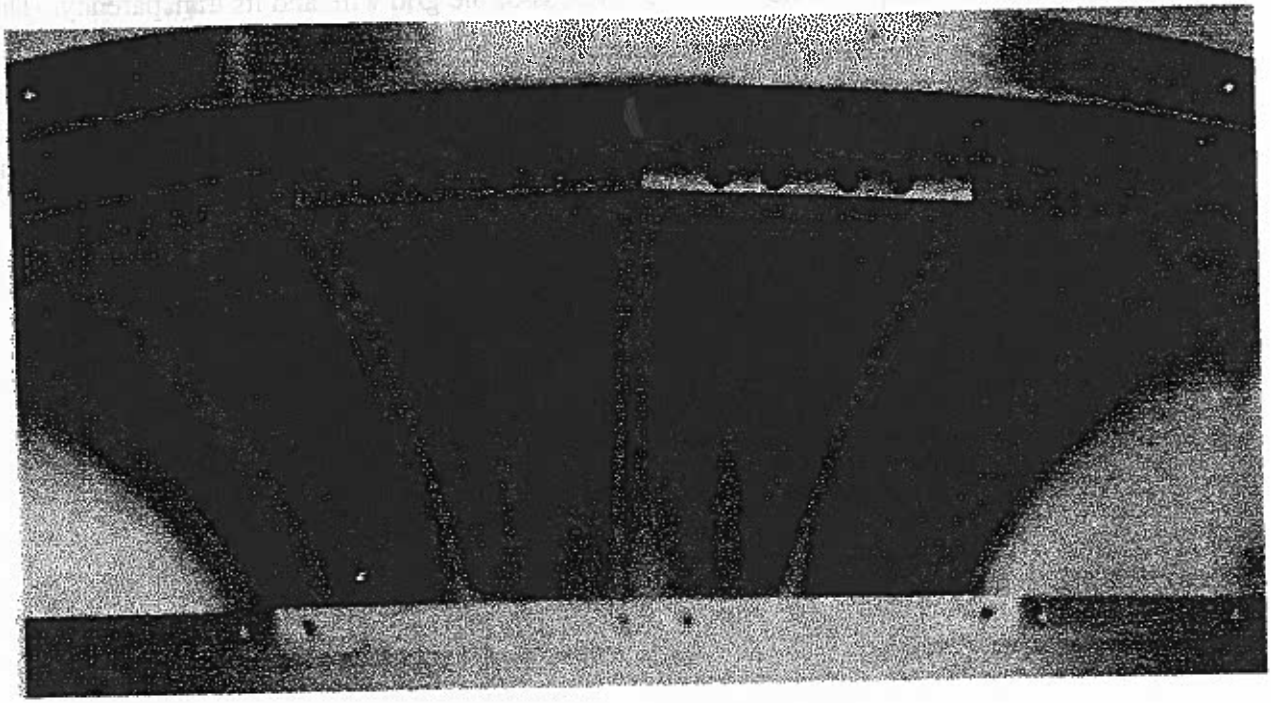

Consider the geometry shown in Figure 3.1-3. The tangent to the front (case potential) grid, at an arbitrary point along it, is indicated along with a charged particle trajectory. The rear (biased) grid is assumed to be located at a fixed distance along the normal to the front (grounded) grid surface. The electric field between the grids points from the rear toward the front grid. Particles incident from the right, moving along the negative "y" direction, feel no force until they pass through the front grid, apart from that due to grid fringe fields, which introduce some scattering. While between the two grids, these particles are under the influence of the applied electric field. Those particles with large enough velocity components along the field direction pass through the rear grid and are lost to the system. Those with smaller velocity along the field direction are turned by the field and directed toward the focal point, located at (0,f/2). We calculate the mirror geometry by determining the functional form of the front grid as y(x) under the following simplifying assumptions:

(a) The grid is considered to be locally flat. That is, the slope of the curve y(x) is considered to be constant over the region between a reflected ion's entry and exit points. This gives rise to a uniform electric field between the grids

$$\mathbf{E} = \frac{V_m}{D} \bullet \hat{\mathbf{n}} \tag{1}$$

where V_m is the commandable applied mirror voltage, D is the distance between the front and back grids, and n is the local normal to the front grid, pointing from back to front grids.

(b) The curve y(x) is considered to be near enough to parabolic that a perturbation from the parabolic case provides a solution to the derived differential equation.

The first assumption above, in combination with the focusing condition and simple particle dynamics within the electric field region, leads to the following differential equation for the curve y(x):

$$y = \frac{x}{2y'}((y')^2 - 1) + \frac{RD}{\sqrt{(y')^2 + 1}} + \frac{f}{2} \tag{2}$$

where R is the ratio of the nominally selected ion kinetic energy per charge to applied mirror voltage (E/(q V_m)), and y' is the slope of the curve y(x) between the points of particle entry and exit. We have chosen a boundary condition such that, in the limit as x approaches zero, the slope y'(x) should approach zero in the same manner as the parabolic solution does. That is,

$$\lim_{x \to 0}[y'(x)] = \frac{x}{f} \quad \text{and} \quad \lim_{x \to 0}[y(x)] = RD \tag{3}$$

This nonlinear first order boundary value problem for y(x) is solved through a perturbation technique, using the second approximation above, as described by Pollock et al. [unpublished manuscript].

In the TIDE instrument, the following parameters were selected for mirror construction:

Table 3.1-1 TIDE mirror design parameters

Parameter	Value
Focal Length	56.7 mm
Thickness	5.0 mm
Typical R (E/(qVm))	1.60

Figure 3.1-3 Mirror geometry

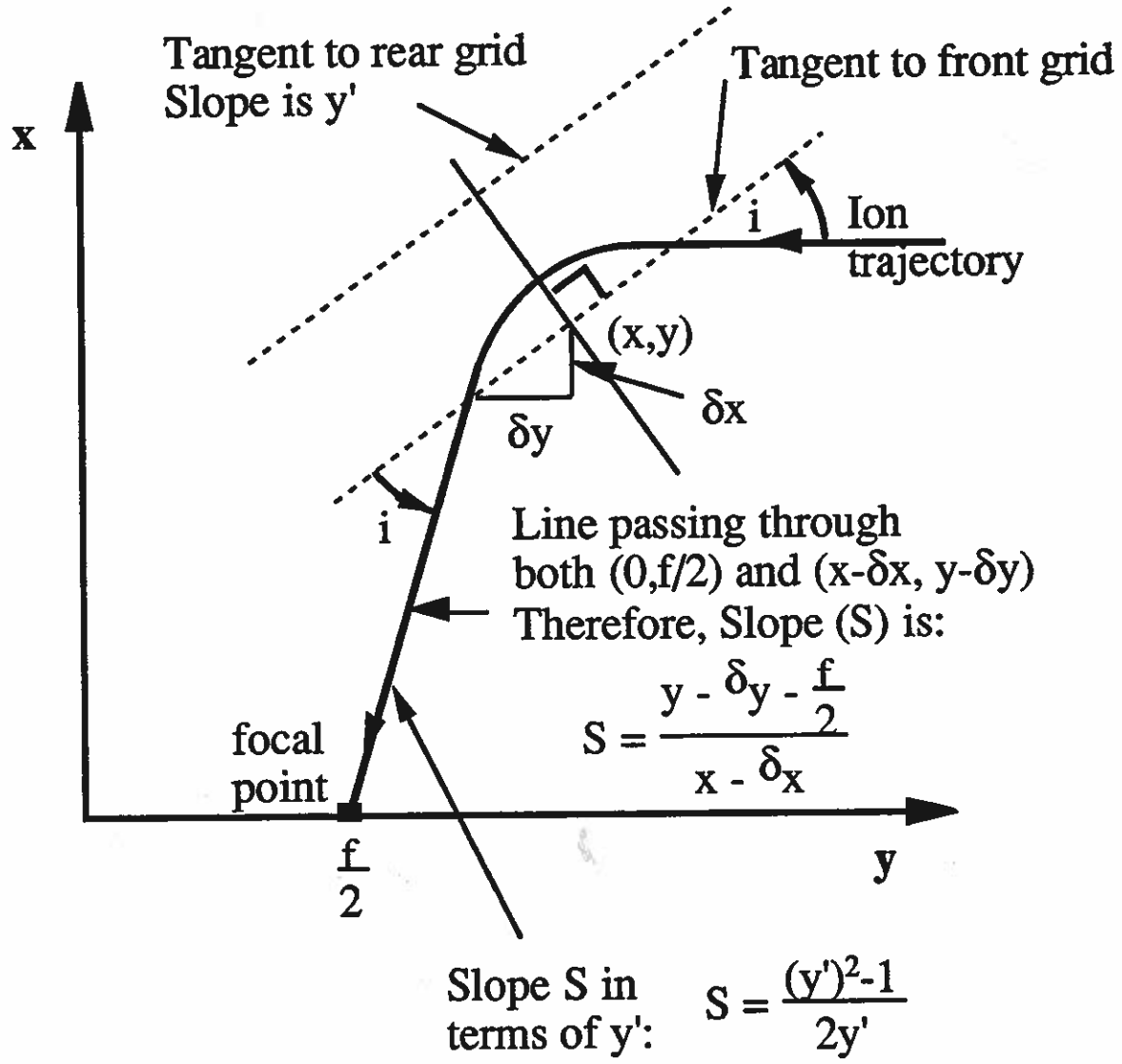

The basis for these choices is as follows: In order that the intergrid spacing be large compared with the grid wire spacing of 0.036 mm (necessary for small fringe field scattering effects), D was chosen to be 14 times as large. In order that the focusing direction angular response of TIDE be a nominal 10°, and in view of the 10 mm aperture of the TOF section, the focal length was chosen as 10 mm x tan(10°) = 56.7 mm. R is chosen to provide optimal focusing at an energy "typical" of TIDE operation, which may extend from approximately one to two times the mirror potential. Maximization of the geometric factor then indicates minimization of the focal ratio, i.e., maximization of aperture size or, equivalently, the range of angles subtended by the active mirror surface with respect to the TOF entrance. The focal ratio of the TIDE mirror apertures is approximately 1.5.

The RPA is a planar device consisting of four grids, as illustrated in Figure 3.1-1. The entrance and exit grids are connected to spacecraft ground, while the two retarding grids are biased at the commandable voltage V_{rpa}.

The electrical biasing scheme employed in this system is as follows: V_{rpa} is commanded with a 12-bit word through a digital-to-analog converter (DAC) providing a range of 0-300 V with 0.073 V resolution. V_m is commanded through an 8-bit DAC which is referenced to the output of the RPA DAC. In this way, the ratio (V_m/V_{rpa}) is directly commanded and can be controlled more precisely at the low end of the energy range than with independent commanding for both V_m and V_{rpa}. This directly controls TIDE sensitivity since the energy pass band (as well as the effective area and solid angle) is directly related to this ratio. The practical range over which TIDE's sensitivity can be varied is over two orders of magnitude, as described in the section below on test results.

3.2. Collimator System

Identical collimator assemblies are installed on each of the seven TIDE polar angle apertures. These collimators consist of two stacks of vanes, one collimating in spacecraft azimuth angle, the other collimating in spacecraft polar angle. The vane stacks are nested with the polar-angle stack in the outer position and the azimuth stack in the inner position. The vanes are positioned so as to eliminate all trajectories which would in any case be unacceptable to the mirror/RPA/TOF optics system; that is, all trajectories which lie outside the angular response and effective area of the instrument. This collimator approach is intended to minimize the number of extraneous particles and photons entering the instrument apertures, and particularly to eliminate such particles or photons which would otherwise be incident upon interior surfaces other than the mirror grids. In this way, the susceptibility of the instrument to extraneous particles and photons is minimized.

Collimation of 10° width in spacecraft azimuth is provided by means of parallel vanes which are 0.50 in. deep, 0.005 in. thick, and set on 0.044 in. centers. It should be noted that the M/RPA is designed for a commensurate angular response when its aperture is fully open. When the M/RPA is effectively "stopped down" by choosing a small ratio V_m/V_{rpa}, its angular response is reduced from 10°, vanishing as do the energy pass band and the aperture effective area.

Collimation of 22.5° in spacecraft polar angle is provided by means of vanes which are set nearly coincident with planes which emanate radially from the instrument symmetry axis. The layout of a single polar angle collimator stack is illustrated in Figure 3.2-1. The individual collimator channels each fully illuminate the focal plane (rejection/deflection system entrance aperture), while cutting off rays which would be incident upon the mirror frames or other interior structures. The oversized collimator openings are masked by a sheet metal aperture mask mounted at the rear of each collimator assembly (not shown).

Figure 3.2-1 Collimator system.

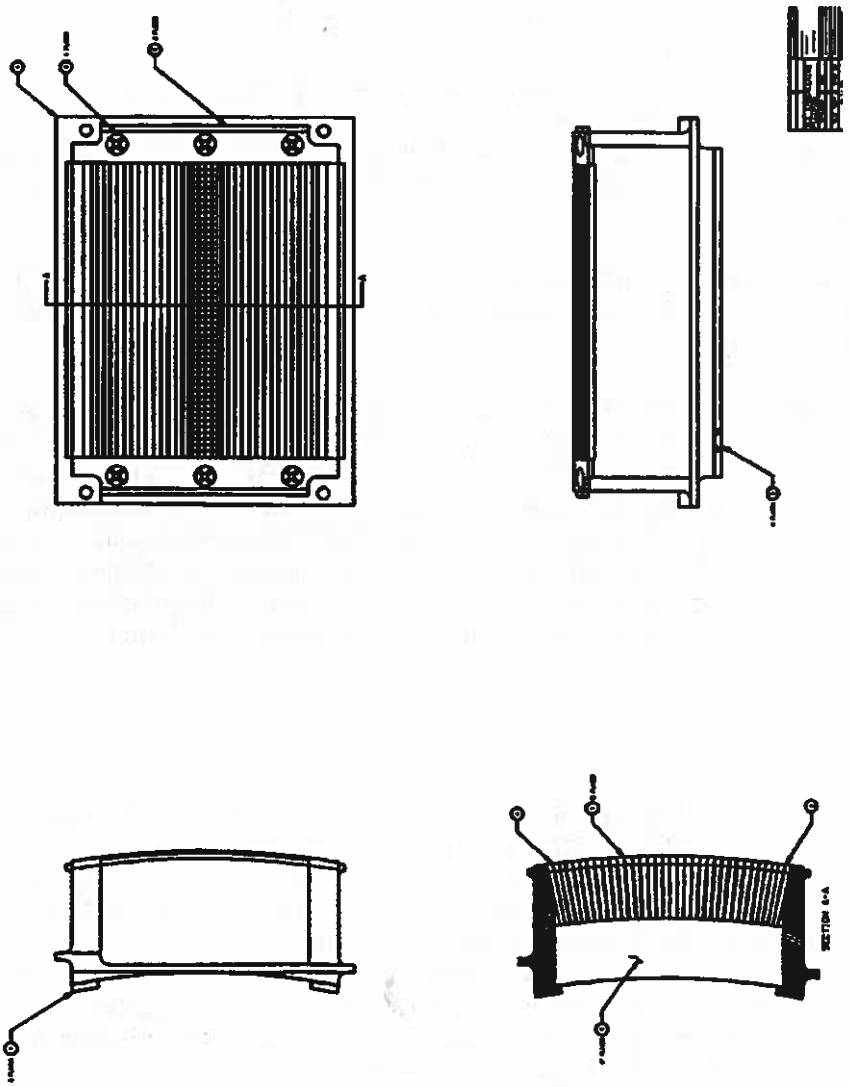

3.3. Mass Analysis Optics

EUV-induced electron contamination of the TOF system is a very serious concern for TIDE, for in contrast to the situation with parallel curved plate electrostatic analyzers, TIDE's relatively open Mirror/RPA system provides little rejection of EUV photons which are incident upon the mirror grid wires beyond the natural transparency of the grids (~90%). The grids have a reflectivity for such photons which is the complement of the grid transmission, approximately 10% for each of the three grids, multiplied by the reflectivity of the surfaces. This reflectivity is diffuse rather than specular due to the curvature and roughness of the electroformed surface. Nevertheless, measures have been taken in TIDE to introduce EUV rejection requiring at least two additional bounces between the grids and the TOF START foils. This is the purpose of the "S" shaped trajectories of ions passing from the M/RPA through the rejection/deflection system to the TOF section, as may be seen in the raytracing of Figure 2.0.2.

Displacement of the ion rays sufficient to cut off all direct paths from the mirror grids to the START foils is accomplished by means of electrodes biased so as to accelerate the ions and accomplish the two opposite deflections. The net translation is radially inward with respect to the symmetry axis of the instrument. The detailed configuration of this Rejection/Deflection system was developed by means of iterative potential solution and raytracing with the goal of accomplishing a deflection and straightening of the ion rays with as little dependence on starting energy as possible, over the energy range 1-300 eV. The result is effective in rejecting EUV photons and in preserving the bundle of ion rays.

Ions passed by the mirror/RPA, and accelerated by the -12 kV potential as they pass through the Rejection/Deflection system, are incident upon an extremely thin ($\leq 1.0\ \mu g/cm^2$) carbon foil suspended on an electroformed grid over an aperture measuring 10 mm x 25 mm. Each ion incident upon the foil creates one or more secondary electrons of a few eV energy, emitted from the rear of the foil as the ion passes through. In the foil, some of the ions are charge exchanged to neutrals and suffer some degree of energy loss and angular scattering, but continue generally along their trajectories toward the first stage of the STOP MCP detectors, arriving with a time delay appropriate to their mass/charge. Electrons produced by the first stage of the STOP MCPs are accelerated by the -12 kV potential onto the remainder of the MCP stack where a TOF STOP pulse is generated.

The electrons produced at the START foil are accelerated by the potential distribution inside the TOF analyzer. As a result, they travel sideways out of the ion flight path and are collected at the START MCP detector, which is biased at a potential more positive than that of the START foil, after a delay which is negligible in comparison with the ion time of flight from START foil to STOP foil. Other surface potentials in the vicinity of the START foils are designed so as to insure that a large fraction of the electrons emitted by the foil are detected. Sample computed electron trajectories are illustrated in Figure 3.3-1.

Analog electronics are used to measure the time elapsed between the START and STOP TOF pulses by charging a capacitor with a constant current source. Typical flight times vary from ~ 10 ns to 300 ns, depending on the ion species. Variations in incident ion energy (0 to < 300 eV) are negligible compared to accelerated ion energies of 12 keV so that ion TOF is largely independent of incident ion energy. Further details are given below in the section on electronic design.

Figure 3.3-1 START electron collection optics.

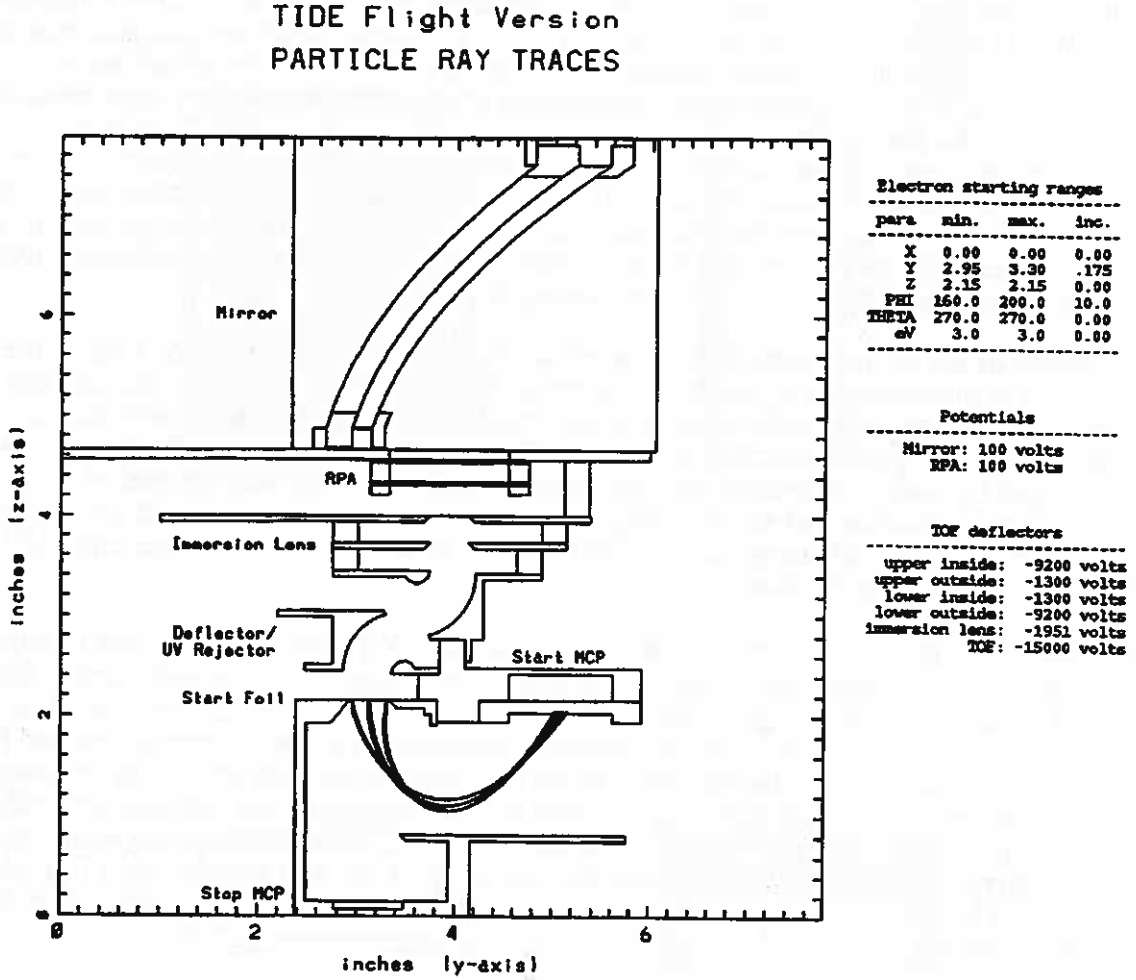

3.4. Microchannel Plates

3.4.1. General

The mechanical design of TIDE is such that the active optical image plane consists of an annular section of 157.5° extent. The individual START and STOP MCPs are arranged to sample the 157.5° annular sections (Figure 3.4-1). The particle optics are configured to deliver the bulk of the particle flux to standard 1 in. circular microchannel plates, which are used throughout for economy and ready availability.

To maintain high pulse S/N, the detector pulses are preamplified by simple emitter followers collocated with the MCP stacks on high voltage boards inside the sensor. These robust signals are then routed to the TOF electronics section for discrimination and processing.

3.4.2. Microchannel Plates

TIDE detectors consist of stacks of 3 individual microchannel plates (MCPs) stacked in so-called Z-configuration with their bias angles set in opposite directions (hence the term "Z") to permit high multiplication gain without ion feedback. Since seven polar view directions are desired there are fourteen stacks of MCPs arranged in seven sectors with each sector consisting of a START-MCP stack and a STOP-MCP stack. Limits on available power restrict the MCP stack resistance to
~ 300 MΩ per stack, which determines MCP strip current and hence maximum counting rates.

Because of the design of the TOF circuitry it is required to have an MCP stack that reliably delivers a gain of $>1.5 \times 10^7$ at the end of the POLAR mission (nominally 2 years). An MCP "Z-stack" of 3 individual plates is used to provide the necessary gain with sufficient reserve. The power supplies for the MCP high voltage bias have 256 levels set by ground command so that gain can be adjusted in flight. The supplies power the MCPs in parallel and therefore they must be set to ensure the gain of the lowest-gain MCP is $>1.5 \times 10^7$. (The dynamic range of the TOF amplifiers is sufficient to handle the variation in MCP pulse heights that results from this requirement.) Thus the gain of the MCP Z-stacks is "reasonably well" matched to within ±20%.

3.4.3. Mechanical Characteristics

Table 3.4-1 Microchannel plate mechanical specifications

Parameter	Value
Diameter	25.4 mm
Active Area Diameter/Shape	18.0 mm, as near circular as possible
Thickness	0.5 mm
Configuration	Z stack, 3 plates with opposed bias angles
Channel Size	12.5 μm
Bias Angle	> 5°

3.4.4. Electro-Optical Characteristics

Owing to the limited rate at which the TOF circuitry can process events, the maximum useful input count rate is $\sim 5 \times 10^5$ c/sec on any given MCP stack. At a gain of 1.0×10^7, and assuming that the maximum fraction of the strip current available to supply output charge is 10%, this corresponds to a required strip current density of >8 μA, which is met by the requirement stated in Table 3.4-2.

Table 3.4-2 Microchannel plate electro-optical specifications

Parameter	Value
Plate Gain	$> 10^3$ per plate
Z Stack Gain	$> 1.5 \times 10^7$
Z Stack Pulse Height Distribution	FWHM ≤ 100% (Δq/q)
Bias Current	10 μa @1000 V ± 10%
Dark Noise	< 10 Hz/cm^2

The MCPs should be of "first quality" without hot spots that could give rise to significant noise in the individual START and STOP measurements. Because this is a space flight instrument and there is an irreducible radiation background contribution in space that amounts to ~10 $cm^{-2}s^{-1}$, we require the MCP stages to have background at or below this level at nominal gain with practical discrimination levels.

In-flight calibration of the MCP gain is not directly possible. An internal pulse generator incorporated in the TIDE electronics is used to stimulate the amplifier discriminator chain of each MCP to determine that pulses are accepted above a preset threshold. It is possible to boost MCP gain as required to maintain sensitivity, as described in the HV power supply section.

3.4.5. Handling

MCPs are handled under cleanroom (Class 1000 or better) and UHV conditions. They are stored in special containers in a high purity N_2 atmosphere. The TIDE instrument has not been constructed so as to minimize the use of organic materials. However, those organic materials that are used, such as plastics, conductive and non-conductive epoxies, have been limited insofar as possible to those identified as MCP compatible by McComas and Bame (*Rev. Sci. Instrum., 53*, 1490 (1982) and *Rev. Sci. Instrum., 55*, 463 (1984)). Once the TIDE sensors are assembled, the entire sensor with MCPs is stored in special containers under high purity N_2 purge.

The required on orbit lifetime is 3 years (10^8 sec) at ion fluxes which can reach 10^9 cm^{-2} s^{-1} in certain regions. The total flux is controlled by adjusting the sensitivity of TIDE electronically. In this way we can limit the total lifetime fluence of ions. If the lifetime of the plates is estimated at $10^{12\text{-}13}$ counts, then the average rate must be limited to $10^{4\text{-}5}$ c/sec per plate stack. In fact, software control of the TIDE aperture is used to insure that rates are never allowed to go above a limit chosen to prevent hard saturation of the TOF circuitry, approximately 10^6 c/sec summed over all seven channels. Running sums of total counts and mean rates are tallied routinely for each MCP stack, and used to further throttle the instrument aperture if necessary.

The MCPs are baked to remove water vapor and burned-in to $>10^9$ counts cm^{-2} in a specially designed UHV system. The burn-in follows procedures developed at LANL for channeltron burn-in. Electrons from Ni^{63} are used for this purpose. It is essential that the MCP stacks be burned in as Z-stack units so that the third plate in the stack receives sufficient scrubbing.

Figure 3.4-1 Sensor axial section: START/STOP detectors.

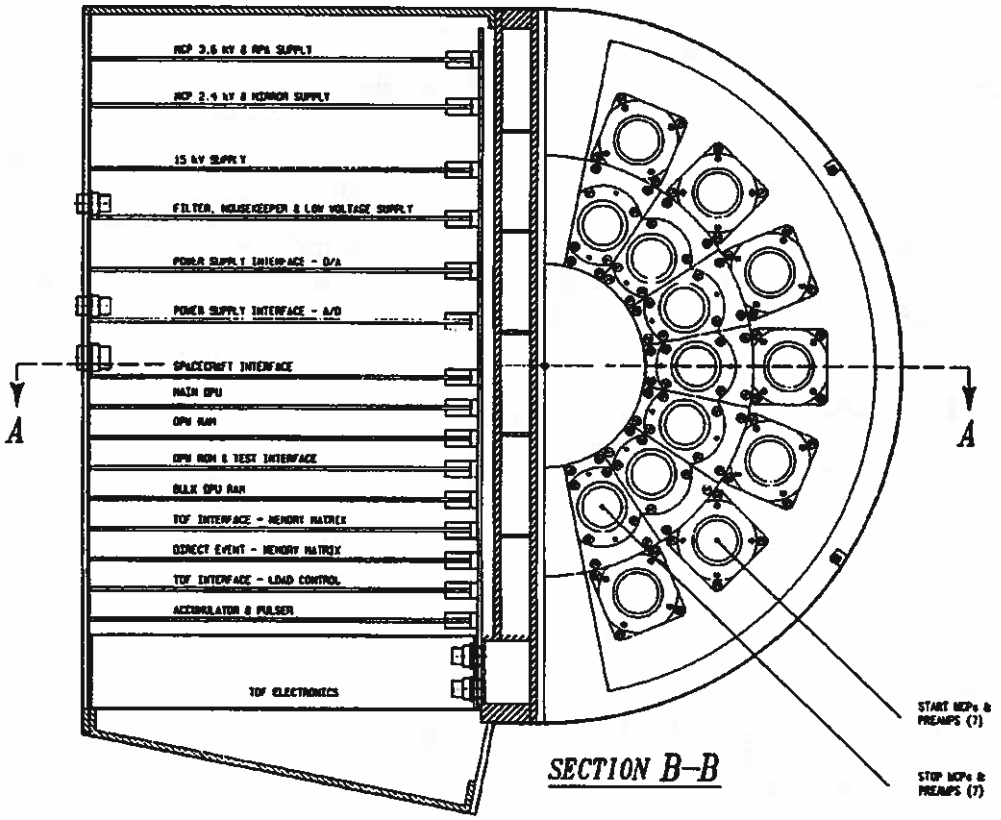

3.5. Preamplifiers

A single preamplifier consists of a bipolar PNP transistor connected in the common-collector (emitter-follower) configuration, as shown in Figure 3.5-1. Power to bias the amplifier is provided by the center conductor of the coaxial cables used to connect the preamplifiers to the TOF electronics module. This conductor serves as both the signal and bias connection for the preamplifiers. The signal connection is ac-coupled into the TOF electronics module. Protection circuitry for the amplifier consists of a 50 Ohm collector resistor, back-to-back diodes from base to ground, a clamp diode on the emitter output, and a 100 Ohm series resistor in the base connection. The amplifiers provide a voltage follower function that buffers the MCP anodes in order to drive the 50 Ohm coax that connects the preamplifiers to the TOF electronics. The common-collector configuration and the use of an RF PNP transistor yield good signal fidelity for the high-speed MCP pulses present on the anodes. The internal pulser system allows stimulation of the preamplifiers for system checkout and test of data handling software.

Figure 3.5-1 Preamplifier schematic/layout diagram.

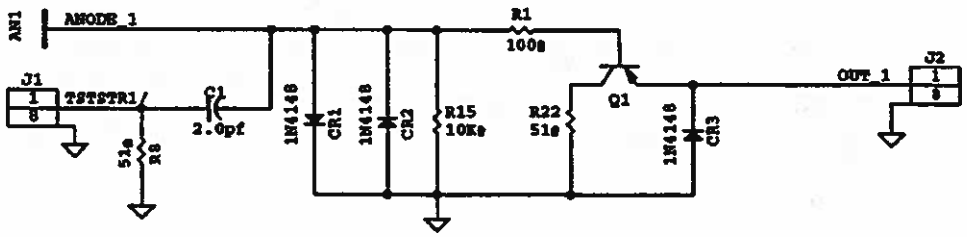

4. MECHANICAL DESIGN

4.1. Interfaces

Figure 4.1-1 shows two views of the TIDE unit including instrument dimensions and location of the FOV. Note that sensor and electronics are integrated into a single unit. Routine access to the sensor components requires removing only the outer cylindrical cover. Routine access to electronics boards requires removing only the rear panel on the electronic compartment. Figure 4.1-2 shows a perspective drawing of the instrument and its orientation on the s/c.

4.1.1. Thermal Design

The operating and storage limits predicted (Pre-Verification issue of Reduced Thermal Model for the TIDE, SwRI document 3348-RTM-1 Rev.B) for the TIDE electronics are:
Non-operating: -24 °C to +44 °C Operating: -3 °C to +38 °C

The operating and storage limits predicted (Pre-Verification issue of Reduced Thermal Model for the TIDE, SwRI document 3348-RTM-1 Rev.B) for the high voltage TOF sensor components are more extreme, because they are thermally well-isolated from the electronics section of the package:
Non-operating: -37 °C to +26 °C Operating: -15 °C to +50 °C

4.1.2. Exterior Surface Finishes

The outer surfaces of the instrument that are in contact with the plasma are electroless nickel plated. The collimator vanes are beryllium copper. Selected optical surfaces within the TIDE sensor are blackened with cupric oxide black (Ebanol-C) to reduce scattering and internal reflections. Estimated UV reflectance at 45° incidence is 1%.

4.1.3. Packaging and Purging

The sensor is designed so that all sensor optical elements are sealed by overlapping joints to normal machining tolerances by the sensor housing. The seal and housing serve as a diffusion barrier against chemical, water vapor and dust contamination of the sensor. The MCPs and carbon foils are particularly sensitive to hydrocarbon contamination and are also strongly hygroscopic. The sensor housing is kept backfilled with high purity nitrogen. The instrument aperture is covered with a tightly fitting cover that is a RED TAG item to be removed before flight. There are purge inlet and over pressure relief valves in the sensor and electronics boxes.

TIDE is fitted with a deployable aperture cover which protects the instrument from contamination during launch within the Delta vehicle's shroud. This cover is a conductively coated (copper) kapton strip. It is unlatched by means of a thermal wax actuator, and is reeled into a spool by a double negator spring mechanism which is very reliable because the double negator spring mechanisms provide nearly constant retraction force.

4.2. Collimators

The polar-angle sectors have a resolution of 10° x 22.5° FOV provided by collimation using 2 sets of thin baffles that form a system of orthogonal slits one behind the other. The outer set of baffles provides 22.5° collimation. These are 0.500" deep with nominally 0.077" wide slots and 0.011" thick baffle walls. Azimuthal collimation of 10° is provided by the inner set which is 0.500" deep with 0.0440" wide slots and 0.005" thick walls.

Figure 4.1-1 Exterior dimensions and mounting.

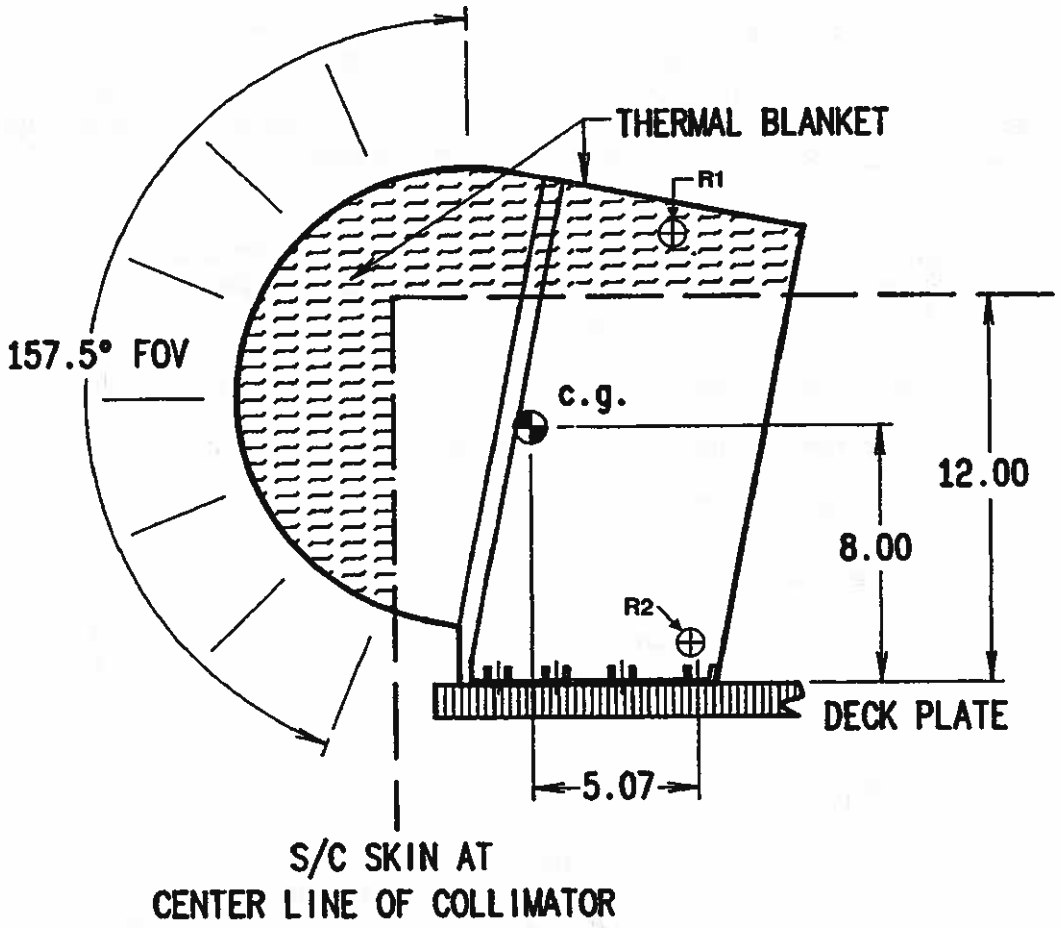

Figure 4.1-2 Perspective view of exterior features.

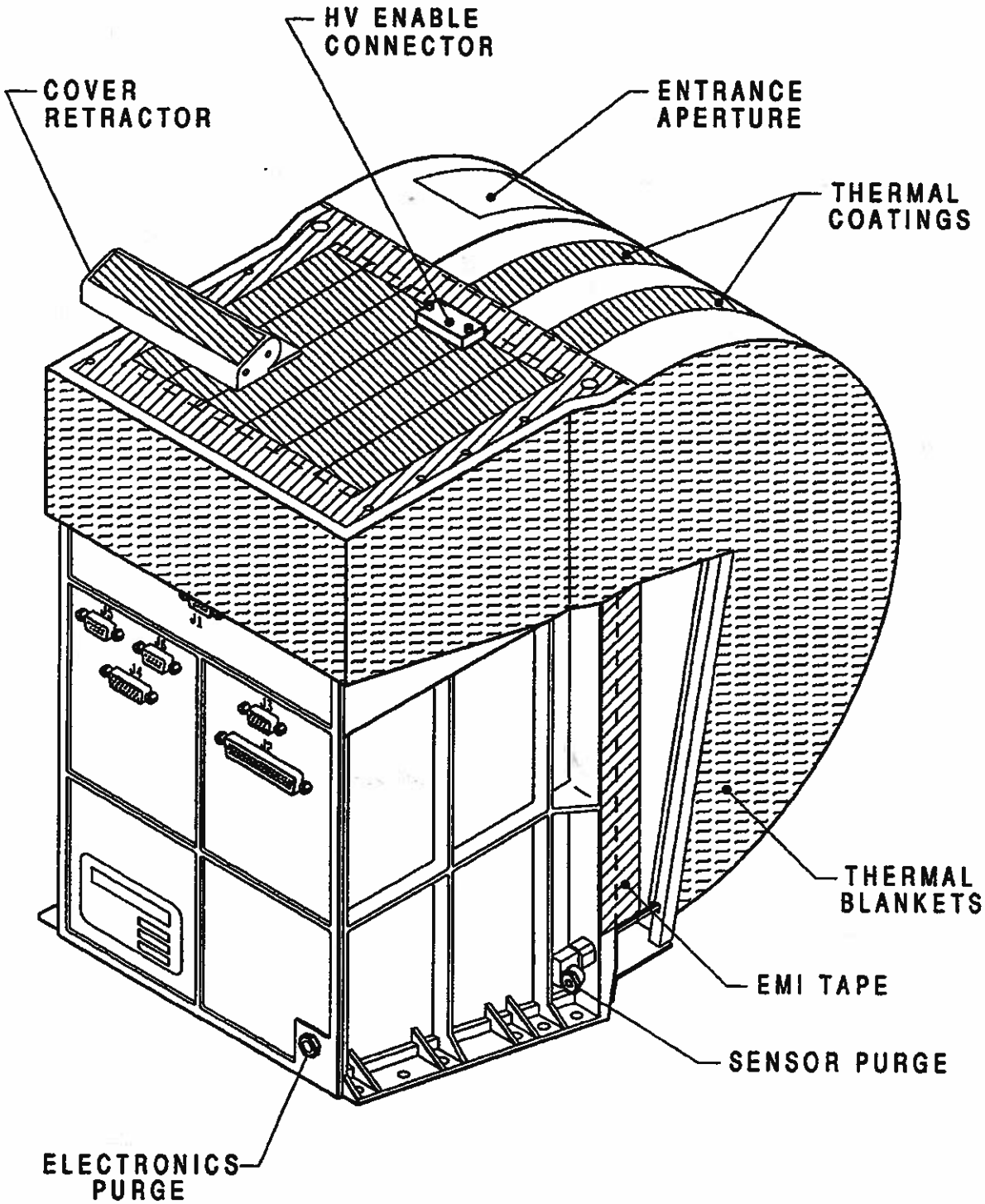

4.3. Interior Structure and Surface Finishes

To keep the TIDE mass within the proposed mass budget, a structural design has been adopted in which a major structural role is played by a built-up noryl optics bench/baseplate, supported upon the aluminum electronics enclosure and in turn, supporting all of the sensor optics components. While a conducting honeycomb structure would have been preferable, this design combines the functions of structural support and high voltage insulation in a single element, saving a considerable amount of mass.

The mirror/RPA assembly is cantilevered from the noryl baseplate on a semicircular aluminum baseplate assembly of its own. All interior metallic surfaces of the M/RPA are bead-blasted aluminum. The mirror and RPA grids themselves are electroformed nickel, and the insulating components are of Noryl.

The deflector/UV rejector components are polished aluminum electrodes, noryl insulating parts, and two toroidal deflection electrodes which are polished aluminum with an Ebanol-C blackening treatment applied. Polished aluminum is used throughout the TOF sensor assembly where scattering of light and particles is not a problem or where high voltage breakdown is a potential problem. All structures interior to the TOF unit of TIDE are carefully finished by polishing to eliminate all roughness and sharp corners. All fasteners have smooth finishes and have been chosen to maximize clearances between elements which are separated by high voltage in operating conditions. The high voltage components have been insulated from each other by Noryl separators which are assembled using Nylon screws.

The mounting arrangement of sensor interior components on the main baseplate assembly is shown in Figure 4.3-1. The sensor is shown in this figure with the M/RPA assembly at the left of the figure, and with the cover removed from the TOF section. From right to left in the figure, one sees the STOP detectors (STOP preamp board is removed), the TOF free flight unit (with "skirt" removed), the START board and detectors, the deflector/UV rejector assembly, and the collimators/apertures of the M/RPA assembly. All of these are approximately axisymmetric but truncated by the baseplate itself.

Along the very top edge of the sensor baseplate, as shown in Figure 4.3-1, the connectors which carry detector signals to the TOF electronics may be seen. Barely visible protruding slightly from within the center of the TOF free flight unit is a tray which holds the resistor divider responsible for producing the various potentials applied to the deflector/UV rejector electrodes. At the right edge of the baseplate are the high voltage feedthroughs for detector and accelerating potentials.

4.4. Radiation Shielding

Radiation shielding for TIDE is made up of structural components of the sensor and electronics housing ("box") plus materials added to the TIDE box as supplementary shielding. Table 4.4-1 summarizes all elements of TIDE housing and additional shielding with thickness given in mils of aluminum equivalent.

GE developed a 512 ray radiation dose model for POLAR that divides the unit sphere into 512 regions of equal solid angle. The 512 ray model was applied to TIDE to calculate dose at two locations, R1 and R2 (indicated in Figure 4.1-1). R1 is located at the top of the TIDE box, 1 inch inside the skin; R2 is located deep inside the electronics unit near the TOF board. A simple model of the TIDE box (40 mils Al walls for electronics box, and 116 mils equivalent in the direction of the sensor) was used to calculate 351 krads at R1 inside their version of TIDE and 162 krads at R2 (GE AstroSpace Doc. GGS-RAD-0003 dated 1/9/90).

Figure 4.3-1 Sensor baseplate assembly layout.

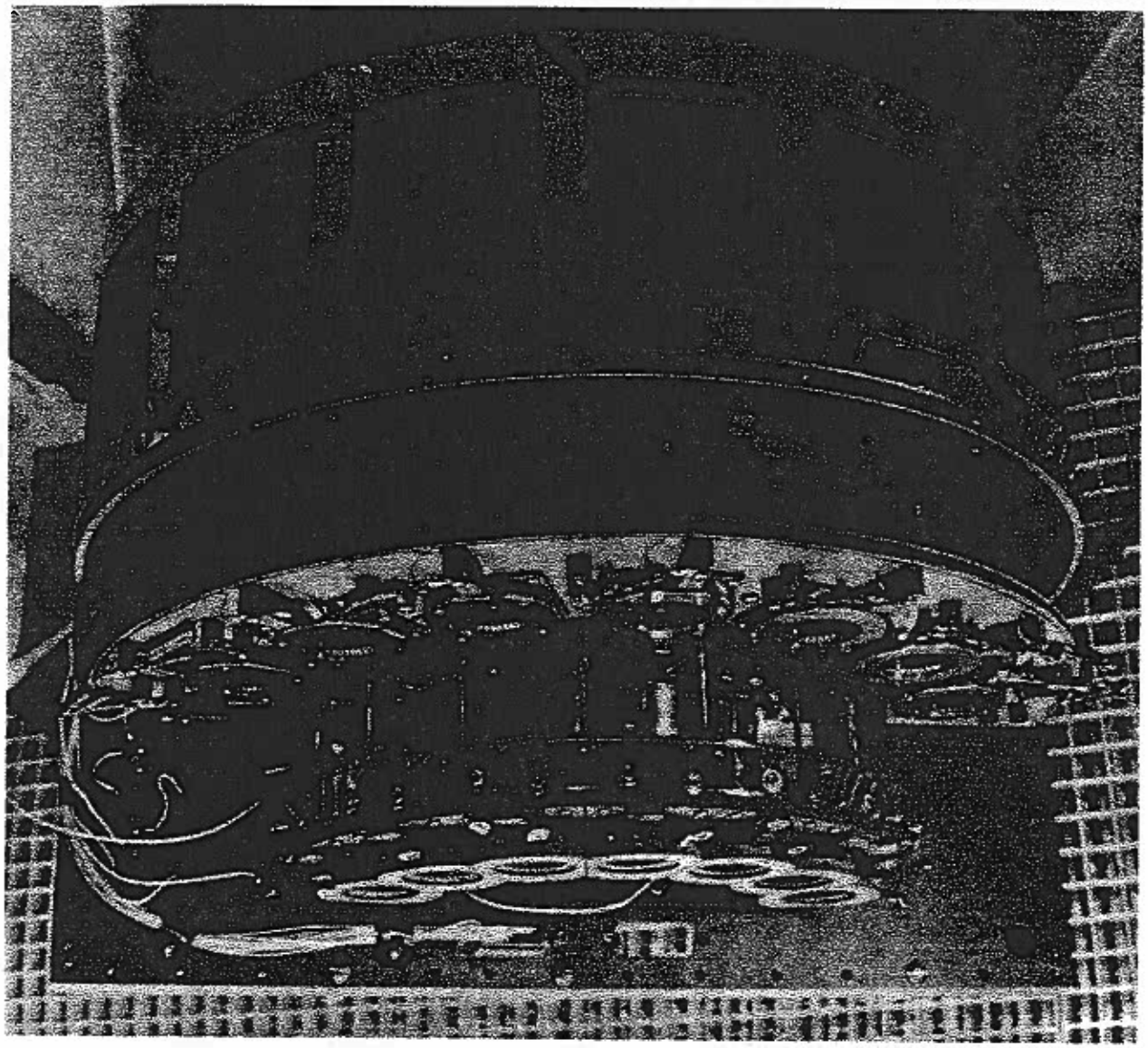

Additional radiation shielding was placed around TIDE (see Table 4.4-1), bringing the average shielding thickness (including slant path effects) up to > 200 mils Al equivalent. The added attenuation varies from a factor of 5 to a factor of 70 depending on direction (Table 4.4-2).

The effective dose inside TIDE with this added shielding was calculated by averaging over the 512 rays of the GE model to obtain 16 sets of ray bundles (cones of equal solid angle), each at a different polar angle relative to the S/C + Z axis. The final GE values were reproduced within 15%, on the high side.

The GE dose values were then multiplied by attenuation factors calculated from the POLAR dose-depth curve dated 6/21/89 for a 3 year mission, taken from the GE/POLAR GIIS. The result shows a total dose at R1 of 41 krad (Table 4.4-3). A similar calculation for R2 (near the LANL TOF box) would yield a significantly lower value. Thus for bulk electronics rated at 100 krad, the TIDE design provides a radiation dose margin (RDM) of 2.5 in compliance with usual NASA requirements for RDM $\geq$ 2.

A few TIDE piece parts (A/D and D/A converters) are particularly vulnerable. They were placed at the center of the electronics housing with individual spot shielding (Table 4.4-1). The 7820 A/D will see a dose of 0.6 krads while the 7623 D/A will see 0.7 krads. This estimate was made by a slightly different method, namely interpolation of the GE shielding tables. This was judged more accurate than the attenuation method for very low dose estimates.

Table 4.4-1 Radiation Shielding Summary

No.	Item (TIDE Dwg. No.)	Material	Thickness (inches)	Equiv. Al thickness (mils)
1	Electronics box side walls -(3348407, 08)	Al	0.100	100
2	Electronics box back wall - (3348409)	Al	0.032	32
3	Electronics box side wall shield - (3348438)	Al	0.050	50
4	Electronics box top panel -(3348424)	Al	0.150	150
5	Sensor baseplate - (3348470)	Noryl GFN3	0.250	125
6	Motherboard - (33481 66-01)	Fiberglass/Cu	0.063	60
7	PC boards - (-------)	Fiberglass/Cu	0.063	95
8	7820 A/D cover - (3348478)	Al	0.160	160
9	7623 D/A cover - (3348473)	Al	0.050	50
10	Support brackets - (-------)	Al	0.032	32
12	TOF box top panel - (3348401)	Al	0.032	32
13	TOF box side panels -(3348403,04)	Al	0.032	32
14	TOF box front panel - (3348405)	Al	0.063	63
15	TOF box rear panel - (3348406)	Al	0.032	32

Table 4.4-2 Added Radiation Attenuation

Ray set #	Θ_0(1)	d_T(2) (mils)	d_{T+SC}(3) (mils)	d_a(4) (mils)	$d/\cos\Theta_0$(5) (mils)	d_{eff}(6) (mils)	Atten.(7) factor
1	14.5	40	45	110	114	159	.067
2	35.2	40	55	110	135	190	.050
3	46.4	40	65	110	160	215	.043
4	55.7	40	85	110	195	280	.014
5	64.0	40	125	110	250	375	.015
6	71.7	40	160	110	350	510	.015
7	79.2	40/116	145	77	78	223	.20
8	86.4	40/116	125	77	77	202	.20
9	93.6	40/116	150	77	77	227	.17
10	100.8	40/116	150	77	78	228	.17
11	108.3	40/116	150	107	178	328	.04
12	116.3	40/116	200	107	154	354	.075
13	124.3	40/116	200	107	147	347	.075
14	133.6	40/116	200	107	150	350	.075
15	144.8	40/116	300	107	170	470	.33
16	165.5	40/116	300	107	325	625	.25

*Based on GE AstroSpace Doc. GGS-RAD-0003 dated 1/9/90, calculated dated 6/21/89.

Notes:

1. Θ_0 measured from S/C + Z-axis.
2. d_T = actual TIDE box wall thickness assumed by GE in mils of Al.
3. d_{T+SC} = average TIDE box + S/C thickness (including slant paths) assumed by GE.
4. d_a = average thickness of material added to TIDE for shielding.
5. $d_a/\cos\Theta_0$ = average slant path thickness.
6. d_{eff} = total of all material = effective shield thickness.
7. Atten. = attenuation relative to original GE calculation due to added shielding.

Table 4.4-3 Radiation Dose at Location R1

Ray set #	Avg. dose[1] (rads)	Attenuation[2]	Atten. dose[3] (rads)	Cum. atten.[4] dose (rads)
1	8.3 (4)	.067	5.6 (3)	5.6 (3)
2	6.4 (4)	.050	3.2 (3)	8.8 (3)
3	4.8 (4)	.043	2.1 (3)	1.1 (4)
4	2.88 (4)	.014	0.4 (3)	1.1 (4)
5	0.96 (4)	.015	0.14 (3)	1.1 (4)
6	0.96 (4)	.015	0.14 (3)	1.2 (4)
7	3.84 (4)	.20	7.7 (3)	1.9 (4)
8	4.8 (4)	.20	9.6 (3)	2.9 (4)
9	4.8 (4)	.17	8.2 (3)	3.7 (4)
10	1.6 (4)	.17	2.7 (3)	4.0 (4)
11	0.32 (4)	.04	0.13 (3)	4.0 (4)
12	0.16 (4)	.075	0.12 (3)	4.0 (4)
13	0.32 (4)	.075	0.24 (3)	4.0 (4)
14	0.22 (4)	.075	0.17 (3)	4.0 (4)
15	0.03 (4)	.33	0.10 (3)	4.0 (4)
16	0.03 (4)	.25	0.08 (3)	4.1 (4)

Total = 41 krads

Notes:
1. Dose (rads) from GE calculation (without extra TIDE shielding).
2. Attenuation due to extra shielding (Table 4.4-2).
3. Attenuated dose (rads).
4. Cumulative dose (sum of doses in (3)).

4.5. Mass Properties

The mass of the integrated TIDE sensor and electronics is 17.13 kg. Location of center of gravity is shown in Figure 4.1-1.

4.6. Mechanical Ground Support Equipment

4.6.1. Instrument Shipment Container

The mechanical design of the TIDE instrument includes an instrument shipping container that is tightly sealed and has a pressure relief valve and purge fittings. The container is fabricated to clean room standards on both inside and outside surfaces. It includes a shock absorbing suspension to protect the instrument during shipment. The container is as lightweight and compact as practicable for ease in transport.

4.6.2. Mechanical Spares

A kit has been made up containing spare screws, nuts, washers, fittings, lugs, etc., as are needed to perform minor repairs on the instrument in the field. Most instrument parts have been fabricated in duplicate as spares.

4.6.3. Tools

A tool kit has been made up containing the usual mechanical and electrical tools, but also in addition containing any special tools that have been fabricated especially for TIDE assembly and operations. This includes the handling fixture used to lift and orient the instrument during mounting in vacuum chambers and on the POLAR spacecraft, and tools required to operate the retractable instrument aperture cover.

5. ELECTRONIC DESIGN

5.1. Introduction

The nominal TIDE operational power allocation is 10.0 W. The major TIDE electronics subsystems are: spacecraft power and data interfaces; low voltage power supplies and filters (±3, +5, ±10, ±15, and 28V); high voltage power supplies (0 to +300V RPA, 0 to +300V Mirror, 0 to -2.4 kV, 0 to -3.6 kV, 0 to -15 kV), TOF electronics, TOF-ADC interface, DPU and associated memory, and EGSE.

Figure 5.1-1 is a simplified schematic diagram of the major components. The major electrical subsystems are discussed in the sections that follow.

The TIDE electronics are built in a modular fashion such that, to the greatest extent possible, similar groups of electrical functions are on the same electronics board. Performance of the spacecraft interfaces and of the low voltage power supplies is as required to make the other subsystems function properly and is not addressed explicitly in this document.

5.2. Board Layout

Individual boards plug-in to a single multi-layer motherboard that is mounted on the Noryl baseplate. The boards for all TIDE electronic components are 7.500 wide x 7.400 in. long. Figure 5.2-1 shows the board layout and illustrates the presence of a stiffening member which is attached across the boards to insure that their fundamental frequency is above 100 Hz. Figure 5.2-2 shows the physical layout of the electronics boards. Board functions are listed in Table 5.2-1 from the top of the stack down. In addition there are two preamplifier boards of non-standard shape that are mounted in the sensor (see section on preamplifiers).

Table 5.2-1 Electronics board functions

Board #	Function	
1	-3.6 kV, +0.30 kV HVPS	
2	-2.4 kV, +0.30 kV HVPS	
3	-15.0 kV HVPS	
----------	(shield) ----------	
4	Filters and LVPS	
----------	(shield) ----------	
5	Power supply D/A and HV enable	
6	Power supply ADC	
7	Spacecraft I/F	
8	Processor (IMP and DP)	
9	Processor RAM	(144 kB)
10	Processor ROM	(72 kB)
11	Bulk RAM	(384 kB)
12	TOF memory matrix	(64 kB)
13	TOF Direct Event memory matrix	(8 kB)
14	TOF load control	
15	TOF accumulator and pulser	
16	TOF electronics (with 15 daughter cards)	

Figure 5.1-1 Simplified functional block diagram.

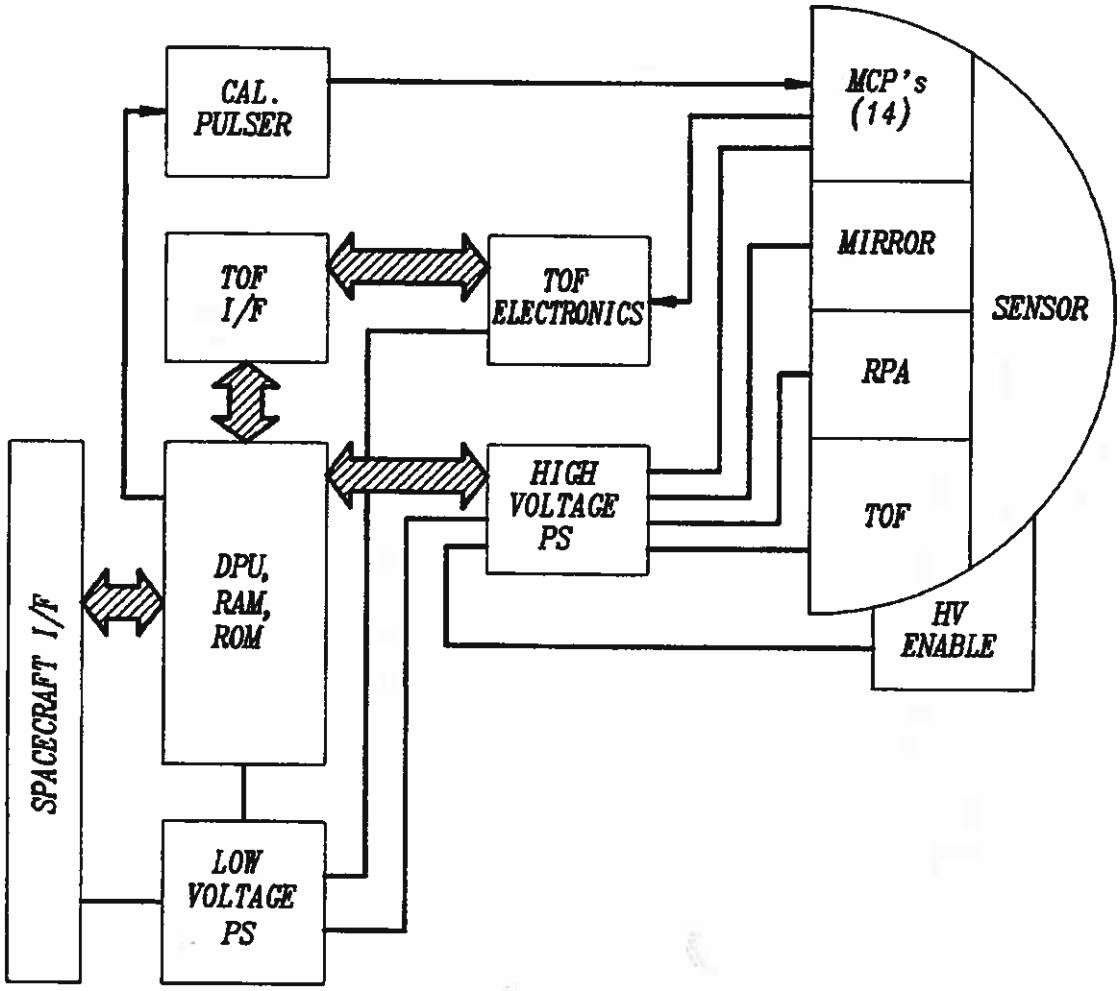

Figure 5.2-1 Circuit board template.

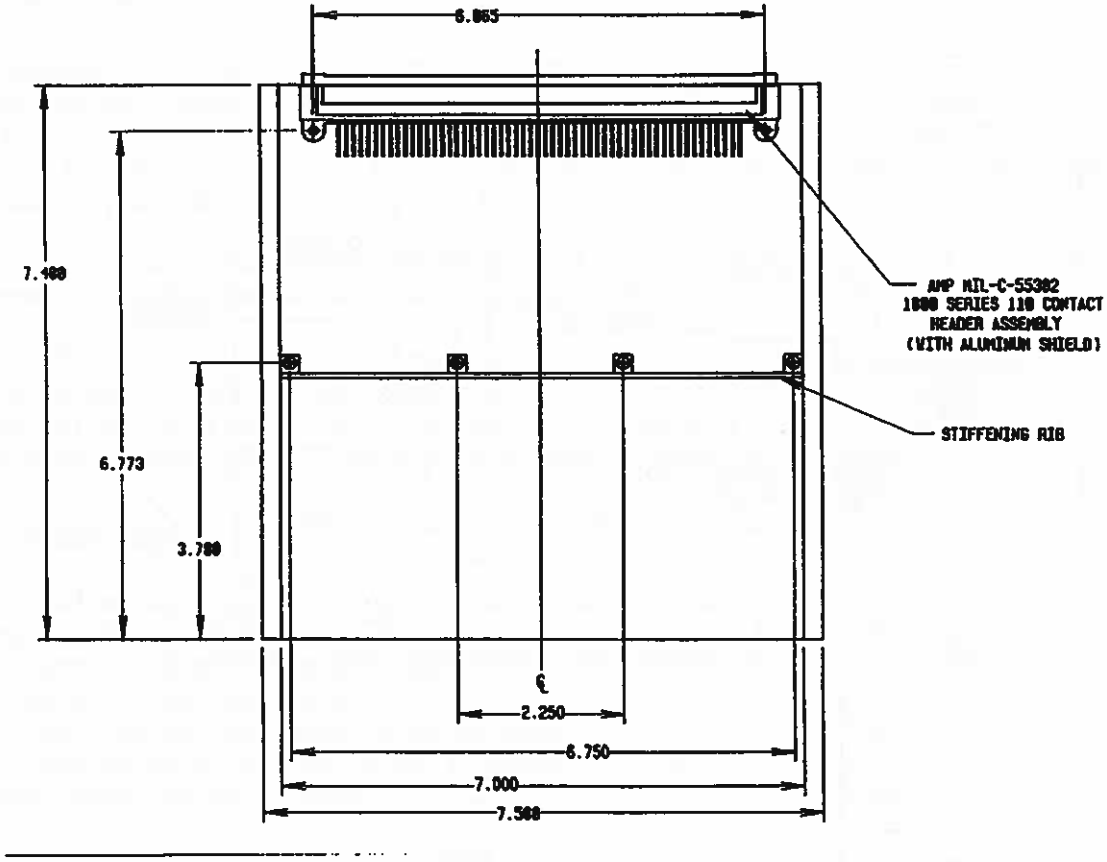

Figure 5.2-2 Circuit board arrangement.

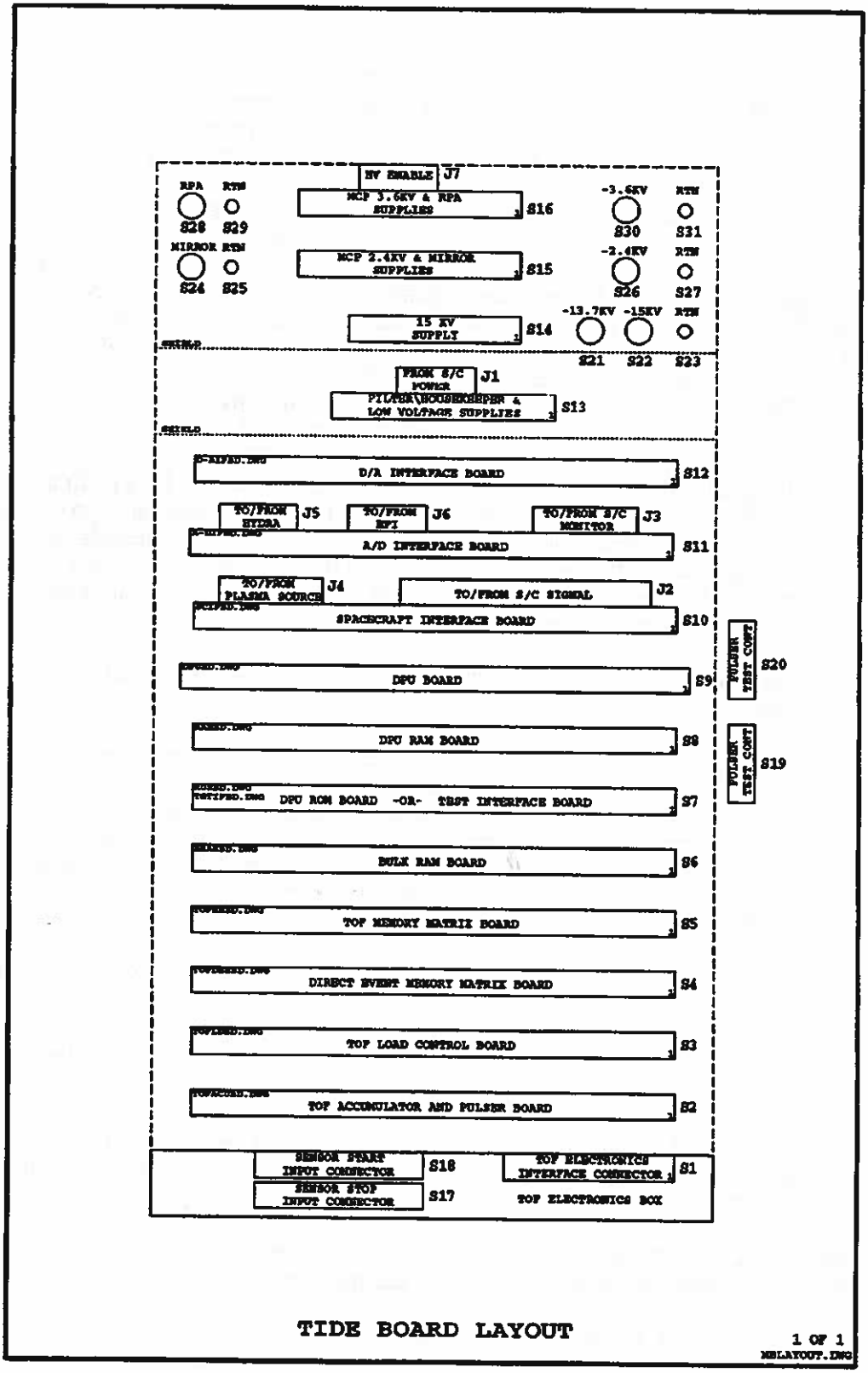

5.3. Time-Of-Flight Electronics

5.3.1. Introduction

The seven START and seven STOP signals are are intputs to the TOF unit. The seven STOP signals are combined into a single STOP trigger by a logical OR operation. Discrimination of MCP pulses occurs after the OR operation. Figure 5.3-1 shows an overall schematic diagram of the TIDE TOF logic while Figure 5.3-2 shows a breakdown of the circuit by board functions.

The mass identification process consists of converting the time interval between correlated START and STOP pulses into a digital word and combining this information with the encoded polar sector. The detectors rates are also monitored without regard to coincidence to monitor instrument processing efficiency. The process begins with the reception of a level-discriminated START pulse from one of the seven START MCP preamplifiers. Provided that previous processing is complete, the error and reset logic provide signals to initiate a TOF interval measurement. The time interval between the received START and STOP pulses (0 to 300 ns) is converted to a voltage pulse of proportional amplitude by the time-to-amplitude converter (TAC). The TAC is implemented using a gated current source to charge a small capacitor. The current source is enabled by a START signal and disabled by a STOP signal. The capacitor voltage is stored in a peak-hold circuit for conversion to 8-bits resolution by a flash analog-to-digital converter (ADC). The reset logic provides timing and synchronization signals to strobe the ADC and to sense ADC conversion complete. Additionally, for time intervals that exceed the 300 ns maximum, the TAC inhibits the logic strobe to the ADC and generates a "Time-Out" single for logging in the singles accumulator. Once the A/D conversion is completed, the TAC is reset, generating another counted event, and processing resumes.

Coincident with the time interval measurement, angular information is obtained by encoding the START singles outputs. The START singles are logic-level pulses from each of the seven START channels. The pulses are provided by one- shots resident on each of the START amplifier boards and are latched in a register during each TOF interval measurement. (Stop pulses are not latched.) The register contents are then encoded to 3-bits to yield a digital value indicating polar arrival angle (sector ID). The time interval/angle combination is then accumulated into TOF memory where it is stored for subsequent analysis by the DPU. In addition, the "singles" counts are accumulated in counters during each sample interval.

5.3.2. Scientific Data Types

The TIDE TOF electronics produces four types of events which are counted and accumulated separately:

1. Detector pulse "singles" rates corresponding to the seven START channels and the one STOP channel.

2. TOF logic "singles" rates corresponding to "Time-Out," "Start Convert," and "Reset" events. Since all valid coincidence events result in either a "Start Convert" or a "Time-Out," the "Reset" rate is equal to the sum of their rates.

3. "Direct Events" are accumulated into an array of 256 TOF bins by 7 polar-angle sector ID over 32 spins without regard to energy step or spin azimuth sector.

4. Coincidence pairs are also, in parallel, accumulated into an array of accumulators encompassing eight broad TOF bins corresponding to the major species of interest, 32 E/Qbins, 7 polar-angle bins, and 32 spin azimuth bins.

Figure 5.3-1 TOF electronics schematic block diagram.

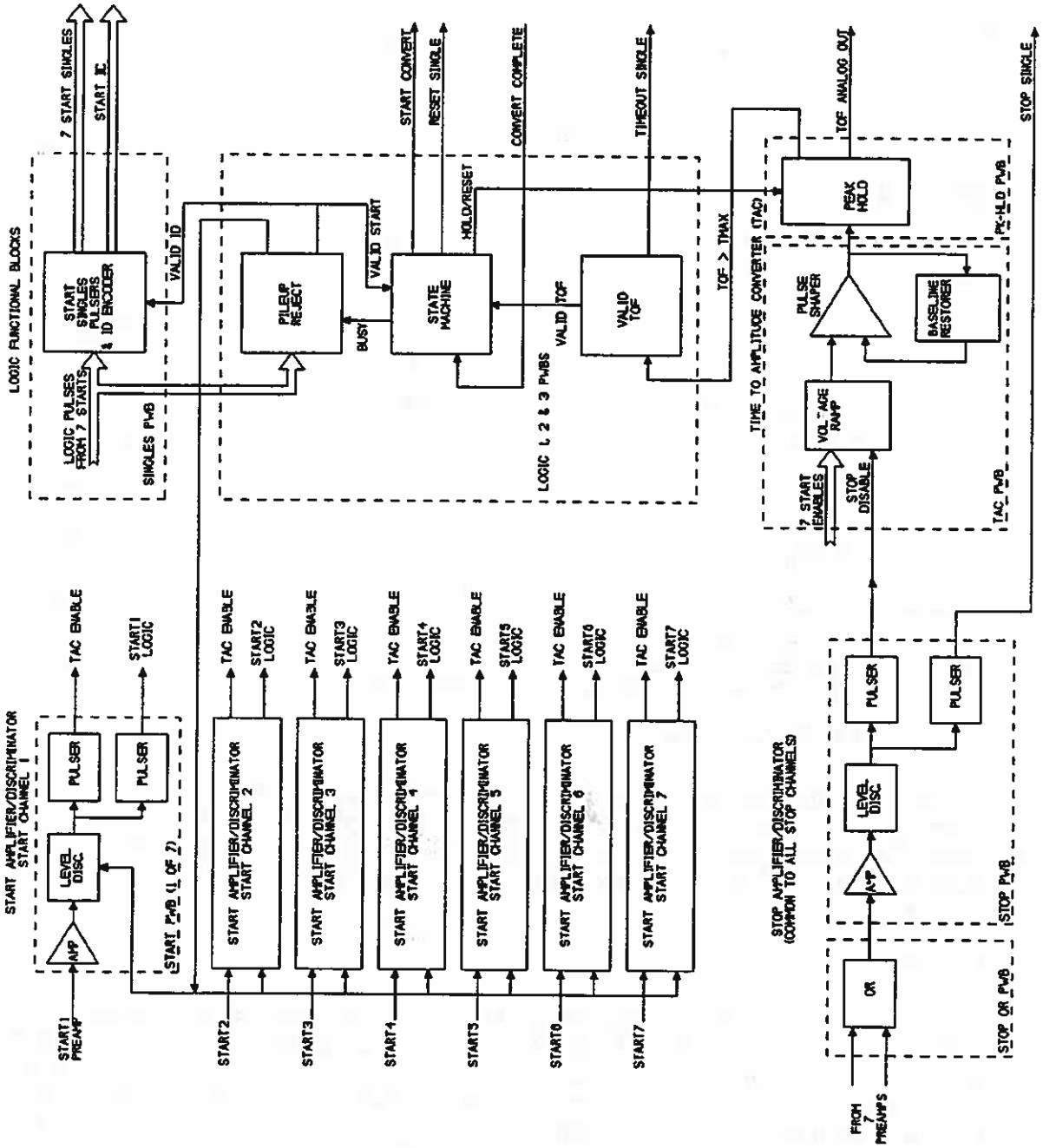

5.3.3. Dead Time

Dead time corrections are performed on the START Singles and the TOF data on-board by the TIDE DPU. The START Singles are subject to a 1.1 μs dead time when not accompanied by valid coincidence event (START CONVERT) and to an additional 2.0 μs dead time when accompanied by START CONVERT. Data associated with TOF events are always subject to the full 3.1 μs dead time. The relevant dead times associated with various TIDE signals are given in Table 5.3-1.

Table 5.3-1 TIDE Dead Times and Live Times

SIGNAL	START CONV ALSO	TIME
START SINGLES	N	2.1 μs
START SINGLES	Y	3.1 μs
RESETS	N	1.1 μs
RESETS	Y	3.1 μs
TIMEOUTS	N	3.1 μs
START CONVERTS	-	3.1 μs
STOPS	-	0.6 μs
TOF, M/Q data	-	3.1 μs
TOF Direct Event Data	-	10.1 μs
Sample Period (Live fraction)	-	5274 μs
Sample Period (Dead fraction)	-	586 μs

Note: All values are preliminary and subject to update based on further calibration analysis.

5.3.4. In-Flight TOF Test Pulser

A pulser circuit is included in the TOF electronics section to directly stimulate the START and STOP preamplifiers in all seven sectors. Pulses from the preamplifiers in turn test the entire signal chain. The pulser is able to generate a range of selected delays between START and STOP pulses in order to test TOF circuitry. These TOF data are fed into the DPU memory and are used to test DPU routines.

5.3.5. TOF Logic

In the ideal case every ion passing through the START foil creates one or more secondary electrons. These in turn are all collected and create a corresponding START pulse in the MCP. Every ion (or neutral) then proceeds from the foil to the STOP MCP and there creates a STOP pulse. (In fact, none of these events has a unity probability and the expected efficiency of the entire TOF event chain is ~ 0.25.) In addition, there are random START and STOP signals due to penetrating radiation (in space) and to noise in the individual MCPs (field emission of electrons) giving rise to random coincidences. The possible cases may be summarized at follows:

Start/Valid Stop

In this case a "start convert" pulse is generated and, at the conclusion of the process, a valid TOF value is also generated.

Start/No Stop

In this case the TOF circuit "times-out" at a predetermined maximum time (nominally 300 ns). The resulting TAC signal is not analyzed by the ADC because it contains no information and would only slow up processing. A "time-out" signal is generated for each such event.

Start/Second Start/Stop

After the first START pulse the TOF circuit ignores any further START pulses that occur before either a STOP pulse or a "time out." Subsequent START pulses which occur during the 300 ns TOF window are not processed, and this time therefore serves as a (non-paralyzable) dead time for the circuit (Table 5.3-1). Recall that the chance probability of a valid second START within the time-out window is small unless the count rate is extremely high, which would not ordinarily be permitted (see below).

Stop/No Start

The logic does not respond to a STOP pulse unless a valid START pulse has occurred within the previous period. By definition a START event is required to fire the logic.

Start/Stop in Random Coincidence

Nothing can be done about this possibility and a random TOF value is recorded. However, note that truly random coincidences are scattered uniformly across the TOF spectrum and this background can, in principle, be measured and subtracted. The expected rate for random coincidences is: $R_{12} = R_1 R_2 (\tau)$ where R_1 and R_2 are the START and STOP detector random rates, and τ is the TOF dead time of 300 ns. (The factor τ is the resolving time of the TOF circuit.) Taking $R_1 \sim R_2 \sim 100\ s^{-1}$ for all seven START and STOP MCPs (which would correspond to relatively high background levels) gives:

$$R = (10^2)(10^2)(3 \times 10^{-7}) = 3 \times 10^{-3}\ s^{-1}$$

Thus the random rate should be very low, if the MCPs can be kept to background rates near 10 $cm^2\ s^{-1}$, a high upper limit except in the radiation belts. This also means that in the presence of a high flux of ions the random coincidence rate increases because it is proportional to either of the single rates.

5.3.6. TOF Interface Signals

The TOF electronics accepts low level analog pulses from the seven START and seven STOP preamplifiers located adjacent to the MCP detector anodes. The seven starts are kept separate to identify ion arrival sector. The seven STOP signals are combined through a logical OR operation, into a single composite pulse.

The TOF measurement accuracy is strongly dependent on MCP pulse characteristics, including modal gain, pulse distribution shape, and the shape of individual pulses (ringing is a problem). Impedance matching of the preamplifier circuits and the MCP anode structure and gain matching of the MCPs are critical elements in obtaining TOF spectra which are consistent from channel to channel.

The TOF electronics process the MCP pulses for TOF information and output a voltage pulse with amplitude proportional to the TOF in the range 0-300 ns. Also output are signals used for

error logging, event rate monitoring, START sector address and ADC synchronization. A digital input is returned to the TOF electronics to signal that conversion is complete and that pulse processing can resume.

Low end (small TOF) nonlinearity and/or noise at this interface is compensated for by introduction of a delay line in the combined STOP signal to raise the proton peak by approximately 15 ns.

5.4. High Voltage Power Supplies

Figure 5.4-1 shows a schematic layout of the TIDE high voltage power supplies and the related voltage dividers and HV feedthrus connecting sensor and electronics. Table 5.4-1 summarizes the requirements for these supplies, which are further discussed in the subsections below.

Table 5.4-1 High voltage power supply specifications

Label	Range	Resol.	Ripple	Drift	Monitor	Comments
TOF	0 to -15.0 kV	8 bits	±1%	±1%	0-4.5 V, 8bits	2nd tap @14.2 kV nominal armed, enabled AND commanded
START MCP	0 to -3.6 kV	8 bits	±0.5%	±2%	0-4.6 V, 8bits	Load: 85 µA armed, enabled, AND commanded
STOP MCP	0 to -2.4 kV	8 bits	±0.5%	±2%	0-4.6 V, 8 bits	Load: 85 µA armed, enabled, AND commanded
RPA	0 to 300 V	12 bits	±1% or ±50mV @< 5V	±1%	0-4.6 V, 8 bits	Settle to 5% in 0.6 ms, ΔV<60 V. No resistive load.
Mirror	0 to 300 V	8 bits	±1% or ±50mV @< 5V	±1%	0-4.6 V, 8 bits	Settle to 5% in 0.6 ms, ΔV<60 V. Controlled as 8-bit fraction of the current RPA supply potential. No resistive load.

Figure 5.4-1 High voltage supply block diagram.

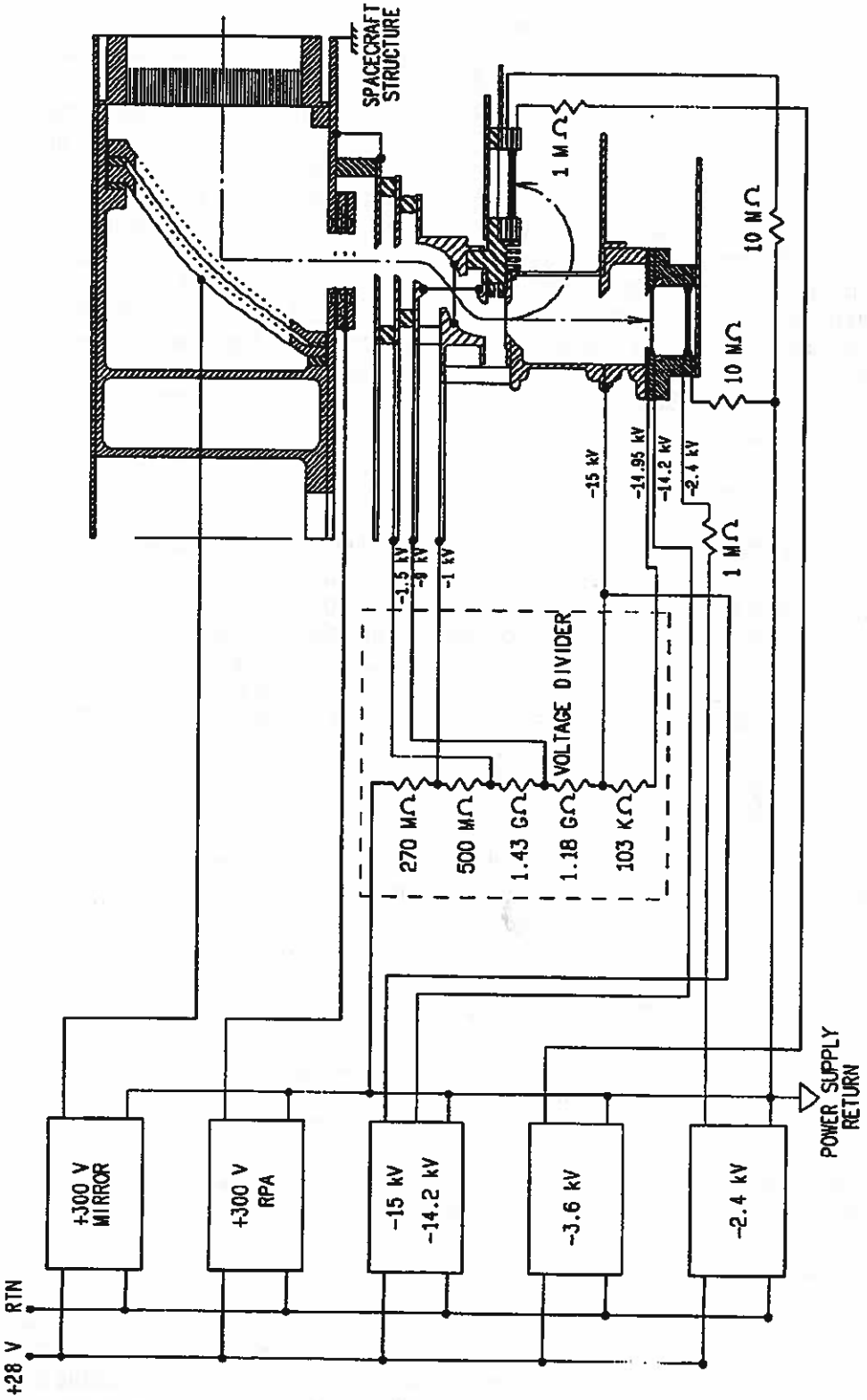

5.4.1. Time-of-Flight HVPS

Power to the STOP MCPs mounted at the TOF HV is provided by a direct tap on the -15.0 kV supply. Although this requires an extra HV wire and feedthrus to the sensor, it lowers total power requirements by eliminating the low ohmic divider. The remainder of the HV values needed for the TOF are provided by a high ohmic ($>10^{10}$ Ω) divider mounted inside the sensor housing. The supply should be commanded to high voltage in a number of steps in order to allow the sensor to condition itself to the applied voltage, and also to provide a lower voltage to operate at in case we cannot achieve the -15 kV maximum. As is the case for other HV supplies on TIDE there are 8 bits of usable control available in the DAC and buffer registers so that a resolution of 58.6 V can be used to adjust the TOF high voltage. The -15.0 kV supply monitor provides an analog voltage scaled at 0 to 4.6 V for 0 to -15.0 kV (5000:1 divider). The monitor voltage is digitized to 8 bits of accuracy. The time sequence for raising the TOF HV to -15.0 kV consists of two stages. First, the instrument must be exposed to high vacuum for a duration sufficient to insure thorough outgassing of the entire instrument. In practice, we have had good success by turning on TOF high voltage only after the instrument has been at a chamber pressure of $\leq 1 \times 10^{-6}$ T for a minimum of 24 hours.

5.4.2. Microchannel Plate HVPS

The START and STOP MCPs are operated from separate HVPS for reliability and because each stack needs to run at a different potential in any case. In order to avoid individual high voltage bias supplies for each sector while maintaining good uniformity from sector to sector, the MCPs have been specified to have consistent impedances from plate to plate and stack to stack (±10%). The resistance per plate is approximately: R ~100 MΩ. Thus a single START stack (3 plates) is ~300 MΩ, and the STOP stack (2 plates) are ~200 MΩ. Since a stack of 3 START MCP plates has a resistance of ~300 MΩ, a full set of 7 in parallel has a total resistance of R ~45 MΩ and at -3.6 kV maximum voltage the total strip current is ~80 μA. The stack of 2 STOP MCPs has a resistance of 200 MΩ, so that a full set of 7 in parallel gives R ~ 31 MΩ. At -2.4 kV the total strip current is ~80 μA.

MCP Z stacks are chosen for consistent multiplication gains, by dividing into START, STOP, and SPARE groups. During calibration, the optimum MCP bias operating points for START and STOP detectors is determined by varying the biases and observing the integral rate of discriminated pulses.

5.4.3. Retarding Potential Analyzer Supply

The voltage varies from 0.00 V to 300.0 volts with 12-bit resolution. This corresponds to a voltage resolution $\Delta V = 0.0732$ v. The shortest sample period is 5.86 ms and we require settling times <10% of this period. The stepping profile requirement is illustrated in Figure 5.4-2.

The RPA supply output monitor provides an analog signal scaled at 0 to 4.6 V for 0 to 300 V input. This is monitored in TM to 8 bits of accuracy.

5.4.4. Mirror Supply

The voltage varies from 0.0 V to 300 V, but is controlled as a fraction of the RPA potential ranging from zero to unity with 8 bits of resolution. Thus the default is for the Mirror to track the RPA potential in a fixed ratio during a sweep. However the ratio is commandable on each step of the energy sweep, and is in fact the parameter which controls the overall instrument sensitivity. The mirror voltage is the specified fraction of the RPA voltage to an accuracy equal to that of the 8-bit command resolution (0.4%) or 40 mV, whichever is greater.

Figure 5.4-2a M/RPA sweep wave form requirements.

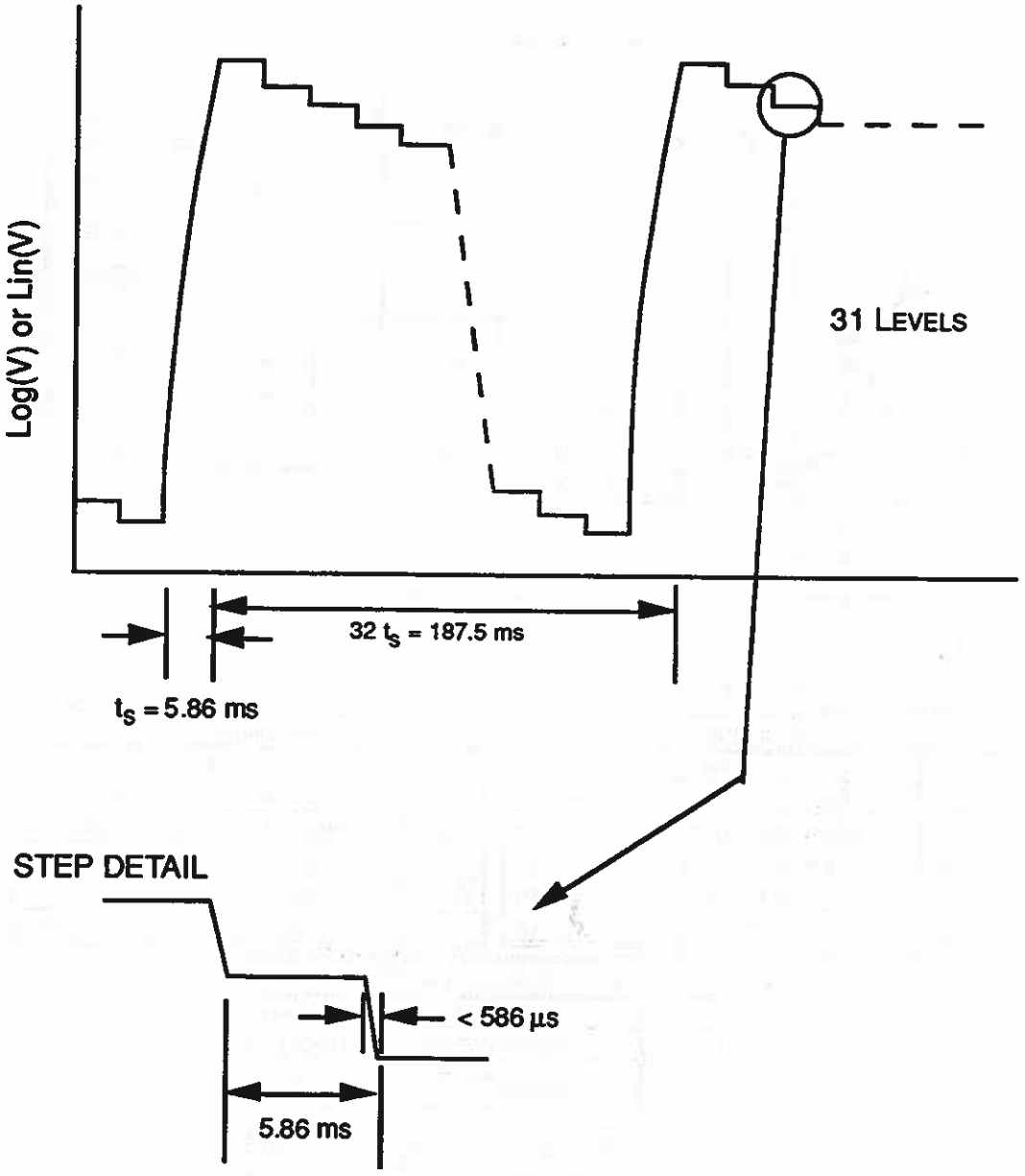

Figure 5.4-2b M/RPA ratio control data.

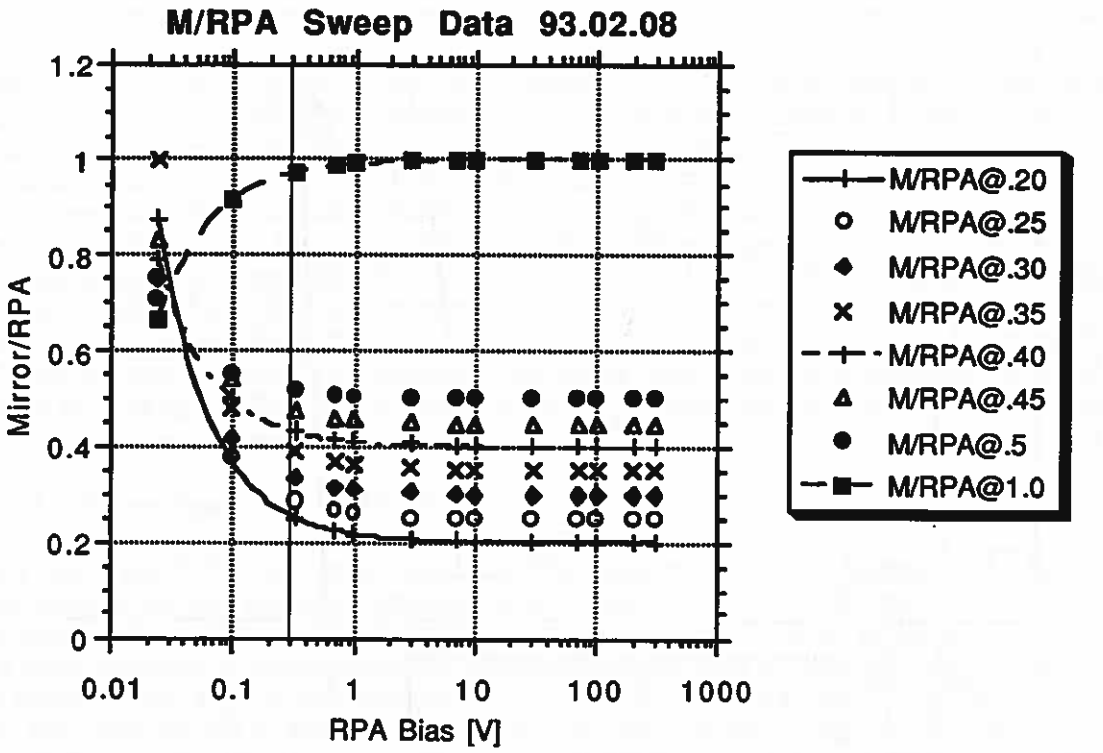

y = ((m0+m2)*m1+m3)/m0		
	Value	Error
m1	0.40149111567	0.000554184
m2	0.0099634674747	4413.39
m3	0.0053848944191	1771.94
Chisq	3.4342537411e-05	NA
R	0.99987770421	NA

y = ((m0+m2)*m1+m3)/m0		
	Value	Error
m1	1.0006472239	0.00027414
m2	-0.0059435748062	2429.26
m3	-0.0020715884072	2430.83
Chisq	8.4036603308e-06	NA
R	0.9999590041	NA

y = ((m0+m2)*m1+m3)/m0		
	Value	Error
m1	0.2016203194	0.00107714
m2	0.027490693707	48641.5
m3	0.010679681358	9807.11
Chisq	0.00012973850474	NA
R	0.99984537489	NA

5.4.5. Aperture Bias Supply

Because of the presence of the Plasma Source Instrument on POLAR, the requirements for an aperture bias potential was dropped by the TIDE team during 1988.

5.5. Data Processing Unit

The following describes the general functions of the DPU. A separate specification was to be written to provide detailed design information on the DPU. Figure 5.5-1 shows a highly schematic overview of the TIDE DPU and control system.

5.5.1. Microprocessors

The data processor (DP) is a Sandia SA3300 microprocessor with a 16-bit external and 32-bit internal bus, running at 8 MHz. This processor is used to execute computation intensive tasks, primarily the calculation of moments from the spin by spin data arrays. Hardware capability is provided to interrupt the processor on critical events such as the spin pulse, minor frame, etc.

The instrument mode processor (IMP) is also a Sandia SA3300 microprocessor, running at 5 MHz. It is used to perform housekeeping tasks such as telemetry formatting, HV control and associated TIDE control functions. In addition, the IMP performs bulk data compression when that function is enabled. Interrupt capabilityis also provided for events such as minor frame sync, command, telemetry, etc.

Memory configuration is as summarized in Table 5.2-1. The IMP and the DP have shared access to 144 kB of RAM and 72 KB of PROM. The processors obtain their data through data acquisition memories which are incremented independently of the processors by the load control circuit. These amount to 8 kB and 64 kB for the IMP and DP, respectively. In addition, the DP has a bulk RAM allocation of 384 kB for intensive calculation space.

5.5.2. TOF Interface

The TOF interface requires digitizing the TOF signal by a flash ADC to 8-bits resolution. The 8 bits are then filtered through a mass/charge lookup table, which is RAM based and can be updated in flight, that generates a 3-bit mass address. Along with a 3-bit sector identification, these data are binned according to azimuth and energy. These data are acquired in a 128 kilobyte memory system over a 6-sec spin period. There are two such memory systems so that at a spin boundary the memory systems are swapped. This allows the data processor access to the previous spin of data while acquisition is occurring in the other memory system.

The ADC digitizes the analog TOF signal to an 8-bit channel number, which determines the bin location for sorting events, both in Direct Event memory (full 8-bit resolution) or in the main Angle-Energy array memory (3-bit resolution). The ADC input must have an input impedance sufficiently high that it is adequately driven by the TOF output driver.

Singles rate outputs from the TOF electronics are accumulated in 16-bit registers, sorted according to azimuth angle and energy step. This data is acquired in the same memory system as described above. The 8-bit output of the TOF ADC along with the 3-bit sector ID is used in a separate (direct event) data acquisition system that bins the 11-bit data over a 3-minute accumulation time. Upon an ADC start pulse, each direct event is binned during a dead time period which exceeds that for the binning of ordinary TOF events into mass bins, as indicated in Table 5.3-1. To accomodate the longer accumulations, 32 bit accumulation words are used.

Figure 5.5-1 IMP/DP block diagram.

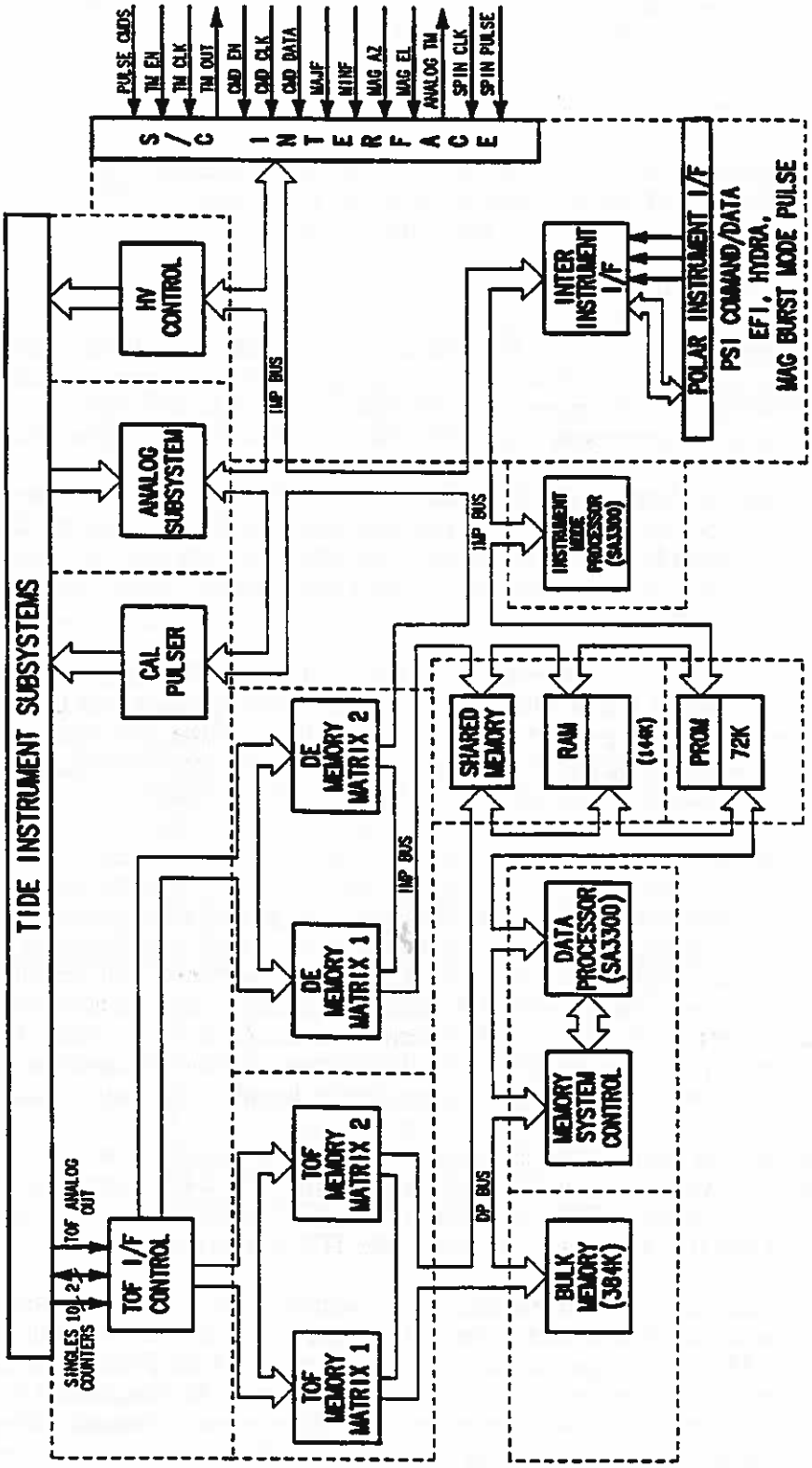

5.5.3. Random and Read-Only Memory System

Hardware capabilities are provided to the data processor for copying memory contents from the data acquisition memory to general purpose memory. In addition to the copy function, a hardware lookup table function is supplied to encode the data in a compact floating point representation, as further described in the section below on Flight Software. Finally, a hardware block add/subtract function is provided. All of these hardware functions are under software control and are intended to reduce software overhead of the data processor.

5.5.4. High Voltage Power Supply Interface

Logic is provided to turn on the HV power supplies in three stages. Spacecraft pulse commands are used to arm the supplies for microprocessor commanding. The three pulse commands arm the RPA/MIR, MCP (START and STOP) and TOF high voltage supplies. A fourth pulse command is provided to act as a "breaker" switch for all HV supplies. Once the supplies have been armed, (major) commands can then be issued to individually enable commanding any of the five HV supplies. Finally, the appropriate control levels, which are generated by digital-to-analog converters (DACs), can be commanded (minor commands) to complete the HV turn-on. Upon DPU power up the control levels reset to zero. Control of the RPA and MIRROR HV control levels is done via sweep tables which are either resident in ROM or built up in RAM by (minor command) upload and then executed by minor command. The stepping of the supplies according to the tables is synchronized to the sample period. The RPA and MIRROR HV have 12-bit and 8-bit control voltage resolution, respectively. The Start MCP, Stop MCP, and TOF HV have 8-bit control voltage resolution.

5.5.5. Spacecraft Interface

All of the spacecraft interfaces described are in accordance the GE General Instrument Interface Specification (GIIS) document number 3282065. The interface consists of a 40-bit serial command channel, together with three 8-bit parallel/serial registers that are provided for the s/c to acquire telemetry data on greater than 1 millisecond centers per minor frame. MAGAZ and MAGEL signals are received from the s/c and utilized in computations. The spin phase clock and pulse is used to synchronize the operations of the instrument to the s/c spin. Analog housekeeping signals for ascertaining the health and safety of the instrument are digitized using a general purpose analog to digital converter. A PSI "Squirt" signal is provided to the EFI and Hydra instruments so that they may be aware of the status of PSI operations. Signal interfaces are provided to the HYDRA and EFI experiments in order to determine when they enter a "burst memory" state indicative of rapid temporal fluctuations in the local plasma or fields.

5.6. Electrical Ground Support Equipment

5.6.1. EGSE Functions

The EGSE is the sole electrical interface to the integrated TIDE sensor, electronics, and PSI. Because of the complex nature of TIDE and of the TOF technology, the instrument test and calibration functions are dependent to a large degree on a well designed and powerful EGSE. In addition to meeting the requirements of the TIDE team, the EGSE conforms to all project requirements for EGSE spelled out in ISTP interface requirements documents. The GSE provides or receives the following signals to/from the TIDE instrument in order to simulate all spacecraft interfaces and their functioning:

Spacecraft power (+28 V)

Telecommand (including clock and address)

Telemetry (including clock and address)

Auxiliary data (spin clock, MAGEL, MAGAZ, plasma source bias level, HYDRA burst signal, EFI burst signal)

In addition to spacecraft functions, additional signals must be provided to test or stimulate the sensor unit:

Housekeeping signals not included in telemetry (e.g., temperature, power, and voltage monitors)

Direct access to sensor data at the point where this data is handed over to the TIDE DPU. This requirement arises from the need to verify DPU operations on the sensor data as discussed below, and is accomplished by means of a test interface board which substitutes for the PROM board.

Finally, signals are required to simulate the sensor functions that are provided to the DPU:

A simple PSI simulator to interface with TIDE and TIDE GSE functions so that TIDE testing can proceed without the PSI present.

5.6.2. Tests to be Conducted with the GSE:

Self-test of GSE

Functional test to provide full checkout of all electronics components and functions. The test must serve for aliveness and bench tests of TIDE following shipment, environmental tests, etc. This test should be broken down into tests of the main subunits alone: LVPS, HVPS, DPU, TOF electronics, sensor preamplifiers, and PSI aliveness. The test must collect all data needed to benchmark the instrument.

Development of TIDE sensor and electronics (i.e., with the sensor in the beam, while undergoing shakedown of the integrated TIDE system)

Calibration of TIDE sensor with DPU:

Verify that DPU correctly interprets TOF data as mass values as well as sorting and binning in angle/energy.

Verify that DPU correctly controls the sensor for any onboard feedback functions (e.g., control of energy pass band in response to high particle fluxes).

Verify that DPU correctly computes items such as moments based on pulser programs developed so as to test the full system.

Verify overall data compression using pulser and real TOF data.

5.6.3. GSE Design Approach

The GSE is based on a functional emulation approach. It contains separate PC computers to simulate the POLAR spacecraft and the controlling ground station. It also contains a Sun workstation to serve as an emulator for the Remote Data Analysis Facility, where the full data

displays are developed. This is a complex system, but the approach is designed to test all phases of the data link between TIDE and the investigators.

All power supply, pulser calibration, and similar functions are computer controlled by the GSE computer. There is never a need for persons conducting a test to "turn a knob"--the setting of which then has to be written down or otherwise entered manually into the test data record.

The GSE is rugged, transportable and easily set up and checked out.

The GSE, its software, and its operation must be well documented in order to meet the requirement that it be easy to set up and operate.

Figure 5.6-1 Ground support equipment block diagram.

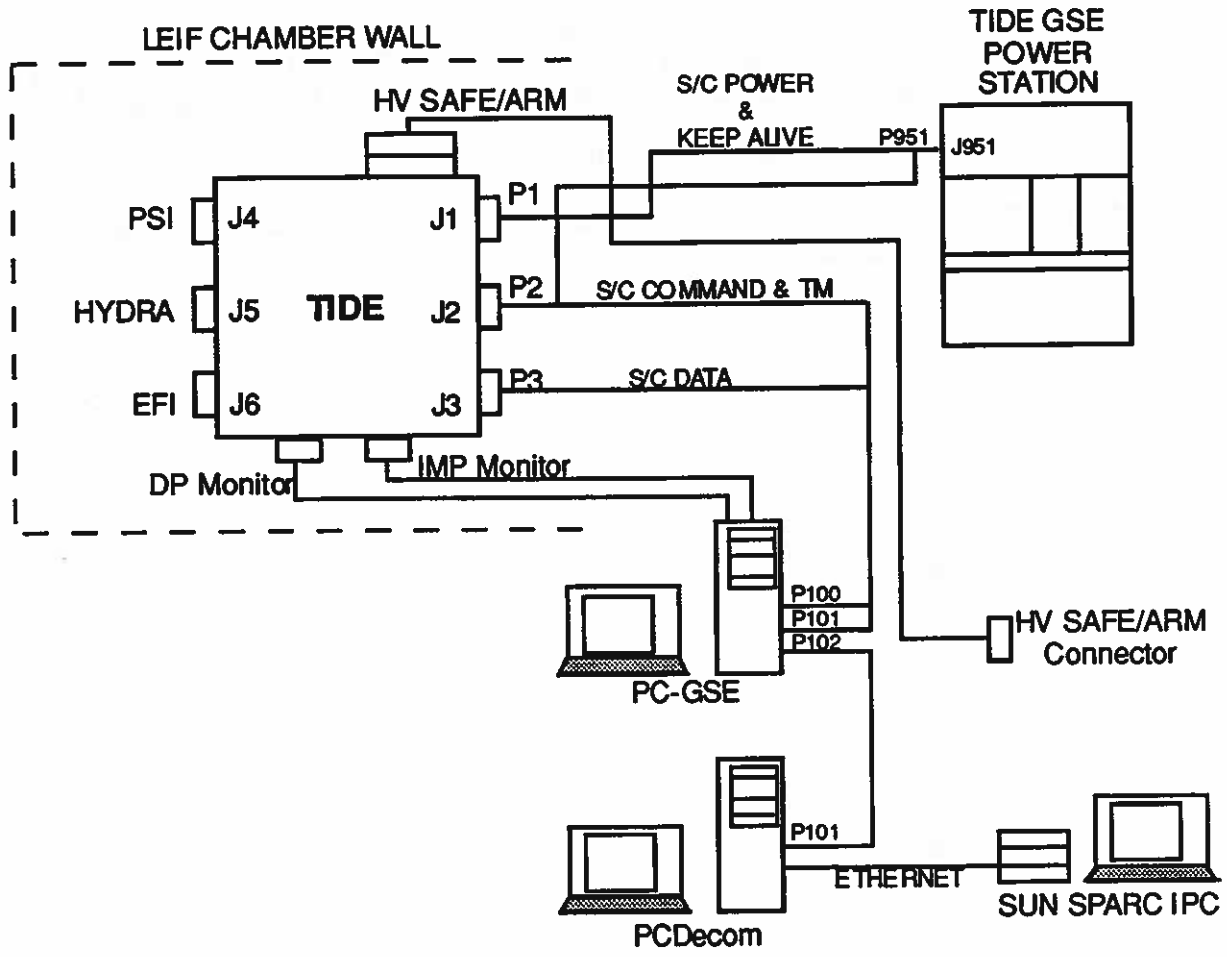

6. PLASMA SOURCE INSTRUMENT

6.1. Objectives and Specifications

The fundamental goal of PSI is to establish a means for the reduction of the spacecraft floating potential to values much smaller than normally associated with spacecraft in low-density plasmas in sunlight. The Plasma Source Instrument (PSI) is an essential adjunct to TIDE, because control the potential of the POLAR spacecraft will allow measurements of low-energy ions. Spacecraft immersed in plasmas in general attain a potential different from plasma potential. A charged particle starting far from the spacecraft and arriving at the spacecraft surface will do so at an energy which differs from its initial energy by the spacecraft floating potential. The origins of this spacecraft potential are many, but the fundamental principle is that the net current to the spacecraft surface has to be zero in the steady state. The currents flowing between the spacecraft and the plasma are all functions of this potential, and the potential adjusts self-consistently on a time scale of seconds to changes in plasma environment or solar irradiance so as to satisfy a zero-current condition. Equilibrium spacecraft potentials can range from several volts positive (to retain emitted photoelectrons) when the spacecraft is in a low-density plasma, to thousands of volts negative when the spacecraft is simultaneously in the shadow of Earth and in a very hot plasma such as is found in the plasma sheet during substorm activity. Positive floating potentials prevent low-energy ions from reaching the spacecraft at all, while negative floating potentials raise the apparent energy of the ions and render it impossible to implement an energy sampling strategy which will be effective in resolving the ambient energy distribution.

Experience with plasma source and accelerator devices on the ATS-6 and SCATHA spacecraft has shown that it is feasible to render the spacecraft relatively immune to swings in floating potential brought about by changes in external plasma or sunlight conditions. This is done by establishing a plasma in the vicinity of the spacecraft with the following properties:

(a) The generated plasma must have an ion thermal flux which is larger than the electron thermal flux of the photoelectron cloud generated by the incident EUV flux on spacecraft surfaces. In addition, the local plasma electron thermal flux must be larger than that of any naturally occurring plasma expected to be encountered by the spacecraft.

(b) The generated plasma electron temperature is small, a few tenths of eV at most.

(c) The generated plasma ions are chemically inert, with a mass per charge which is distinct from that of naturally occurring ions.

Condition (a) insures that the thermal flux of local plasma ions will be capable of neutralizing the flux of photoelectrons away from the spacecraft which will result if spacecraft floating potential is maintained at values much less than the mean energy of the photoelectrons. Condition (a) further insures that the thermal flux of local plasma electrons will be capable of neutralizing the flux to the spacecraft of very hot plasma electrons frequently encountered near synchronous orbit. Condition (b) insures that the equilibrium floating potential will be much smaller than either the several volts corresponding to the photoelectron mean energy, or the thousands of volts corresponding to plasma sheet electron temperatures. Condition (c) insures that the operation of the plasma source will not create a plasma which can be confused with the ambient plasma.

Figure 6.1-1 Photograph of the plasma source.

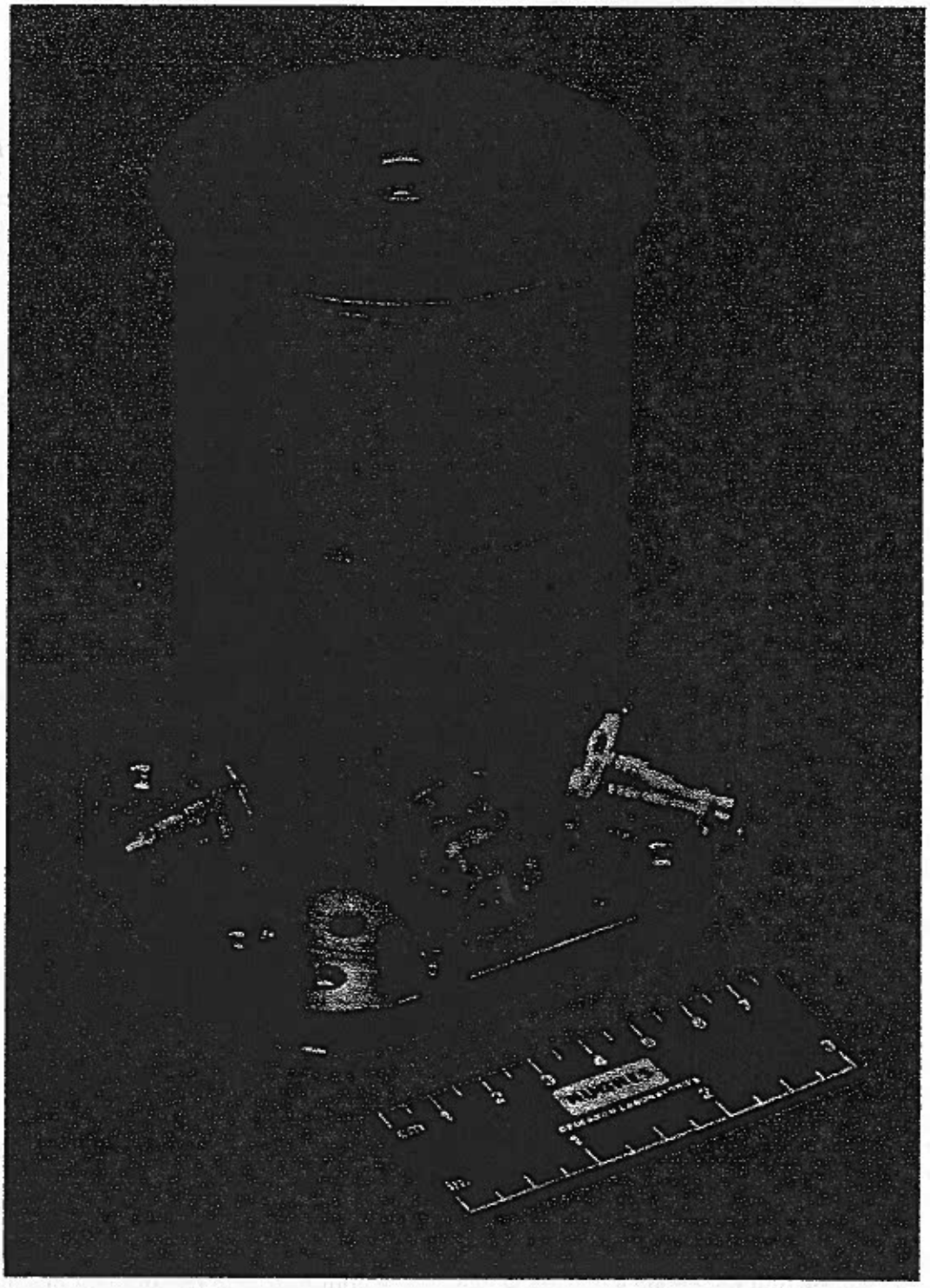

The design of a source which produces a suitable plasma is based on earlier experiences with ATS-6 and SCATHA. This design has been developed by the Hughes Aircraft Corp. under a contract with the U.S. Air Force. Flight hardware has been previously produced, tested, and flown by Hughes in connection with these programs, and the design is mature. Table 6.2-1 provides a summary of the technical specifications for PSI which details the capabilities of the system.

The Plasma Source Instrument (PSI) is an integral part of the TIDE investigation. Its presence on the POLAR spacecraft is essential to the correct operation of TIDE at very low ion energies (<10 eV). The PSI emitter is provided by Hughes Research Labs, while all tankage, tubing, power supplies, and electronic controls are provided by SwRI.

6.2. Functional Description

The PSI consists of the plasma source, a gas feed system with appropriate tanks, plumbing, and valving and an electronics system capable of powering and monitoring the operation of the PSI. The relationship among these components is illustrated in Figure 6.2-1.

The plasma source is a compact arrangement of a hollow-cathode, keeper and anode electrodes, a magnetic structure, and a grounded shield. Xenon gas flowing through the plasma source is ionized by bombardment with electrons released from a low-work-function surface within the hollow cathode. The ionized gas flows out of the plasma source, providing a medium-density ($\sim 10^{10}$ cm^{-3}), inert-gas plasma to neutralize differential charge buildup between various surfaces of the satellite and also to form an electrically conducting "bridge" between the satellite and the natural space plasma.

Table 6.2-1 PSI performance and resources requirements

Parameter	Value	Unit
Expellant Gas: Xenon	131	amu
Expellant Flow Rate	0.5	sccm
Discharge Voltage	~ 25	V
Discharge Current	< 200	mA
Keeper Voltage	~ 18	V
Keeper Current	< 250	mA
Total Power (Into Source - Running)	15.1	W
Total Power (Into Source - Startup)	45	W
Startup Time	5	min
Lifetime	20,000	hrs
Startups	> 10,000	starts
Saturation Particle Emission Currents:		
- Ions	req'd >25, actual > 1000	μA
- Electrons	actual > 500	mA

It is anticipated the plasma source will bias the satellite such that the plasma source anode is within a few volts of space potential. To hold the satellite within +1 V of space potential it may be necessary to bias the plasma-source anode relative to spacecraft ground. A vernier bias control permits this. Plasma source characteristics are listed in Table 6.2-1.

Figure 6.2-1 Plasma Source Instrument schematic diagram.

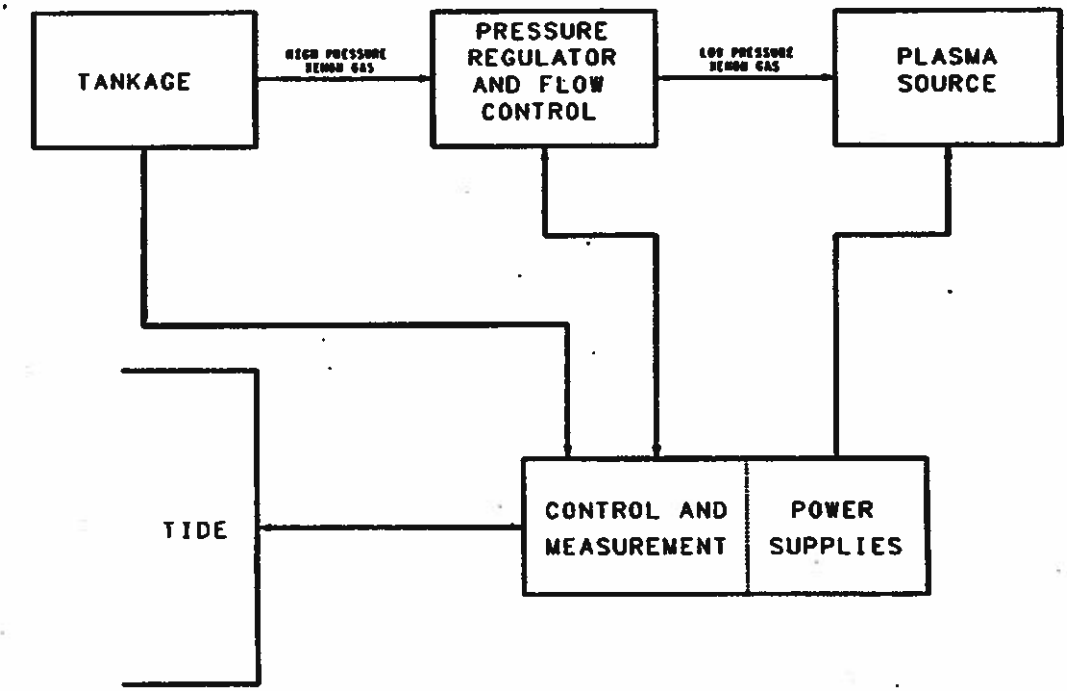

The plasma source has a porous-tungsten insert. The cathode, keeper, and anode are all electrically isolated from the outer can so that the return current from the satellite can be measured. The outer can is fabricated from cold rolled steel and thus serves as a magnetic shield for the permanent magnets inside the source. A solenoid valve in the gas feed plumbing is an additional source of stray magnetic fields. Both have been tested thoroughly, and their exceedances have been waived.

6.3. Source System

The hollow-cathode source is illustrated schematically in Figure 6.3-1. The cathode is a porous-tungsten material impregnated with barium aluminate, a material with a low work function. Initially the cathode is heated with an external filament to begin thermionic emission. Xenon gas flowing through the hollow cathode is initially ionized by the thermionic electrons accelerated by the potential on the keeper electrode. The axial magnetic field serves to confine the electrons and increase the probability of an ionizing collision, thereby minimizing the rate of gas flow required to obtain a given ion current. Once the keeper discharge is initiated, a fraction of the positive ions is accelerated back to the cathode and produce local impact heating. After an initial heating time, the filament can be turned off and the thermionic emission is maintained without the penalty of heater power.

The keeper electrode and anode are biased +18 and +25 volts, respectively, relative to the cathode. The neutral Xenon gas flows throughout the entire region between the gas inlet and the outer shield exit. The potential structure accelerates electrons toward the anode, and production of plasma therefore occurs throughout the region. The distribution of plasma generation can be controlled to some extent by the magnitudes of the keeper and discharge voltages. A plume of low-energy plasma therefore exits the anode orifice, and the current can be "fine-tuned" by adjusting the magnitude and polarity of the bias supply. This supply biases the entire plasma source relative to spacecraft frame ground, and an electrometer measures the net current produced by the source.

6.4. Gas Feed System

The feed system consists of the storage tanks, valves, pressure regulators, flow impedance, and pressure transducers required to provide the source with a steady-state 0.5-sccm flow rate. Its overall layout is illustrated in Figure 6.4-1. The Xenon gas supply is contained in two pressure vessels located symmetrically on the spacecraft to maintain balance and provide gas flow over the anticipated range of temperature. The storage tanks are a pair of 4.8 L, cylindrical high pressure vessels rated for 3100 psi. The tankage is fitted with high and low pressure transducers (to indicate the quantity of remaining expellant) and a manually operated fill valve. The nominal gas supply is 3.5 kg, or 600 standard liters, of Xenon, which is sufficient for 20,000 hrs of continuous operation at the specified flow rate. The valves and regulators reduce the pressure to 10 psi which is applied to the upstream side of a constant flow impedance plug to maintain a flow rate into the cathode of 0.5 std cm^3/min, or 0.37 micro mole/s. Saturation ion current is 1.0 mA; hence, the maximum ion production efficiency is approximately 3%.

The Xenon flows from the tank through a high-pressure valve to the pressure regulator. The pressure regulator reduces the Xenon pressure to a constant 10 psia. The 10 psia is applied to the upstream side of a constant flow impedance to maintain a steady state flow rate of 0.5 sccm. No low-pressure valve is provided to turn the flow to the plasma source on/off, so the high pressure valve must be turned off in advance of the desired shut down time so that the small volume of high pressure Xenon left downstream of the valve can be scavenged.

Figure 6.3-1 PSI source functional block diagram.

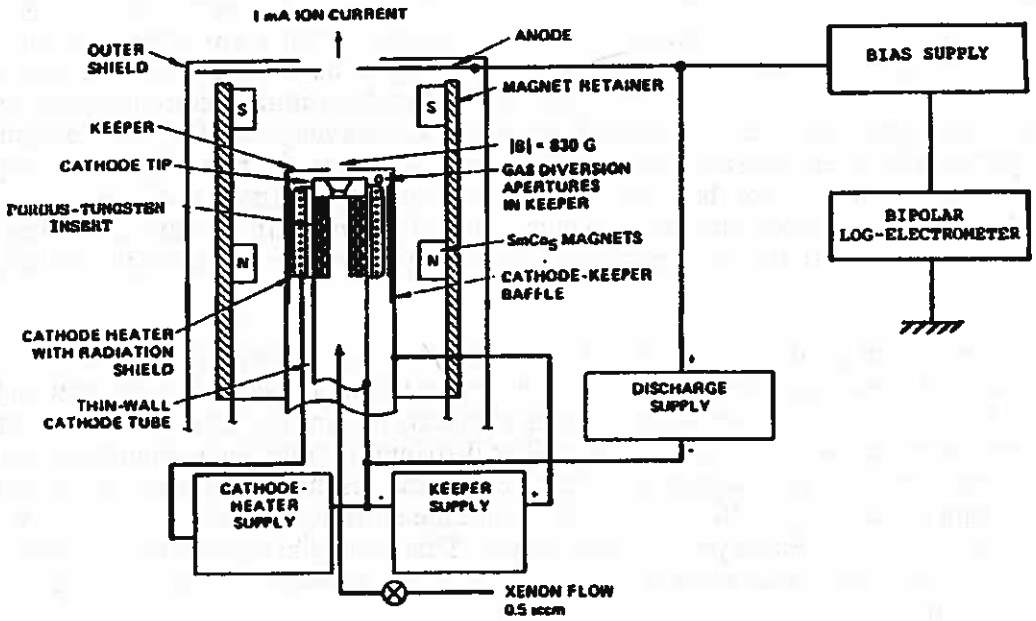

Figure 6.4-1 PSI Gas feed system block diagram.

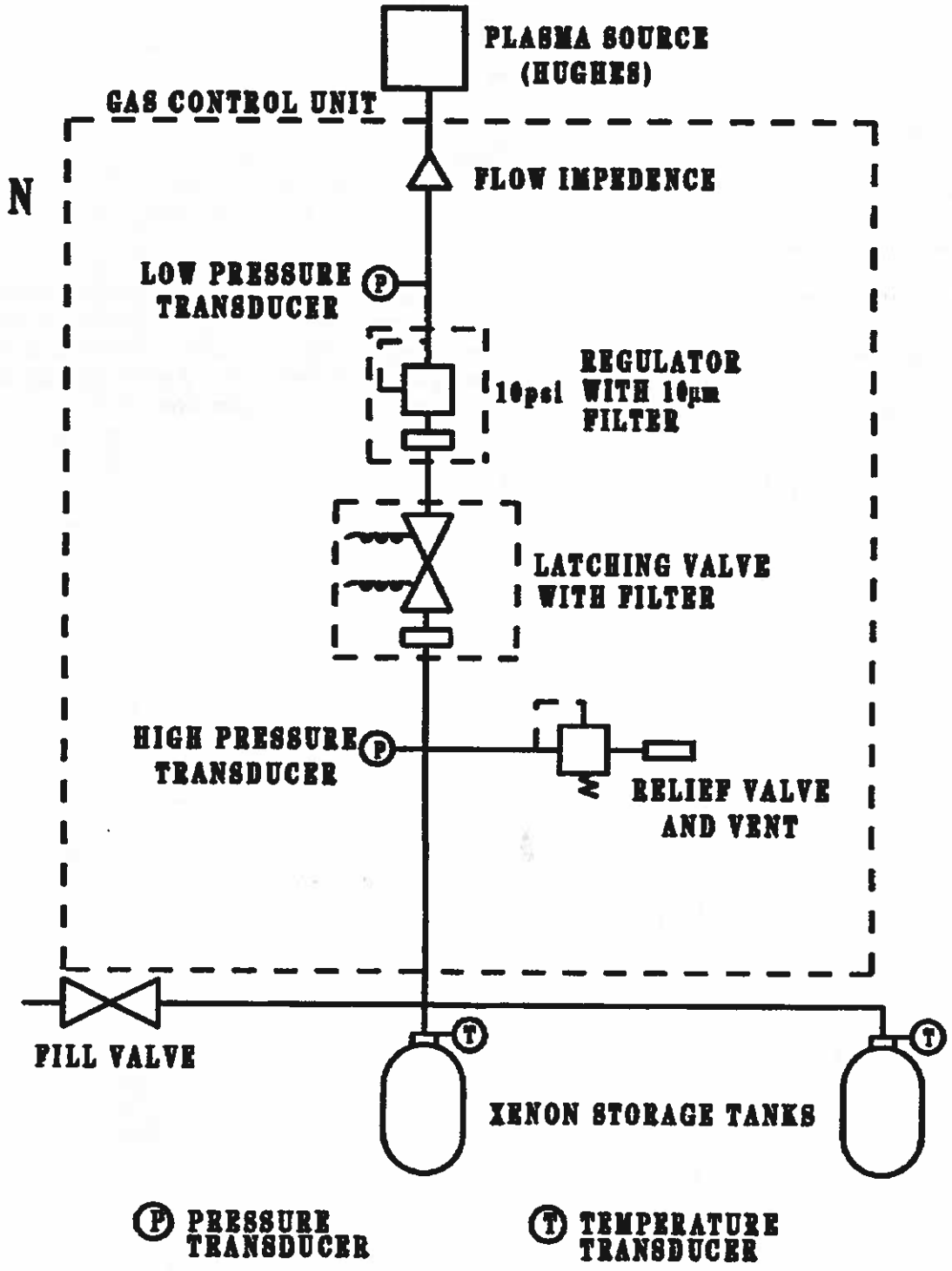

6.5. Electronics System

The PSI electronics system is illustrated schematically in Figure 6.5-1. It contains the discharge, keeper, heater, and bias supplies for operation of the source, a bipolar log-electrometer to measure the net emission current from the source (this constitutes the return current from the satellite), valve drivers, analog telemetry signal conditioning, and the TIDE interface.

The remaining components of the PSI are the various control electronics and interface circuitry necessary for interfacing with the TIDE power, data, and command system. The primary controls are the startup heater, the keeper potential, anode potential, and the bias supply. The primary data reported to the data stream are the emission current and power supply monitors, which are reported in the TIDE data stream.

The TIDE instrument controls all phases of PSI operations. The application of 28-V power and a simple on command is all that is required to start the plasma source. A maximum of 20 other commands are required to set the level of the bias supply and make minor adjustments to the operation of the source (including manual control of all power supplies). Approximately 20 telemetry words are used to monitor the status of the source and its operation.

Figure 6.5-1 PSI Electronics unit block diagram.

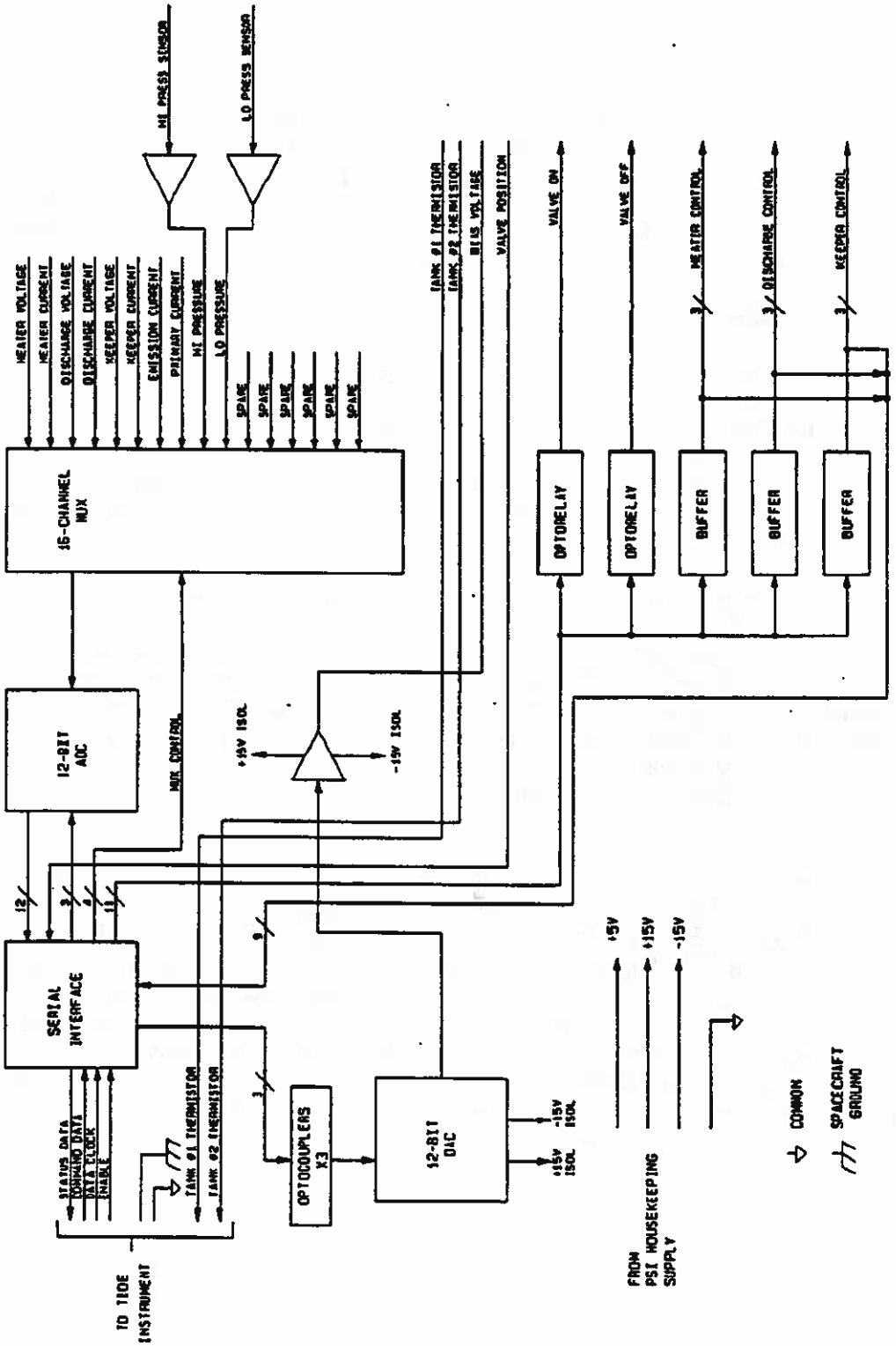

7. FLIGHT/GSE SOFTWARE DESIGN

7.1. Overview

With TIDE's capability to monitor multiple directions and mass species simultaneously, only the ion energy needs to be swept. Since TIDE has only one swept measurement, all its operating modes consist of repetitive sweeping of the mirror/RPA potentials in an uplinkable pattern coordinated with the spin sweep of the seven sectors in spacecraft azimuth with a period of 6 sec. TIDE has two sampling modes. The "standard" sampling mode provides for 32 energy steps per sweep with 32 sweeps per 6-sec spin, dividing the spin into 11.25 ° sectors. A phase-locked-loop maintains precise spin sectoring during each spin, and provides for the phase to be adjusted by up to 22.5 ° of spin in 256 steps.

The fundamental organization of the TIDE data consists of a triplet of arrays: First, the species array has dimensions: energy, azimuth angle, polar angle, and mass, with 16 bits of accumulation depth. Second, the singles array has a similar structure, but with four additional rates in addition to sectors 1-7: STOPS, StartConverts, TimeOuts, and Resets. Finally, the direct event array stores full mass spectral information (8-bit address) for each of the 7 sectors, without regard to spin or energy, and with 32 bits of depth to accomodate accumulations of durations up to several minutes.

The data reside in the spin data acquisition memory which includes two pairs of identical banks (64 k x 16 bits each) that collect data during alternating spins for the species data and singles/direct events, respectively. While data are being acquired in one pair of memory banks, processing is performed on previously acquired data, resident in the alternate pair of memory banks. During processing, specified data sectors can be copied, summed, or differenced with selected portions of bulk dynamic RAM memory (384 kB) that serves as the main working memory of the Data Processor. A schematic showing the basic functional elements of the TIDE data flow is shown in Figure 7.1-1. Timing with respect to the spacecraft spin is illustrated in Figure 7.1-2.

In view of the large size of the TIDE data "images" (Species: 32 energies x 32 azimuths x 7 polar-angle channels x 5 masses x 16 bits = 70kB, Singles: 11 x 32 x 32 x 16 bits = 22 kB, and Direct Events: 256 x 7 x 32 bits = 7 kB; Total: 99 kB), and the rate of generation of images (once per 6-sec spin), the intrinsic data output of TIDE may be seen to be ~ 10^5 Bytes/spin or ~130 kbps. The allocated telemetry rate is 3000 Bytes/spin or 4000 bps, so it is clear that tradeoffs must be made between temporal resolution and comprehensiveness of data reporting. TIDE has two data handling modes, which provide considerable flexibiltiy for trades in favor of the one or another aspect of the data set. In addition, onboard data processing techniques such as data compression and moment computation are used to maximize the effectiveness of the available data rate.

Figure 7.1-1 Data flow block diagram.

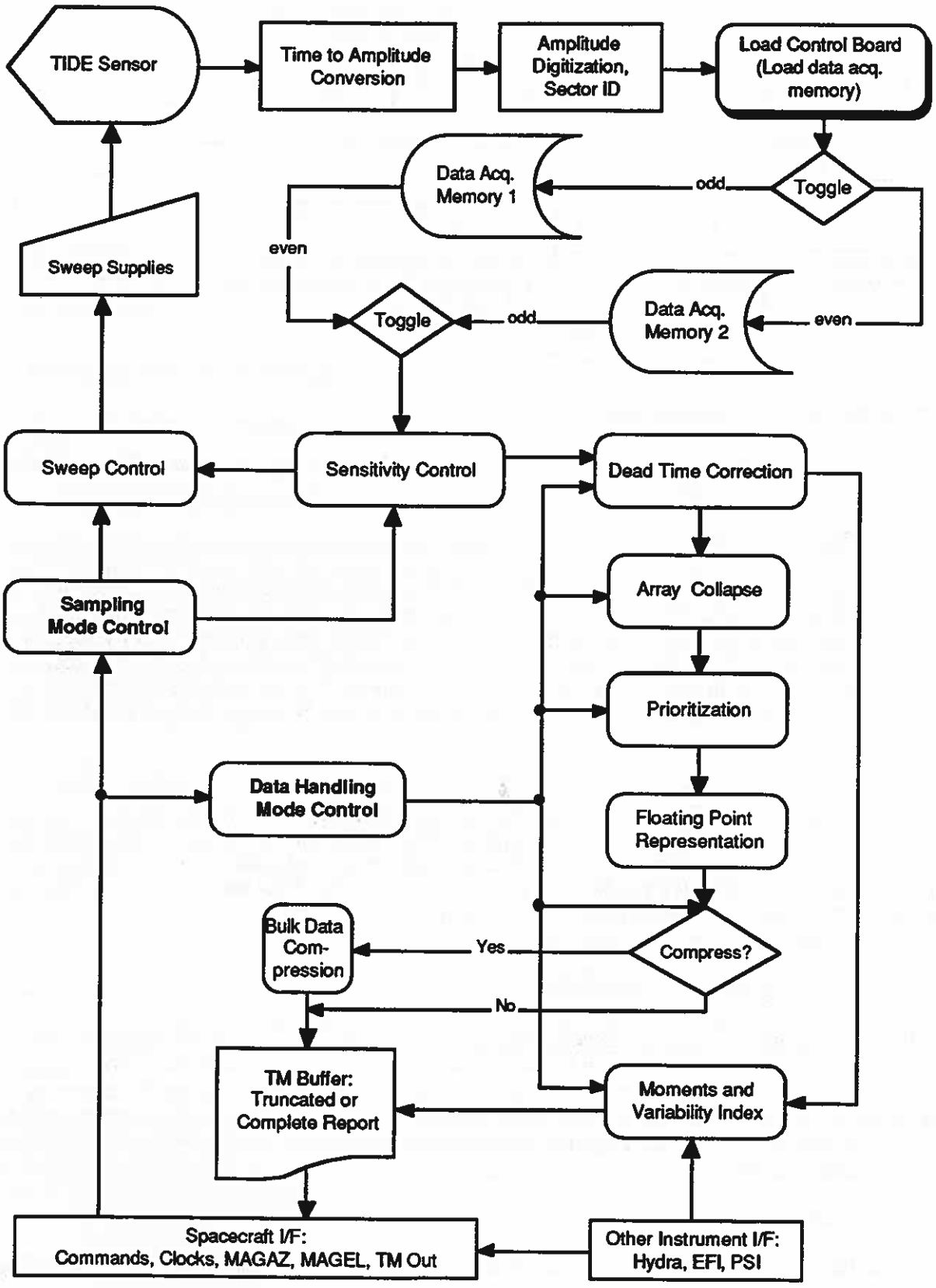

Figure 7.1-2 Data flow timing diagram

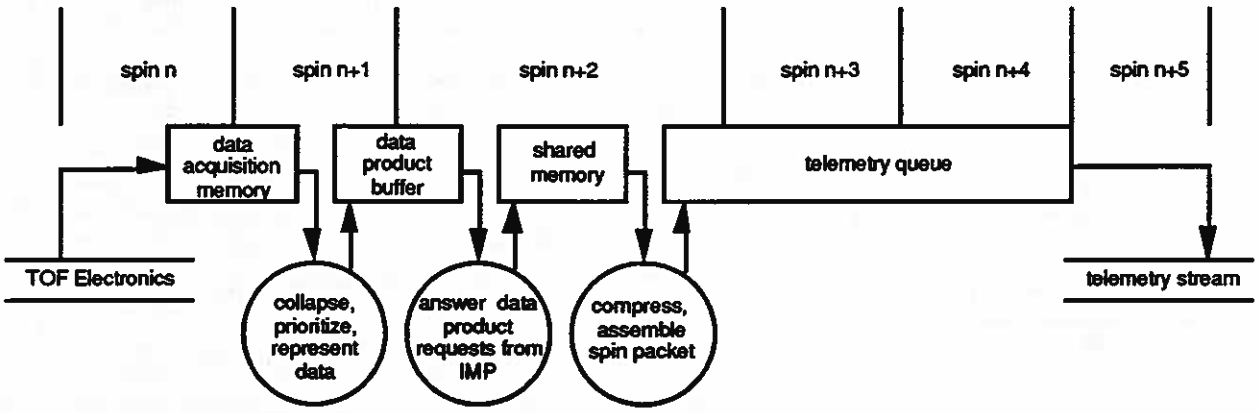

7.2. In-flight Data Decimation

The following methods implement the necessary trades by reducing the content of one or another aspect of the data to be telemetered:

7.2.1. Priority Ordering

The first form of prioritization of the TIDE data is the drawing of a distinction between the reporting of species data and direct events. Since the purpose of direct event reporting is to provide information about species which may not be sampled among the top priority species data, it is intrinsically of lower priority. It is therefore accumulated over a longer time scale of 32 spins (a superspin, see below). This requires larger accumulation registers, but drastically reduces the data rate requirement for this information, down to 56 words (long 4 Byte) per spin (of 3000).

The TIDE species data are also routinely priority ordered from the most important species to least important species. The ordering is controlled by a default table in ROM, but may alternatively be controlled by means of an uplinked table. The START singles rates (seven of them) may be treated as a distinct, composite mass species and introduced into the telemetry as such. By default, the START singles data is the highest priority mass species in the priority ordering. The other four singles rates, STOPS, StartConverts, TimeOuts, and Resets, are reported only after reduction to spin moments, as described below.

7.2.2. Floating Point Representation

TIDE count accumulations are reduced from 16 bits to 8 bits (or 32 bits to 16 bits in the case of direct event data) by implementing a special form of floating point representation with a resolution of ~3% and a range of 2^{16}, conserving scarce telemetry and limiting the reporting precision to a level commensurate with the overall measurement accuracy. The mapping of 16-bit internal data acquisition accumulator words to encoded bytes is handled in hardware by a memory lookup table.

7.2.3. Azimuth Collapse

To make the angular sampling which occurs near the spin axis directions in the TIDE sampling

scheme more commensurate with the angular response of the instrument, data from the polar angle sectors can be increasingly collapsed as they approach the spacecraft spin axis. This yields a collapse factor of 1.9 without significant loss of detail in the data. To provide additional collapse at the cost of real loss of angular resolution, an additional collapse option combines alternate bins for a collapse factor of 3.8. Another collapse option simply combines 32 spin rows into two rows for laboratory test and calibration purposes where spin sectoring is not needed. Only the second of the two spin rows is reported, so that the first half of each "spin" period may be used to make adjustments to the laboratory setup in real time without invalidating the entire spin of data.

7.2.4. Energy Array Collapse

In cases where additional collapse is desired, an energy collapse is provided in which adjacent energy columns of data are combined, for a collapse factor of 2, with corresponding loss of energy resolution.

7.3. In-Flight Data Processing

In order to minimize the impact of data decimation, the following in-flight processing techniques are used:

7.3.1. Bulk Data Compression

Collapsed arrays of floating point represented data are further compressed by a lossless encoding technique similar to those used for telecommunications of computer files. This eliminates data with little information content and provides reductions in the total data volume by a factor ranging from approximately 2 to several, depending on the information content of the specific data. The resulting data volume depends in general upon the nature of the data collected, but this uncertainty is handled by truncation or by allowing as much time as is needed for reporting. The result is the transmission of more data content per spin (less truncation), or a reduced number of spins between complete reports, respectively.

7.3.2. Moments

Moments computed each spin provide an important measure of variability from spin to spin when full distributions can only be sent at less frequent intervals. In addition, moments of the singles rates provide useful diagnostic information concerning the operation of the instrument detectors and electronics.

Selected simple moments of the species and singles, angle and energy distributions, are computed from the raw data arrays and reported on a single spin basis. A short history of these moments is updated by the Data Processor each spin and used to judge the variability of the data for purposes of triggering a high time resolution mode. The criterion for the switch is that the standard deviation within the current record of selected moments exceeds an uplinkable threshold.

Due to limited computational speed, even with two 32-bit processors, the moments computed are simple mean bin numbers and effective widths for Azimuth and Polar Angle. The energy distribution is weighted to provide the energy of maximum phase space density and the effective width of the phase space density distribution.

7.3.3. Dead-Time Correction

The finite dead time of the TOF analysis circuits, and the desirability of operating with large counting rates to maximize the statistical significance of the TIDE data, indicate that TIDE requires a dead-time correction onboard to support the computation of accurate collapses and moments. Therefore, it is necessary to perform an onboard dead-time correction of all counts samples based upon the overall rate of TOF events. This is done on the basis of the current START CONVERT rate, by means of a look up table stored in DPU memory.

7.4. Operations and Commanding

7.4.1. Mode Summary

The strategies for reducing TIDE data volume therefore involve a number of options, the selection of which defines a TIDE operating mode. In addition, the basic partitioning of energy and angle sampling can be modified so as to gain fine angular resolution at the cost of reduced energy resolution and/or range. The mode structure is summarized in Table 7.4-1. In the following paragraphs, the major mode options are described:

Table 7.4-1 TIDE operating mode summary

Mode Nomenclature	Energy bins	Azimuth bins	Mass bins	Comments
"Standard" Sampling:				
Calibration Collapse	32	1,1,1,1	5	collapse out spin information
Truncate (High Time Res.)	16	16, 8, 4, 2	3	maximum collapse
Complete	16-32	32, 16, 8, 4	1-5	on trigger -> Truncate
High Ang. Res. Sampling:				
Phase Stepping superposed on any mode above	16-32	(32, 16, 8, 4)x4	3-5	step phase by 2.81° per spin or report, through 22.5°

NOTE: The series of numbers under "Azimuth Bins" corresponds to the number of azimuth bins in polar angle sectors 4&5, 3&6, 2&7, and 1, respectively.

7.4.2. Calibration Mode

In this mode the normal 32 spin sectors are summed into two sectors, one of which is discardedto allow for settling of changes made in the test setup, while the latter of the two is reported. This reduces the data volume by a factor of 32, removing over sampling which is inappropriate at the time of calibration, and making it possible for all of the collected data to be reported within a single "spin," as defined by the simulated spacecraft spin clock provided by the GSE.

In addition, a unique additional data product is defined for this mode containing all singles rate data, which is plotted in real time to facilitate management of detector and TOF high voltages during testing.

7.4.3. Truncate (High Time Resolution) Mode

Data are truncated to the amount which can be sent in a single spin of telemetry, but with priority ordering to insure that the most important data are sent. To maximize the number of species reported on in this mode, maximum collapses are used for both energy and azimuth angle. Since each species requires approximately 940 Bytes at this level of collapse, while 3000 Bytes can be telemetered per spin, only the three highest priority species can be monitored in this mode. By default, the three species reported are START singles, Mass 1 (H^+), Mass 2 (He^{++}). However,

this designation can be modified by uplink of an alternate priority table.

7.4.4. Complete Report Mode

In order to report a larger number of mass species or to regain the full available resolution in energy and azimuth, or both, it is necessary to give up time resolution and report the full data set over a period of multiple spins. The full ordered data array is queued for telemetry, in general leaving a partial spin of telemetry unfilled. In order to fully utilize the available telemetry, the next spin header is introduced at mid-spin followed by the next spin record without waiting for the next spin clock pulse. This is possible because of the buffered nature of the data processing. The mean number of spins required to report a data array is, to a large extent, controlled by the level of collapse which is implemented and the character of the data itself.

The Complete Report mode operations result in a time series of data arrays for a selectable number of species (from 1 to 5 plus START singles), at time intervals ranging from every spin to every several spins, depending on the collapse level. Moments of the data, computed and reported every spin, may be used to identify the existence of variability on time scales shorter than the current number of spins between distribution samples (see below).

TIDE monitors the EFI (electric field investigation) and Hydra (three dimensional energetic plasma) experiments' "burst" modes by means of dedicated lines connecting the instruments. It also monitors the reduced moment data from the most recent several spins of data. TIDE can be enabled to switch to its high time resolution mode, truncating data to permit single spin reporting, when a specified combination of these sources indicates the presence of variability in the plasma environment meeting criteria which can be defined by uplink. It dwells in the high time resolution mode for an uplinkable duration.

7.4.5. High Angular Resolution Mode

As noted above, the "standard" sampling is based on 32 energy sweeps of 11.25° duration each. The M/RPA optics supports a finer sampling of Spin Azimuth angle when operated at reduced sensitivity. The ultimate angular resolution of the optics is limited by the available flux, but it is thought that resolutions down to approximately 3° can be supported.

A "high angular resolution" sampling mode is based on the capability to vary the sector phase from spin to spin. By stepping the phase of the sectors through a submultiple (N) of 11.25° each spin for N spin reports (plus another spin to restore the phase to baseline), a factor of N finer angle sampling is supported at the cost of a loss of time resolution by a factor (N+1). The value of N commensurate with maximum practical angular resolution is approximately 4. The spin phase is incremented once per telemetry report so that both truncated and complete reporting would be supported by this mode.

7.4.6. Over Counting and Automatic Sensitivity Control

The basic strategy involves sampling the entire data acquisition memory and counting the number of saturated counting values which exceed a hierarchy of thresholds. For each energy (RPA) step of the current spin of data, if a significant number of samples exceed a particular threshold in the hierarchy, the sensitivity is reduced by a corresponding number of "stops", where the term "stop" is used by analogy with mechanical aperture systems. The next spin of data is again tested for saturation as described above and further reduction is imposed if needed, continuing until the over counting criterion is no longer met.

When a low threshold is exceeded by an insufficient number of samples, the sensitivity can be increased, at a maximum rate of one "stop" per spin. The spacing between thresholds and "stops"

is determined from laboratory testing of the control algorithm. The overall control strategy is best described by an analogy with the human eye. Upon encountering a bright light the eye blinks and then slowly recovers by squinting and slow reopening.

The testing process is repeated and implemented every spin. More elaborate recovery algorithms using the number of saturated counting values from previous spins in a linear scaling procedure could also be implemented if deemed necessary. However they would require additional coding and control functions, and thus they are not implemented in the baseline software scheme.

TIDE sensitivity control is implemented in flight software at two levels. At the default level, over counting in a particular energy step at any point during a spin triggers a proportionate reduction of the sensitivity level for that step in the energy sweep. Cessation of over counting does not, however result in an increase in the sensitivity for that energy step, and the instrument becomes adjusted to the largest fluxes encountered at each given energy step of the sweep. At the optional level, the instrument responds to low counting levels by returning the sensitivity to higher values at each energy step, at a maximum rate of one "stop" per spin.

Default sensitivity control is considered to be necessary at all times when the instrument is not being monitored in real time, to protect against over counting. The lowest available sensitivity 'stop' is designed to totally shut down the flux to the detection system. In the event that this still fails to eliminate over counting on any given energy step, the control software causes shutdown of the High Voltage supplies, TOF first, then MCP bias. The default sensitivity control can be disabled by means of an appropriate command which is designated as hazardous.

7.4.7 Command Summary

The overall command structure for TIDE and PSI is summarized in Tables 7.4-2 and 7.4-3.

Table 7.4-2 Commands for power, testing, and operations

Commands	Class.	No. Bits	Processed	Effective
POWER SUPPLY COMMANDS:				
M/RPA HV Arm	major pulse		N/A	O/R
MCP HV Arm	major pulse		N/A	O/R
TOF HV Arm	major pulse		N/A	O/R
HV Master Off	major pulse		N/A	O/R
Mirror HV Enable	major serial		O/R	O/R
RPA HV Enable	major serial		O/R	O/R
TOF HVEnable	major serial		O/R	O/R
START MCP HV Enable	major serial		O/R	O/R
STOP MCP HV Enable	major serial		O/R	O/R
RPA HV Disable	major serial		O/R	O/R
Mirror HV Disable	major serial		O/R	O/R
START MCP HV Disable	major serial		O/R	O/R
STOP MCP HV Disable	major serial		O/R	O/R
TOF HV Disable	major serial		O/R	O/R
START MCP HV Update	minor	16	O/R	SP
STOP MCP HV Update	minor	16	O/R	SP
TOF HV Update	minor	16	O/R	SP
Sweep Table Select	minor	16	O/R	SP2/SSP
Sweep Table Fill and Select	minor	24	O/R	SP
TEST PULSER COMMANDS:				
Resync w/ GSE	major		SP	SP
Single commanding enable	major serial		O/R	SSP
Delay/Rep rate select	minor	16	O/R	SP
TOF sector select	minor	7	O/R	SP
Sequence commanding enable	major serial		O/R	SSP
Pulser disable	major serial		O/R	SSP
Data processing test sequence enable	major serial		O/R	SSP
Data processing test sequence disable	major serial		O/R	SSP
OPERATION COMMANDS:				
S/C spin sun pulse lock	major serial		O/R	O/R
S/C spin free run mode	major serial		O/R	O/R
Constant spin phase shift enable	minor	8	SSP	SSP
High Ang. Res. mode enable	major serial		SSP	SSP
High Ang. Res. mode disable	major serial		SSP	SSP
Spin phase shift disable	major serial		SSP	SSP
Execute stored SSP commands	major serial		O/R	SSP
Default sensitivity control enable	major serial		O/R	SP
Optional sensitivity control enable	major serial		O/R	SP
Sensitivity control disable	major serial		O/R	SP
MASS TABLE COMMANDS:				
Select Mass LUT 1	major serial		SSP	SSP
Select Mass LUT 2	major serial		SSP	SSP
Mass LUT Swap	major serial		SSP	SSP
Load powerup default LUT	major serial		SSP	SSP
Mass LUT entry specification	minor	24	O/R	O/R
Mass LUT build	minor	20	SSP	SSP

Table 7.4-3 Commands for Instrument Mode and Data Processing

Commands	Class.	No. Bits	Processed	Effective
MODE COMMANDS:				
Select energy sweep table 1	major serial		SP	SP
Select energy sweep table 2	major serial		SP	SP
Swap energy sweep table	major serial		SP	SP
DP Reset	major serial		O/R	O/R / SP
Clear direct event memory	major serial		O/R	SP
Direct event buffer toggle enable	major serial		O/R	SP
Direct event buffer 1 freeze	major serial		O/R	SP2
Direct event buffer 2 freeze	major serial		O/R	SP2
M/q buffer toggle enable	major serial		O/R	SP
M/q buffer 1 freeze	major serial		O/R	SP2
M/q buffer 2 freeze	major serial		O/R	SP2
Watchdog enable	major serial		O/R	O/R
Watchdog disable	major serial		O/R	O/R
Dump Mode enable (IMP)	major serial		SSP	SSP
Dump Mode enable (DP)	major serial		SSP	SSP
Address for memory dump	minor	24	O/R	SSP
Clear IMP/DP error flags	major serial		O/R	O/R
DATA PROCESSING COMMANDS:				
Dead time correction enable	major serial		O/R	SSP
Dead time correction disable	major serial		O/R	SSP
Accumulation period	mnor	8	O/R	SSP
Rice compression enable	major serial		O/R	SSP
Rice compression disable	major serial		O/R	SSP
Truncated reporting	major serial		O/R	SSP
Complete reporting/fixed ions	minor	5	O/R	SSP
Complete reporting/rotating ions	minor	5	O/R	SSP
Collapse option	minor	8	O/R	SSP
High Time Res. trigger enable	minor	24	O/R	SSP
High Time Res. trigger disable	major serial		O/R	SSP
High Time Res. dwell #Sspins	minor	3	O/R	SSP
Priority ordering of masses/sectors	minor	24	O/R	SSP

7.5. Telemetry Summary

7.5.1. Science Data Telemetry

The TIDE spacecraft telemetry allocation is 4000 bits/s, 3000 Bytes per spin or 4608 Bytes per Major Frame. The Science Data Telemetry can be alternatively used for Memory Dumps. The alternatives for Science Data Telemetry are summarized below:

SCIENCE DATA MODE

The Science Data is reported in a packet-organized hierarchical format as indicated below:

Superspin Header X
- Data Product 1 Header
- Data Product 1
- Data Product 2 Header
- Data Product 2
- .
- .

Spin Header 1
- Data Product 1 Header
- Data Product 1
- Data Product 2 Header
- Data Product 2
- .
- .

Spin Header 2
- Data Product 1 Header
- Data Product 1
- Data Product 2 Header
- Data Product 2
- .
- .

.
.

Superspin Header (X+1)
- etc.

The superspin structure is a means of reducing the overhead associated with reporting of mode parameters, and coincides with a beat period between the spin and telemetry major frame periods. A superspin consists of 32 spin packets of data. A superspin header contains all mode information about the instrument operation which is valid at the beginning of that superspin. This includes active sweep tables, current mass lookup table, and a complete specification of the operating mode and all uplinkable option parameters. The only mode changes allowed during a spin are variations of the Mirror sweep table made by the auto sensitivity control algorithm, and a switch to Default Science (Truncate or High Time Resolution) Mode triggered by EFI, HYDRA, or TIDE's own variability indices. Under the complete report mode, each full data array translates into an integer number of spin packets, and these packets are labeled to indicate their position in the report. Single spin and trickled data continue through these full report groups of spin packets.

The formats for the headers are given in Table 7.5-1. The detailed data product formats are tabulated in the TIDE Flight Software Design Document.

Table 7.5-1 Spin Packet Formats

ITEM	No. Bytes
SPIN HEADER:	
Sync Word	2
Spin Packet Length	2
Mode ID	1
Spin Counter	1
Time Tag	3
Continue Number (for complete reports)	1
MAGAZ	2
MAGEL	1
Accumulation Period	1
TOF Efficiency Moments	4
Moments	36
Trickled Start Converts	31
Invalid Events	1
Trickled Direct Events	112
Commands Received Counter	1
Data Product Counter	1
Header Checksum	1
DATA PRODUCT HEADER:	
Data Product Sync	1
Data Product ID	1
Data Product Length	2
Data Product Time Tag	3
Data Product Data	variable
Data Product Checksum	1

MEMORY DUMP MODE

In order to facilitate low level trouble shooting, a memory dump mode replaces the science data products with a straight dump of specified sections of memory. The command to go into this mode includes the specification of address limits for the dump. Details are given in the Flight Software Requirements Document.

7.5.2. Engineering and Housekeeping Data Telemetry

In addition to digital scientific data, telemetry must be allocated to power supply monitors, other housekeeping and status functions. This telemetry has been allocated as 46 Bytes per telemetry Major Frame header for TIDE and PSI. The allocation for analog and digital status bytes is shown in Table 7.5-2. Mnemonics and status byte assignments are detailed in Appendix B.

Table 7.5-2 Engineering and housekeeping monitors/status bits/bytes

Description (s/c) indicates acquisition by s/c	No. Bytes	Sample Rate per Major Frame	Bytes per Major Frame
TIDE:			
Input Current (+28 V) (s/c)	1	1	1
Mirror Maximum Monitor	1	1	1
RPA Maximum Monitor	1	1	1
TOF HV Monitor	1	1	1
START MCP HV Monitor	1	1	1
STOP MCP HV Monitor	1	1	1
DAC Ref. Monitor	1	1	1
DAC Temperature Reference	1	1	1
START MCP DAC adjust	1	1	1
STOP MCP DAC adjust	1	1	1
TOF HV DAC ADJUST	1	1	1
+15 V Monitor	1	1	1
+5 V Monitor (s/c)	1	1	1
+10 V Monitor	1	1	1
+3 V Monitor	1	1	1
Flash ADC Monitor	1	1	1
TIDE Temperature (2 Monitors)(s/c)	2	1	2
TIDE Temperature (2 Monitors)	2	1	2
Electronics Temperature (PS, DP)	2	1	2
PSI:			
Bias Current	1	1	1
Input current (28V)	1	1	1
PSI +5 V Monitor	1	1	1
PSI +15 V Monitor	1	1	1
Keeper voltage/current Monitor	2	1	2
Filament voltage/current Monitor	2	1	2
Discharge voltage/current Monitor	2	1	2
PSI Temperature (2 Monitors) (s/c)	2	1	2
Gas Pressure Monitor (hi/low)	2	1	2
DIGITAL STATUS:			
Major Frame Counter	1	1	1
System Status Byte 1	1	1	1
System Status Byte 2	1	1	1
System Status Byte 3	1	1	1
Power Supply Status	1	1	1
IMP Status	1	1	1
DP Status	1	1	1
PSI Discrete Status	2	1	2
Command Counter	1	1	1
Total Bytes per Major Frame			46

7.5.3. Science Data Product Allocations

The straw man allocation of data within a spin record is shown in Table 7.5-4.

Table 7.5-4 Science data allocations

	# Words per Product	# Masses	# Words per Spin
Spin Header Info			
sync, ID, ctrs., etc.			18
Direct TOF Events			112
Science Moments	6	6	36
Diagnos. Moments	4		4
Science Data Products	940	3	2820
Undesignated			10
Total no. of compressed (8 bit) words/spin			3000

7.6. GSE Software

7.6.1. Command and Control

The first responsiblity of the GSE software, after establishing a logic interface with the instrument which is identical to that of the POLAR spacecraft, is to provide an effective and convenient means of issuing commands and data to the instrument and assuring their implementation. This begins with the uploading of the flight software, startup of the DPU processors, and the verification of proper operation. The PCGSE is the subunit of the GSE which has this responsibility first. Later, when the spacecraft substitutes for the PCGSE, the RDAF portion of the GSE inherits this responsibility. Since the RDAF is a SUN rather than a PC, there are portability issues in moving this software functionality.

The GSE supports the development of macros which are test procedure-oriented with hard copy outputs showing pass/fail criteria and results for test buy-off by QA.

The GSE program shell is menu driven and reasonably user friendly so that there is no one key person whose presence is required for tests involving the GSE. At present there is insufficient documentation on the PCGSE software and a guide to the menu structure is badly needed to make possible limited routine operations by multiple staff members and the PI surrogates during I&T.

7.6.2. Data Decommutation and Display

The GSE software includes routines which decommutate the TIDE data from the rest of the spacecraft data stream (PCDecom), and which decommutate the TIDE Science (Spin-organized) data from the Housekeeping/Engineering Data (GETSPINS), which is synchronous with the telemetry major frame structure. PCDecom breaks out the major frame headers containing the housekeeping data, while GetSpins breaks out the spin headers, the data product headers, and all data product arrays in a form which facilitates graphical display on the RDAF component of the EGSE.

PC Decom is a commercial piece of software which is adequately documented. GetSpins requires adequate documentation to be written by the developing teams.

8. TEST AND CALIBRATION

8.1. Safety

8.1.1. HV Arming Plug

The HV plug must be in place during all ground operations at atmospheric pressure. The plug may be removed prior to tests in which TIDE is operated in a vacuum of 10^{-6} Torr or below. The plug must be removed before flight.

8.1.2. N_2 Purging

TIDE is tightly sealed and equipped with a purge cover which must remain in place at all times during ground operations with the exception of testing in vacuum. The cover must be removed before launch. Purging will be continuous with exceptions as allowed in the TIDE Handling Plan (SwRI document 3348-HP-1).

8.1.3. Vacuum Requirements

Because of large detector surface areas within TIDE a vacuum of <10 Torr must be held for >24 hours before HV switch-on can take place.

8.1.4. Beam Intensity Limits

TIDE has a large collecting surface area (~1 cm^2) and therefore a large geometric factor. The TIDE MCPs are extremely sensitive and beam current densities $>10^6$ ions/cm^{-2} s^{-1} (0.16 pA) could damage the multipliers. Care is therefore exercised when bringing up an ion beam for test or calibration purposes. TIDE apertures are closed by application of zero mirror bias, and RPA bias larger than the beam energy, until the beam current can be verified to be within range.

8.1.5. Instrument Handling, Packaging, Transport

Reference is made to the Handling Plan for TIDE, SwRI document 15-3348-HP-1.

8.1.6. Instrument Purge and Cover Removal

Reference is made to the Handling Plan and Cleanliness Requirements for TIDE, SwRI documents 15-3348-HP-1 and 15-3348-CR-1; and to the Purge Operating Procedure for TIDE, SwRI document 15-3348-POP-1.

8.2. Commanding

8.2.1. Low-Voltage Power

The low-voltage power used to drive DPU, TOF, and all HK functions is commanded on by a single pulse command. The electronic circuitry always come on in a state that poses no danger to the instrument or its GSE.

8.2.2. HV Arming Connector

In order to prevent accidental switch-on of the TOF, MCP, RPA or mirror high voltage supplies

with the electronics on and operating, there is an HV arming plug accessible from outside the instrument (Figure 4.1-2). This plug is a RED TAG item to be removed before launch. The arming plug circuit controls the low voltage side of all five HVPS in question. This is preferable to breaking the actual HV lines. In addition a line is run through the shorting plug to indicate to the GSE and operator the status of the shorting plug.

8.2.3. HV Arming Commands

In addition to the HV Arming Connector, the HV supplies themselves are armed by three pulse commands in the following way:

-15.0 kV HVPS armed separately

-3.6 kV and -2.4 kV MCP HVPS armed together

+300 V mirror and +300 V RPA armed together

Memory Load Commands Based on the required voltage resolution of the various power supply commands (see Section on high voltage supplies):

Table 8.4-1 Command resolutions

Function	# bits
RPA Voltage	12
Mirror Ratio	8
Stop MCP Voltage	8
Start MCP Voltage	8
TOF HV	8
Sample Phase (0 to 22.5 °)	8
Command word	40

8.3. Testing

8.3.1. Functional Test

The functional test is designed to test most of the instrument systems by operating it in a mode which exercises as many functions as possible. As new software modes and functions are added during the development period, the procedure is expanded to exercise the new modes/functions. This test is specified in the TIDE/PSI Functional Test Procedures, SwRI documents numbered 3348-FTP-01 for TIDE and 3348-FTP-04 for PSI.

8.3.2. Comprehensive Test

The comprehensive test involves operation in a live ion beam in the case of TIDE, or generating a plasma in the case of PSI, so that all optics and detector functions are thoroughly tested. These tests are specified in the TIDE/PSI Comprehensive Test Procedures, documents numbered MSFC-TIDE-CTP-00 in the case of TIDE, and SwRI-15-3348-FTP-04 for PSI.

8.3.3. Spacecraft Level Tests

Spacecraft environmental testing will be conducted per the TIDE/PSI I&T Plans, as referenced in the section on relevant documentation.

An important aspect of the spacecraft integration testing is the checkout of the links between TIDE/PSI and the other instruments on the spacecraft. Several other instruments receive a signal indicating that PSI is operational, while TIDE receives signals indicating that HYDRA and EFI have gone into "burst memory mode" indicating that these instruments have detected interesting time variations of their data. TIDE optionally responds to these signals by switching to a maximum time resolution mode.

8.4. Calibration

Reference is made to the TIDE Calibration Procedure (MSFC-TIDE-CP-01), which is based upon the following requirements for calibration information:

8.4.1. Channel Survey Configuration

This part of the calibration provides broad information on all seven sectors of the instrument. This includes the basic mass calibration of the TOF system, as well as the absolute sensitivity measurements. It is the highest priority measurement at the time of refurbishment when flight MCPs are installed.

8.4.1.1. MCP gain characterization

The idea here is to determine how each stack plateaus, i.e. obtain its count rate saturation curve with respect to MCP bias, an integral measure of its pulse height distribution. In the case of the Stop detectors, all 7 stacks have to be done together.

8.4.1.2. Mass calibration

The data consists of DE mass spectra obtained using H^+, H_2^+, He^+, Ne^+, H_2O^+, N_2^+. This information serves as the basis for assigning bin limits to define the binning of species data.

8.4.1.3. Dead time effects

This is to determine response non linearity for selected channels at M/RPA centroid in RPA, Azimuth, and Polar angle.

This is basically a way to empirically measure the dead time, and requires accurate beam current measurements.

8.4.1.4. HV bias and beam energy response dependence

This provides a measurement of TOF and MCP bias, and beam energy dependence for selected channels at M/RPA centroid in RPA, Azimuth, and Polar angle.Bias dependencies should be primarily in the mass spectrum and effective area, but may include angular response changes.

8.4.1.5. Normal Incidence Energy Response

This provides measurement of the response of the M/RPA at a full range of energies, for each sector, at normal incidence upon each sector aperture.

8.4.2. Single Channel Setup

This part of the calibration provides detailed energy and angular response characteristics of an individual sector. It is to be repeated on as many channels as time permits. Any channels not

studied this way during the main calibration period will be done at highest priority during the refurbishment period.

8.4.2.1. Energy centroid and pass band vs. R_m

This test provides measured energy centroid and pass band vs. Rm, based on the collapsed count rate array for the principal beam species: ΣAz [CR(RPA, R_m, Az)]. This needs to be done with a very intense beam to get good data at the lower values of R_m.

8.4.2.2. Azimuth centroid and pass band vs. R_m

This test provides measured azimuth centroid and pass band vs. Rm, based on the collapsed count rate array for the principal beam species: ΣRPA [CR(RPA, Rm, Az)]. This is actually formed from the same data set as test 8.4.2.1, by the complementary collapse.

8.4.2.3. Polar angle centroid and pass band vs. R_m

This test provides measured polar centroid and pass band vs. Rm, based on the count rate array for the principal beam species: CR(Rm, Pol) @ RPAc, AZc, where the subscripts denote the centroid positions in RPA and Az, as determined by 8.4.2.1, above. This assumes that the CR(POL) response is factorable from the other responses. We have data which already demonstrate this.

8.4.2.4. Effective area Vs. Rm

This test provides measured Aeff vs. Rm, based on CRmax and Jcup (at RPAc, AZc, POLc, centroid positions) for each Rm in tests 8.4.2.1-2. This information is actually derived from the tests 1-2 if cup currents are recorded systematically.

8.4.2.5. Mirror Tracking

This test provides a measurement of the response as a function of Rm vs. RPA/Ebeam, based on conduct of tests at low energies, where Rm is known to vary from that commanded due to power supply inaccuracy. This will be based on a model of Rm involving a known offset in the sweep supplies. Measured mirror voltages show that Rm varies from the commanded ratio at RPA biases below approximately 2 V. All sweeps must take account of this, for which this test provides the required information.

8.5. Test Data Examples

As examples of the test performance of TIDE/PSI, the following are offered: In Figure 8.5-1, a set of lab test data from a TIDE prototype TOF sensor known as the Hot Plasma Composition Analyzer (HPCA) is given. This is a composite TOF spectrum representing the sum of spectra obtained with beams whose composition varied, producing the peaks shown, and providing a basis for the expected mass resolution and S/N of TIDE.

In Figure 8.5-2, a similar set of data is shown, collected from the TIDE protoflight model during testing.

In Figure 8.5-3, we show the energy-azimuth response of the TIDE front end optics as tested using the TOF mass analyzer for detection. The data illustrate the modulation of response to a constant ion beam which is obtained by modulation of the mirror potential ratio.

Figure 8.5-1. TOF spectrum from the HPCA prototype.

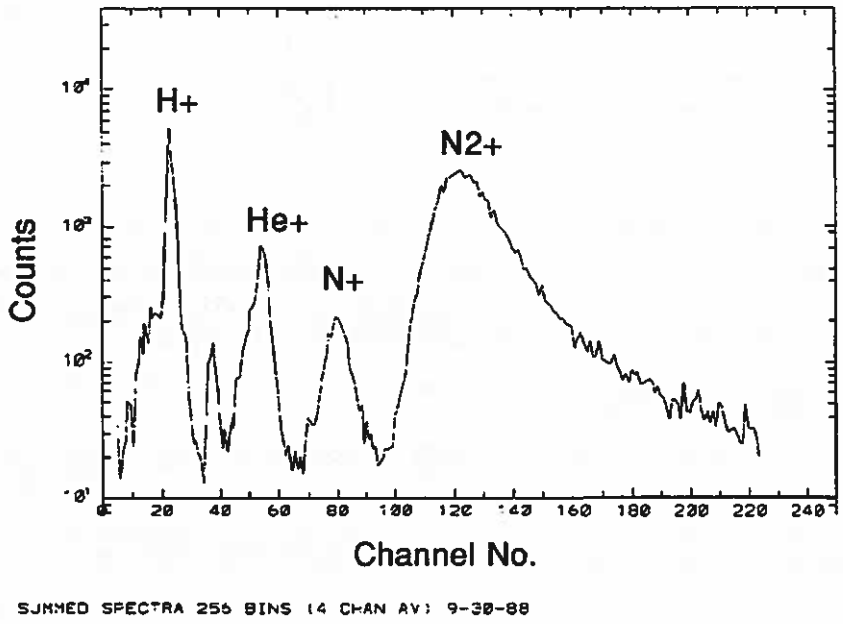

Figure 8.5-2. TIDE flight model mass spectrum.

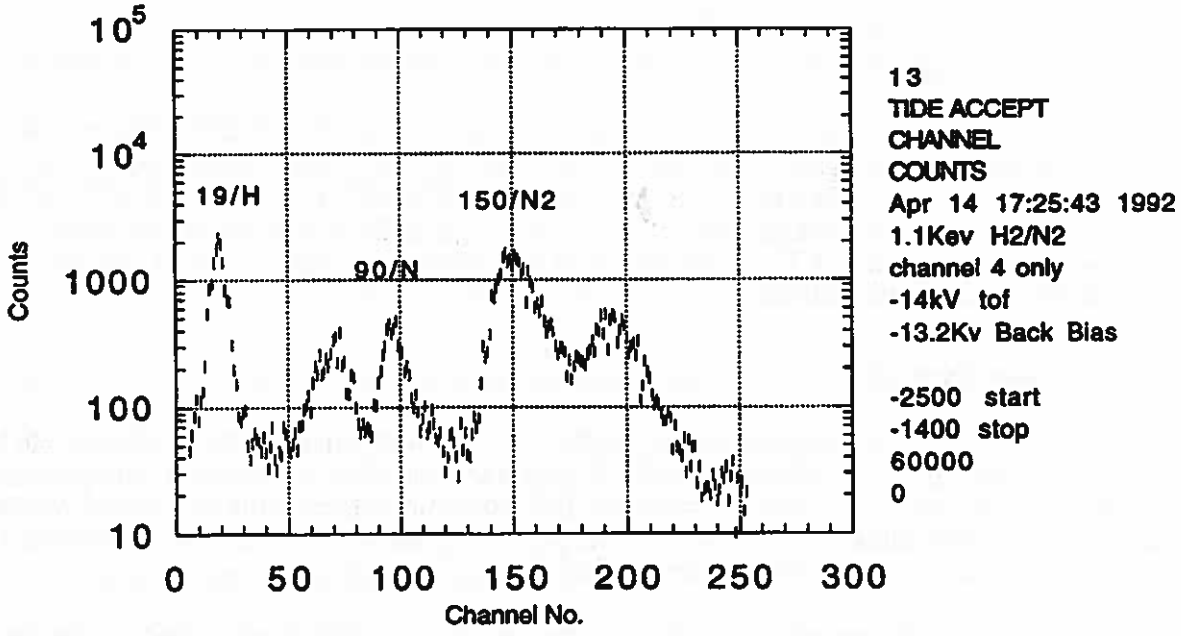

Figure 8.5-3 M/RPA energy-azimuth response vs. Rm.

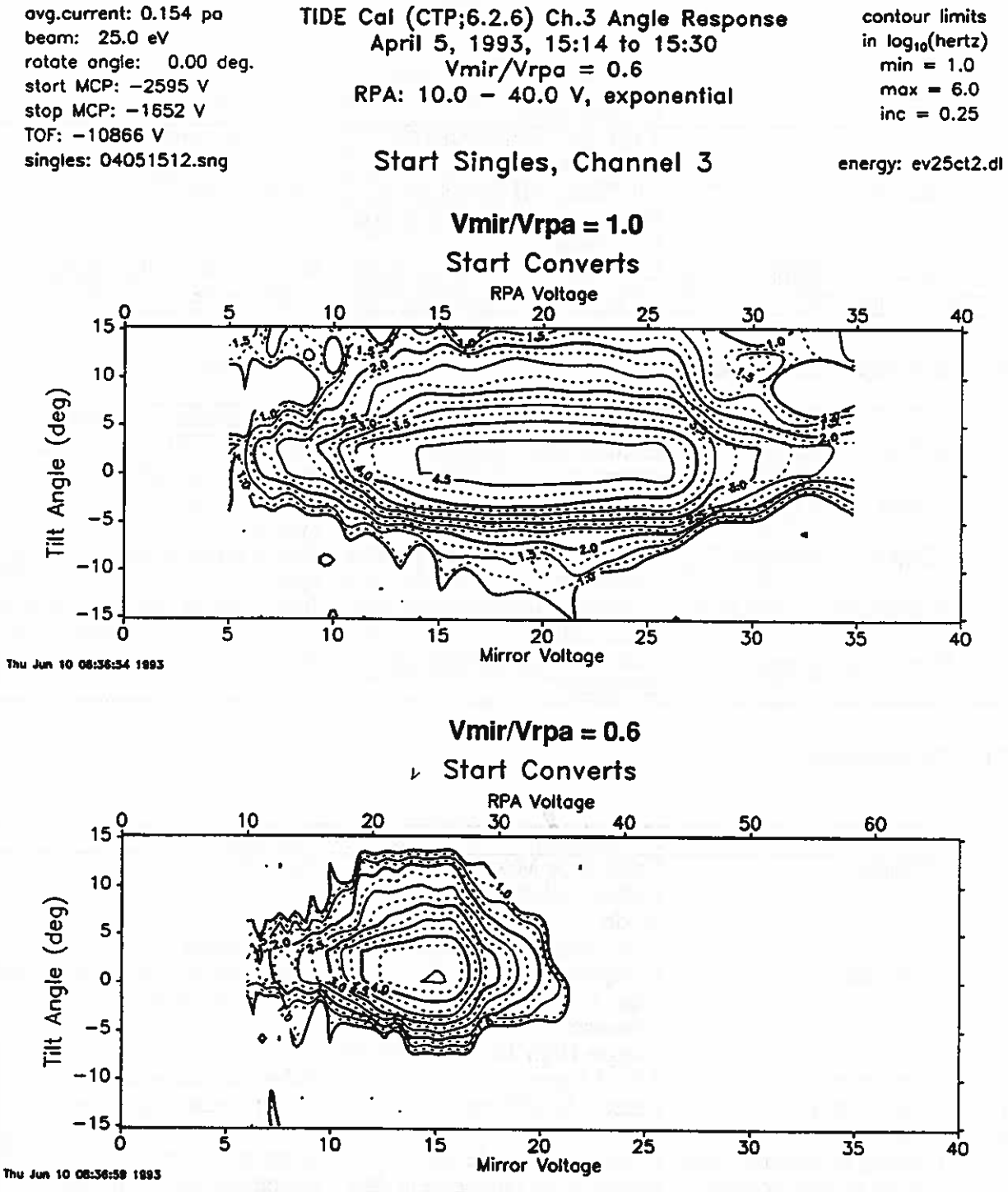

APPENDIX A: COMPREHENSIVE TEST CRITERIA

Interfaces

Item	Requirement	Test Method
Mass	≤ ICD mass for TIDE, PSI	Certified weigh-in
Power Consumption	≤ ICD power for TIDE, PSI	GSE measurement
Command Functions	All TIDE, PSI function per Flight Software Specification Document	Exercise via GSE
Physical Configuration	Envelope, mounting per ICD	Measurement, fit checks
Surface Conductivity	All points ≤ 1 ohm to ground	VOM probe

Power Supply Performance

Item	Requirement	Test Method
RPA and Mirror Supply	Settling times per this document	Bench test of boards driven with flight program
RPA Supply Wave form	Accuracy, ripple, drift per this document	Bench test of board in full up system
Mirror Supply Wave form	Accuracy, ripple, drift per this document	Bench test of board in full up system
MCP Bias Supplies	Accuracy, ripple, drift per this document	Bench test of board
TOF Bias Supply	Accuracy, ripple, drift per this document	Bench test of board

DPU Operations

Item	Requirement	Test Method
Phase I Modes	Calibration Mode	Pulser macros
	Default (High Time Res.) Mode	
	Auto Sensitivity Control	Beam testing
Phase II Modes	Complete Report	Pulser macros, designed to test features of each mode.
	High Ang. Res. Mode	
	Moments	
	Trigger High Time Res. Mode	
TOF Dead Time	2.0 - 3.1 μsec	Pulser or saturation?
TOF Singles Rates Relationships	Reset = Sum(TimeOut + StartConvert	Pulser macro sequences
Time Tagging of Science Data	Accuracy to single spin	Beam pulse test
GSE Display of Engineering Data	Access to all engineering data	Automatic during testing
GSE Archival, Playback, Display	Access to all science data words	Pulser testing with appropriate macros

Sensor Operation

Item	Requirement	Test Method
Vacuum High Voltage Stability	Operable at 11 kV 24 hours after reaching ≤ 1 x 10^{-6} Torr	Automatic in vacuum testing
Detector Gain/Threshold Uniformity	Low gain Start/Stop stack enters saturation plateau before High gain Start/Stop shows ion feedback.	Saturability test in beam
Detector Dark Rates	Starts ≤ 100 Hz Stops ≤ 700 Hz	Vacuum test w/ beam off
H-alpha Response	≤ 10 Hz at 1 solar constant	Krypton UV source test
TOF Mass Response	M/ΔM ≥ 4 @ N_2	Beam testing
TOF Single/Noise	Coincidence Dark Rate ≤ 0.1 Hz S/N ≥ 100 @ 10 kHz	Beam testing
Singles Data Crosstalk Rejection	Adjacent sectors: ≤ 10% Other sectors: ≤ 1%	Beam testing
TOF Data Crosstalk Rejection	Adjacent sectors: ≤ 1% Other sectors: ≤ 0.1%	
Energy Response	RPA cutoff ±1% FWHM 60%±10% at Rm=1	Beam testing
Azimuth Angle Response	Centroid 0°±5°, FWHM 10°±5	Beam testing
Polar Angle Response	Centroid 0°±5°, FWHM 22°±5	Beam testing
Effective Area	≥ 0.3 cm^2 per sector for Rm=1	Beam testing
Effective Area Commandability	≤ 0.003 cm^2 reproducible to 10%	Beam testing
Effective Area Uniformity	Standard Deviation ≤ 25 %	Beam testing

APPENDIX B. Houskeeping Data

	MiFr No. (0-249)	Byte No.	Description	Mnemonic
	5	11	Major Frame count	TMAFRCNT
	5	12	Command counter	TCMD_CNT
	17	11	Power supply status	TPWR_STX
	17	12	System status 1	TSYSST1X
	29	12	IMP status	TIMP_STX
	41	12	DP status	T_DP_STX
	53	11	System status 2	TSYSST2X
	53	12	System status 3	TSYSST3X
*	61	11	Input current	TINPCURR
	65	11	PSI Bias current	TPBSCURR
	65	12	TOF DAC adjust	TTOFDACA
	77	11	PSI status 1	TPSIST1X
	77	12	3.6KV DAC adjust	T36KDACA
*	79	11	+5V monitor	T_P5VMON
*	85	11	Temperature 1	T_TEMP_1
	89	11	PSI status 2	TPSIST2X
	89	12	2.4 KV DAC adjust	T24KDACA
*	91	11	Temperature 2	T_TEMP_2
*	97	11	PSI temperature 1	TP_TEMP1
	101	12	-15 KV monitor	T15KVMON
*	103	11	PSI temperature 2	TP_TEMP2
	113	11	PSI keeper voltage	TPKEEPRV
	113	12	-3.6KV monitor	T36KVMON
	125	11	PSI keeper current	TPKEEPRI
	125	12	-2.4 KV monitor	T24KVMON
	134	11	Temperature 4	T_TEMP_4
	137	11	PSI filament voltage	TPFILMTV
	137	12	+3 V monitor	T_P3VMON
	149	11	PSI filament current	TPFILMTI
	149	12	Temperature 3	T_TEMP_3
	161	11	PSI discharge voltage	TPDISCHV
	161	12	Flash ADC monitor	TFADCMON
	173	11	PSI discharge current	TPDISCHI
	173	12	+15 V monitor	T_P15VMN
	185	11	PSI hi gas pressure	TPHIGASP
	185	12	+10 V monitor	T_P10VMN
	197	11	PSI lo gas pressure	TPLOGASP
	197	12	+10 V DAC reference	T10VREFV
	209	11	PSI +5 V monitor	TPP5VMON
	209	12	10V DAC temperature ref	T10VREFT
	221	11	PSI +15V monitor	TPP15VMN
	221	12	Power supply temperature	TTEMP_PS
	233	11	PSI +28V current	TPP28V_I
	233	12	DP temperature	TTEMP_DP
	245	11	RPA peak voltage monitor	T300VRPA
	245	12	MIR peak voltage monitor	T450VMIR

* Acquired by S/C

Power supply status

Bit	Description	Mnemonic
0 (LSB)	15 KV enable (0=disable, 1=enable)	T15KVENA
1	3.6 KV enable (0=disable, 1=enable)	T36KVENA
2	2.4 KV enable (0=disable, 1=enable)	T24KVENA
3	RPA enable (0=disable, 1=enable)	TRPA_ENA
4	MIR enable (0=disable, 1=enable)	TMIR_ENA
5	15 KV Arm (0=safe, 1=arm)	T15KVARM
6	2.4/3.6 KV Arm (0=safe, 1=arm)	T2436ARM
7	RPA/MIR Arm (0=safe, 1=arm)	TRPMIARM

System status 1

0 (LSB)	Auto sensitivity (0=default, 1=optional)	TAUTOSEN
1	Watchdog (0=disable, 1=enable)	TWATCHDG
2	Hardware arm status bit 0 (0=safe, 1=1/10, 2=N/A, 3=arm)	T_HVSTAT
3	Hardware arm status bit 1	
4	PSI Squirt (0=off, 1=on)	TPSQUIRT
5	Pulser status (0=off, 1=on)	TPULSSTA
6	Boot mode (0=normal, 1=alternate ROM)	TBOOTMOD
7	Auto sensitivity (0=disable, 1=enable)	TAUTOENA

System status 2

0 (LSB)	Command received (0=OK, 1=error)	TCMD_REC
1	Command executed (0=OK, 1=error)	TCMD_EXE
2	Data load (0=OK, 1=error)	TDATA_LD
3	Telemetry queue (0=OK, 1=error)	TTLM_QUE
4	Telemetry (0=invalid, 1=valid)	TTLMSTAT
5	DE memory (0=OK, 1=error)	T_DE_MEM
6	PSI status (0=OK, 1=error)	TPSISTAT
7	spare	

System status 3

0 (LSB)	Super spin counter bit 0 (lsb)	TSS_CNT
1	Super spin counter - bit 1	
2	Super spin counter - bit 2	
3	Instrument mode - bit 0 (lsb)	TINSMODE
4	Instrument mode - bit 1	
5	Instrument mode - bit 2	
6	Instrument mode - bit 3	
7	Mode change pending (0=no, 1=yes)	TCHG_PEN

IMP status

Bit	Description	Mnemonic
0 (LSB)	RAM memory (0=OK, 1=error)	TIMP_RAM
1	ROM memory (0=OK, 1=error)	TIMP_ROM
2	Shared memory (0=OK, 1=error)	TIMPSHAR
3	MLUT (0=OK, 1=error)	TIMPMLUT
4	Energy sweep (0=OK, 1=error)	TIMPESWP
5	Debug initiated (0=no, 1=yes)	TDBGINIT
6	Acquistion mode (0=Sun, 1=Free)	TSUNMODE
7	Data processor health (0=OK, 1=Error)	TDPHEALT

DP status

0 (LSB)	DP RAM memory (0=OK, 1=Error)	TDP_RAM
1	DP ROM memory (0=OK, 1=Error)	TDP_ROM
2	DP Shared memory (0=OK, 1=Error)	TDP_SHRD
3	DP data acq memory (0=OK, 1=Error)	TDPDATMS
4	DP command (0=OK, 1=Error)	TDP_CMD
5	spare	
6	DP mode - bit 0 (lsb) (0=dump, 1=eng., 2=sci)	TDPMODE
7	DP mode - bit 1	

PSI status 1

0 (LSB)	Bias current - bit 8	TPBSCUR1
1	Bias current - bit 9	
2	Bias current - bit 10	
3	Bias current - bit 11	
4	Heater control level - bit 0 (lsb) (xx = lo, yy=hi)	TPHEATLV
5	Heater control level - bit 1	
6	Heater (0=off, 1=on)	TPHEATST
7	PSI arm (0=safe, 1=arm)	TPSI_ARM

PSI status 2

0 (LSB)	Discharge control level - bit 0 (lsb) (xx=lo, yy=hi)	TPDISCLV
1	Discharge control level - bit 1	
2	Discharge (0=off, 1=on)	TPDISCST
3	Keeper control level - bit 0 (lsb) (xx=lo, yy=hi)	TPKEEPLV
4	Keeper control level - bit 1	
5	Keeper (0=off, 1=on)	TPKEEPST
6	Valve 1 status (0=off, 1=on)	TPVLVST1
7	Valve 2 status (0=off, 1=on)	TPVLVST2